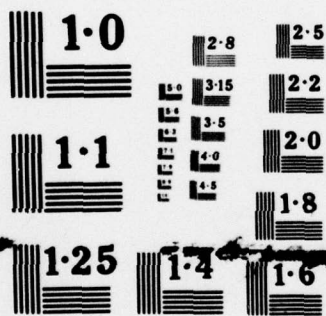


AD-A070 539 ARMY ELECTRONICS RESEARCH AND DEVELOPMENT COMMAND FO--ETC F/G 7/4
PHYSICS OF MESOMORPHIC COMPOUNDS.(U)
SEP 78 A J BROWN, R D ENNULAT
UNCLASSIFIED DELNV-TR-0003

NL

1 OF 2
AD
A070539





NATIONAL BUREAU OF STANDARDS
MICROCOPY RESOLUTION TEST CHART

LEVEL

AD

Report DELNV-TR-0003

12
B.S.

PHYSICS OF MESOMORPHIC COMPOUNDS

by
Arlin J. Brown
and
Reinhard D. Ennulat

DDC
REF ID: A66116
JUN 26 1979
RECEIVED

September 1978

Approved for public release; distribution unlimited.

DDC FILE COPY

**U.S. ARMY ELECTRONICS R&D COMMAND
NIGHT VISION & ELECTRO-OPTICS LABORATORIES
FT. BELVOIR, VIRGINIA 22060**



79 06 25 003

Destroy this report when it is no longer needed.
Do not return it to the originator.

The citation in this report of trade names of commercially available products does not constitute official endorsement or approval of the use of such products.

UNCLASSIFIED

SECURITY CLASSIFICATION OF THIS PAGE (When Data Entered)

REPORT DOCUMENTATION PAGE		READ INSTRUCTIONS BEFORE COMPLETING FORM
1. REPORT NUMBER 14 DELNV-TR-0003	2. GOVT ACCESSION NO.	3. RECIPIENT'S CATALOG NUMBER
4. TITLE (and Subtitle) 6 PHYSICS OF MESOMORPHIC COMPOUNDS	5. TYPE OF REPORT & PERIOD COVERED 9 Final Report May 63 - Jun 71	
7. AUTHOR(s) 10 Arlin J. Brown and Reinhard D. Ennulat	8. CONTRACT OR GRANT NUMBER(s)	
9. PERFORMING ORGANIZATION NAME AND ADDRESS US Army Electronics R&D Command Night Vision & Electro-Optics Lab, DELNV-FIR Fort Belvoir, VA 22060	10. PROGRAM ELEMENT, PROJECT, TASK AREA & WORK UNIT NUMBERS 16 61102A 1T161102A31B/06/003 CJ	
11. CONTROLLING OFFICE NAME AND ADDRESS 17 06	12. REPORT DATE 11 September 1978	
13. MONITORING AGENCY NAME & ADDRESS (if different from Controlling Office) 12 124 PI	14. SECURITY CLASS. (of this report) Unclassified	
15a. DECLASSIFICATION/DOWNGRADING SCHEDULE		
16. DISTRIBUTION STATEMENT (of this Report) Approved for public release; distribution unlimited.		
17. DISTRIBUTION STATEMENT (of the abstract entered in Block 20, if different from Report)		
18. SUPPLEMENTARY NOTES		
19. KEY WORDS (Continue on reverse side if necessary and identify by block number) Mesomorphic compounds Cholesteric liquid crystals Temperature-sensitive, cholesteric liquid crystals Liquid crystals		
20. ABSTRACT (Continue on reverse side if necessary and identify by block number) This final report summarizes the physical behavior of over 200 cholesteric liquid crystals including transition temperatures, heats of transition, temperature sensitivity of visible selective reflection spectra, the effect of impurities, combining liquid crystals, and behavior in a thermal-imaging system. Eleven homologous series of alkanoates, <i>omega</i> -phenylalkanoates, alkyl carbonates, and S-alkyl thiocarbonates of cholesterol, cholest-5-en-3 β -thiol, and 5 α -cholestan-3 β -ol were investigated. Twenty liquid crystals were found to have a cholesteric color spectral range of 0.2°C or less. alpha beta gamma		

DD FORM 1 JAN 73 1473 EDITION OF 1 NOV 65 IS OBSOLETE

UNCLASSIFIED

SECURITY CLASSIFICATION OF THIS PAGE (When Data Entered)

79 06 25 003

PREFACE

The hundreds of cholesteric liquid crystals which are characterized in this report were synthesized and purified by Dr. W. Elser, Dr. J. L. W. Pohlmann, and P. R. Boyd.

Accession For	
NTIS GRA&I	<input checked="checked" type="checkbox"/>
DDC TAB	<input type="checkbox"/>
Unannounced	<input type="checkbox"/>
Justification	
By	
Distribution/	
Availability Codes	
Dist	Avail and/or special
A	

CONTENTS

Section	Title	Page
	PREFACE	iii
	ILLUSTRATIONS	vi
	TABLES	x
I	INTRODUCTION	
	A. Purpose of Program	1
	B. Approach to Project	1
II	BACKGROUND	
	A. The Cholesteric Mesophase and its Textures	2
	1. Mesophases and Molecular Arrangement	2
	2. Types of Mesophases	7
	3. Relation Between Mesophases and other Phases	8
	4. Textures of Cholesteric Mesophases	8
	a. Unexplored Textures	8
	b. Focal Conic Textures	9
	c. Planar Texture	10
	5. Helix-forming Tendency of Molecules	11
	B. Selective Reflection	14
	1. Experimental Considerations	14
	2. Typical Experimental Results	18
III	EXPERIMENTAL: CHARACTERIZATION OF LIQUID CRYSTALS	
	A. Hot-Stage Microscopy	25
	B. Differential Thermal Analysis	27
IV	RESULTS	
	A. Physical Properties of Liquid Crystals	28
	1. Homologous Series	28
	2. Transition Temperatures	30
	3. Multiple Melting Points	30

CONTENTS (Cont'd)

Section	Title	Page
	4. Heats of Transition	30
	5. Temperature of Color Bands	60
	6. Dependence of Selective Reflectance on Temperature and Wavelength	74
	7. Chain-Length Dependence of the Color Band	77
	8. Extremely Temperature-Sensitive Selective Reflectance	79
	9. Crystal Colors	83
	10. Mixtures and impurities	85
	11. Hysteretic Cholesteric Mixtures	94
	12. Effects of Electric Fields	96
	13. The Depolarization of Light Scattered from Liquid Crystals	96
	B. Thermal Imaging System	96
V	SUMMARY AND CONCLUSIONS	105
	BIBLIOGRAPHY	106

ILLUSTRATIONS

Figure	Title	Page
1	Geometry for Selective Reflection in Planar Texture	16
2	Reflection Spectrum of a Mixture of Cholesteryl Acetate, Chloride, and Nonanoate at 24° at Normal Incidence	19
3	Intensity of Selectively Reflected Light as a Function of Wavelength	20
4	Intensity of Light Selectively Reflected by the Planar Texture as a Function of Wavelength and Temperature	20
5	Wavelength of Maximum-Selective Reflection as a Function of Temperature	21
6	Normalized Intensity of Selectively Reflected Light as a Function of Temperature	22
7	Wavelength of Maximum Scattering as a Function of Viewing Angle	24
8	Typical Calibration Curve for Mettler FP-2 Microscope Hot Stage	26
9	Calibration Curve for Differential Scanning Calorimeter	29
10	Transition Temperatures of Alkanoates	31
11	Transition Temperatures of ω -phenylalkanoates	32
12	Transition Temperatures of Carbonates	33
13	Transition Temperatures of Carbonates	34
14	Enthalpy of Fusion of the Alkanoates of Cholesterol and Thiocholesterol	35
15	Entropy of Fusion of the Alkanoates of Cholesterol and Thiocholesterol	36

ILLUSTRATIONS (Cont'd)

Figure	Title	Page
16	Enthalpy Changes at Transitions in the Melt of the Alkanoates of Cholesterol and Thiocholesterol	37
17	Entropy Changes at Transitions in the Melt of the Alkanoates of Cholesterol and Thiocholesterol	38
18	Heats of Transition of the Thiocholesteryl Alkanoates	39
19	Enthalpies and Entropies of Fusion of Cholesteryl ω -phenylalkanoates	40
20	Enthalpies and Entropies of Smectic-cholesteric Transitions of Cholesteryl ω -phenylalkanoates	41
21	Enthalpies and Entropies of Cholesteric-isotropic Transitions of Cholesteryl ω -phenylalkanoates	42
22	Enthalpies and Entropies of Fusion for S-cholesteryl ω -phenylalkanethioates	43
23	Enthalpies and Entropies of Cholesteric-isotropic Transitions and Smectic-cholesteric Transitions for S-cholesteryl ω -phenylalkanethioates	44
24	Entropy of Fusion of Cholesteryl n-alkyl Carbonates	45
25	Entropies of Transitions in the Melt of Cholesteryl n-alkyl Carbonate	46
26	Heats of Fusion of Cholesteryl S-alkyl Thiocarbonates	47
27	Heats of Transition in the Melt of Cholesteryl S-alkyl Thiocarbonates	48
28	Entropy of Fusion of S-cholesteryl Alkyl Thiocarbonates	49

ILLUSTRATIONS (Cont'd)

Figure	Title	Page
29	Entropies of Transitions in the Melt of S-cholesteryl Alkyl Thiocarbonates	50
30	Smectic-cholesteric and Cholesteric-isotropic Transitions	51
31	Entropy of Fusion of 5 α -cholestan-3 β -yl ω -phenylalkanoates	52
32	Entropy of the Cholesteric-isotropic Phase Transitions	53
33	Transition Heats of Cholestanyl n-alkyl Carbonates	54
34	Enthalpies and Entropies of Cholesteric-isotropic Transitions and Smectic-cholesteric Transitions for 5 α -cholestan-3 β -yl S-alkyl Thiocarbonates	55
35	Enthalpies and Entropies of Fusion of 5 α -cholestan-3 β -yl S-alkyl Thiocarbonates	56
36	Typical Shape of a Melting Transition Curve (S-cholesteryl 8-phenyloctanoate)	57
37	Typical Solid-solid Transition Involving Some Melting and Recrystallization Just Prior to Melting (S-cholesteryl 6-phenylhexanoate)	58
38	Solid-solid Transition Occurring Just Prior to Melting (5 α -cholestan-3 β -yl Eicosyl Thiocarbonate)	59
39	Typical Cooling Curve Showing Isotropic-cholesteric Transition and Cholesteric-Smectic Transition (S-cholesteryl Tridecanethioate)	61
40	Typical Heating Curve Showing Unexplained Peak Between Smectic-cholesteric Transition and the Cholesteric-isotropic Transition (S-cholesteryl Heptadecanethioate)	62

ILLUSTRATIONS (Cont'd)

Figure	Title	Page
41	Cooling Curve Showing Unexplained Peak Between Isotropic-cholesteric Transition and Cholesteric-smectic Transition (S-cholesteryl Nonyl Thiocarbonate)	63
42	Heating Curve Showing Two Unexplained Peaks Between the Smectic-cholesteric Transition and the Cholesteric-isotropic Transition (S-cholesteryl Undecanethioate)	64
43	Heating Curve Showing Unexplained Peaks Just Prior to the Smectic-cholesteric Transition and the Cholesteric-isotropic Transition (S-cholesteryl Decyl Thiocarbonate)	65
44	Width of the Color Band of S-cholesteryl ω -phenylalkanethioates as a Function of Chain Length	78
45	Wavelength of Maximum Selective Reflection as a Function of Temperature	80
46	Wavelength of Maximum Selective Reflection as a Function of Temperature	82
47	Maximum Temperature Coefficients of Selective Reflection as a Function of Wavelength	84
48	Temperature Range (Red to Blue) of Selective Reflection of Ternary Mixtures	89
49	Effect of Mixing 10% Cholesteryl ω -phenylalkanoate with 90% Cholesteryl Nonanoate	93
50	Deterioration of Cholesteryl Nonanoate with Time at a Constant Temperature of 75.55°C	95
51	Conversion Principle	98
52	Laboratory Thermal Imaging Device	99

ILLUSTRATIONS (Cont'd)

Figure	Title	Page
53	Thermal Imaging Device	100
54	Cell Unit	101

TABLES

Table	Title	Page
1	Characteristic Textures Suitable for Phase Identification-Optical Features	5
2	Temperature Ranges ($^{\circ}\text{C}$) of Platelet and Regular Cholesteric Colors for 11 Homologous Series	66
3	Liquid Crystals with Cholesteric Color Bandwidths of 0.25° or Less	75
4	Parameters of Curve Fits $\lambda_p(\underline{T})$ to Figure 47	81

PHYSICS OF MESOMORPHIC COMPOUNDS

I. INTRODUCTION

A. Purpose of Program. The purpose of our liquid crystal (mesomorphic compound) program was to synthesize liquid crystals suitable for incorporating into a direct-view, thermal-imaging system for use as a night-vision device.

Many cholesteric liquid crystals possess the unique property of selectively reflecting light so that the compound is visually observed to traverse the entire color spectrum as it is heated or cooled over a temperature interval ranging from a small fraction of a degree to many degrees, depending on the compound. By using suitable optics, an infrared heat image can be focused onto a thin, heat-absorbing Mylar* membrane. A thin layer of a liquid crystal then undergoes color changes with changes of temperature due to changes of intensity in the infrared radiation. When the crystal is illuminated with monochromatic light, changes in temperature translate into changes in light intensity.

B. Approach to Project. The general approach to the project was to synthesize hundreds of previously unknown organic liquid crystals in order to find some which would be superior in performance to those which had already been studied in thermal-imaging systems.

Lack of a good theory linking molecular structure with liquid crystalline properties necessitated an empirical, but systematic, approach to organic synthesis, such as making different substitutions in the steroid moiety of cholesterol and then synthesizing the resulting homologous series — usually the first 20 members.

The effects of impurities on the properties of liquid crystals as well as the effects of mixing different liquid crystals were also studied.

The desirable liquid crystalline properties which were sought were:

- (1) A narrow cholesteric color spectrum, as a function of temperature change, exhibiting bright colors somewhere between 35° and 45°.**
- (2) A time constant less than 1 second, preferably 0.1 second or better.

*Mylar is the Dupont trademark for poly(ethylene terephthalate).

**Unless otherwise stated, all temperatures refer to degrees Celsius (°C).

(3) A reasonably stable compound with a freezing temperature low enough to avoid any solid crystals competing with the liquid mesomorphic state at operating temperatures.

In order to characterize the properties of the liquid crystals, hot-stage microscopy, typically in conjunction with polarized light, was used to determine transition temperatures such as melting, freezing, smectic-cholesteric transition, cholesteric-isotropic liquid transition (clearing point), and the temperature of the cholesteric color band, when these features exist.

Differential scanning calorimetry was used to determine the heats of transition and entropies associated with melting, clearing, and changes of mesophase, as well as to confirm transition temperatures as determined by microscopic observation.

II. BACKGROUND¹

The generally bright color play produced by "selective reflection," or "dispersive reflection," is one of the most significant characteristics of cholesteric mesophases. The observation of this unusual interference effect of visible light in a liquid may have been primarily responsible for the discovery of the mesomorphic state and for the coining of the more descriptive term "liquid crystal" by Lehmann.² This distinct phenomenon together with associated optical effects reveal the basis of molecular arrangement in cholesteric mesophases.

The absence of the color band does not necessarily preclude the existence of a cholesteric mesophase. For example, the selective reflection may not be observed because it occurs in the infrared or because the sample may not be in the state of alignment which exhibits selective reflection when bright field illumination is used. Therefore, features other than selective reflection have to be considered to identify properly cholesteric mesophases in new materials and to induce that manifestation or texture of this phase which exhibits selective reflection.

A. The Cholesteric Mesophase and its Textures

1. **Mesophases and Molecular Arrangement.** Mesomorphic states (mesophases) are characterized according to the structure of molecular arrangement. Definite phase transitions are observed whenever a substance changes to the mesomorphic state or from one mesophase to the other. This allows the detection of mesophases by differential scanning calorimetry.³ But the determination of the structure of a

¹ W. Elser and R. D. Ennulat in "Advances in Liquid Crystals," G. E. Brown, Ed, Academic Press, New York, Vol 2, 1976., Ch 2.

² O. Lehmann, *Z. Phys Chem (Leipzig)* 4, 462 (1889).

³ R. D. Ennulat, *Mol Cryst Liq Cryst* 6, 329 (1970).

mesophase is a more difficult matter. For example, x-ray diffraction patterns are hard to interpret because these structures have a much lower symmetry than three-dimensional translation lattices. Furthermore, the samples cannot always be maintained in sufficiently uniform alignment along a preferred direction because of the liquid nature of the substance and the complex interaction between the substance and its boundaries. The most practical approach to phase identification is the microscopic analysis of those optical properties which are unambiguously related to the structure of the molecular arrangement. These characteristic optical properties are usually observed only in certain textures. In 1907 Vorländer observed that the homeotropic texture of mesophases exhibits an optical behavior akin to uniaxial, solid crystals.⁴ When observed through the Bertrand lens of a microscope in divergent light between crossed polarizers, such textures exhibit an interference cross. It is possible to determine the optical sign of the texture from this cross with the aid of subparallel waveplates even for low birefringence.⁵

When a subparallel waveplate is not used, the cross has very dark, colorless arms and very light, colorless quadrants, in which case the optical sign cannot be identified on the basis of color. However, if interference colors are induced by a subparallel waveplate (such as type Rot I, E. Leitz, Inc., NY) which is placed between the sample and the analyzer of the microscope, identification of the optical sign of the homeotropic texture can be made. When the slow direction lies in the first and third quadrants of the cross and forms an angle of approximately 45° with the horizontal leg of the cross, these quadrants have a blue color and the other quadrants have an orange color, as in the case of a smectic mesophase (positive optical sign). When the colors are reversed, a cholesteric mesophase is indicated (negative optical sign).

In principle, this information could also be obtained from homogeneous and birefringent textures* if all the textures of a given mesophase would have the same uniaxial indicatrix. But even if the latter is established as a fact, it will be difficult to determine the optical sign. Since the orientation of birefringent regions within the sample usually cannot be specified, the direction of the ordinary beam is not known and, thus, the optical sign cannot be obtained. The birefringent feature of such textures can be described by relating the direction of the slow and fast vibrations of polarized light with a reference direction of the texture that can be uniquely defined. Examples for such reference directions are the length extension of a focal conic band (often called an oily streak) or a direction perpendicular to it — the radial or tangential direction of a spherulitic arrangement of birefringent elements, the direction of the rib of the fan-shaped texture, and so on. Once the reference direction is defined, a

⁴ D. Vorländer, *Z. Phys Chem (Leipzig)* 61, 166 (1907).

⁵ F. Laves and T. Ernst, *Naturwissenschaften* 31, 68 (1943).

* The distinction between homogeneous and birefringent textures appears to be necessary, because they can be quite different manifestations of a given mesophase even in spite of the same molecular building principle. (E.g., the homogeneous and the focal conic texture of the smectic mesophase).

unique association can be made between it and the slow and fast vibrational directions of polarized light. The same approach proved to be useful in the field of optical crystallography, when the orientation of the ordinary beam of a crystal fragment cannot be determined. The direction of the slow or fast vibrational component in the crystal section is then determined with respect to a recognizable symmetry axis of the crystal habit. For example, the length extension of a crystal with a prismatic habit could provide such a reference direction. The term "sign of elongation" is used as a shorthand description for the birefringence of crystal sections.⁶ This quantity is positive when the slow, vibrational direction is parallel to this elongation or, more generally, to the chosen reference direction, and negative in the opposite case. It is suggested to include in the definition of the "sign of elongation" also the birefringent mesomorphic textures which have definable and reproducible reference directions. The use of such a quantity not only eliminates unnecessary confusion about the concept of the optical sign of a texture but also provides quantitative criteria for the empirical phase-identification scheme (Table I). The sign of elongation can easily be determined. The insertion of a subparallel gypsum waveplate (first-order red) at 45° against the crossed polarizers changes the color toward orange for focal conic bands approximately aligned along the fast direction of the waveplate and toward blue for bands perpendicular to it. This indicates that the slow vibration of polarized light in the focal conic band lies along its length extension and that the sign of elongation is positive with respect to this direction. According to all previous experience, this result is characteristic for the cholesteric mesophase.

Friedel derived the optical sign for most of the textures from partly assumed and partly known features of the mesomorphic building principle.⁷ Therefore, he does not distinguish between the optical sign of textures, for which the optical axis can be experimentally recognized, and the sign of elongation of textures, which do not have a discernible optical axis. Friedel's contribution significantly advanced the understanding of the mesomorphic state and led to fruitful hypothetical concepts about its molecular building principle. However, additional evidence is required to definitely establish the position of the optical axis for nonhomeotropic textures. Until this is achieved, it appears to be necessary to distinguish between optical sign and sign of elongation. The optical sign or sign of elongation has only an empirical significance for phase identifications, because of the lack of information about the molecular arrangement within a texture and the easy direction of polarization of the respective molecules. For example, the rule that a cholesteric mesophase should always exhibit a negative optical sign could be a dangerous generalization. With only very few exceptions, all known compounds exhibiting this mesophase are sterol derivatives, and thus, all have the sterane skeleton. Furthermore, the homeotropic behavior of this

⁶ N. H. Hartshorne and A. Stuart, "Crystals and the Polarizing Microscope," E. Arnold, London (1960), p. 293; See also E. E. Wahlstrom, "Optical Crystallography," J. Wiley & Sons, New York, NY 1951, p. 141.

⁷ G. Friedel, *Ann Phys (Paris)* 18, 273 (1922).

Table 1. Characteristic Textures Suitable for Phase Identification (Optical Features)

Type of Texture	Nematic	Smectic	Cholesteric	Reference Direction
Birefringent	Homogeneous	Homogeneous	—	—
	Homeotropic O.S.+	Homeotropic O.S.+	See Plane Texture	O.S. optical sign; Optical Axis normal to sample plane
	—	Focal Conic (f.c.)	Focal Conic (f.c.)	S.E. sign of elongation; Reference Directions:
		1. f.c. domain SE+	1. f.c. domain SE-	Long Axis of Ellipse
		2. f.c. bands SE-	2. f.c. bands SE+	Length Extension of Band
		3. fan-shaped SE+	3. fan-shaped SE-	Rib of Fan-Shaped Texture
	—	Batonnets	Batonnets	—
Nematic Droplets	—	—	—	—
Centered Texture	—	—	—	—
Optical Active	—	—	Plane Texture O.S.- Color Band	Optical Axis normal to sample surface
Optical Discontinuities	Threads	—	Threads	—

Sequence of *different* mesophases for rising temperatures:
 Either Solid-Smectic-Nematic-Isotropic Liquid
 or Solid-Smectic-Cholesteric-Isotropic Liquid.
 (For falling temperatures, read sequence from right to left.)

phase cannot be directly related to its birefringent textures, since this behavior is exhibited by the plane texture. In confocal observation, the uniaxial-like interference cross of the plane texture can be seen from temperatures below the coherently scattered light region (i.e., Bragg-like diffracted light or the color band) up to the clearing point. In the color band, the cross is observed when the narrow wavelength region of the diffracted light is filtered out. In this context, often a dull violet-appearing texture is perceived above the color band. This is speculated to be a "homeotropic condition" caused by rapid coalescing of many small and undistinguishable particles.⁸ These particles may be very small plane texture regions of various orientations. A mechanical disturbance such as the slip of the cover glass not only reduces the incoherent scattering but also appears to align these regions and, thus, induces the interference cross in confocal observation. The experimental procedure for identification of mesophases is not perfect. It is still possible to overlook or mis-identify a mesophase. However, such errors can be made less likely by a combination of different methods: temperature-scanning thermal analysis to recognize even small changes of thermodynamic quantities at phase transitions, and careful microscopic investigation to identify the particular phases between the various transitions. There is no reason to doubt that further refinement of thermal analysis as well as an improvement of the optical investigation will permit the recognition of all enantiotropic phases. But monotropic phases may still be overlooked because of the shortness of the observation time due to interfering crystallization.⁹

The identification of mesophases is certain only to the extent that the classification of the mesomorphic state is defined. Because of shortcomings of the present theories of the structure of thermotropic mesophases, it is not possible to derive complete sets of characteristic textures for the various mesophases. As in the past, one has to rely on a purely empirical classification (Table 1). Thus, new findings can modify and refine empirical rules for phase identification. To support this development and to ensure unprejudiced experimental procedures, any phase-identification scheme should be based on a minimum number of carefully chosen hypotheses. The proposed classification of mesomorphic phases is based on a molecular arrangement which excludes a three-dimensional lattice order.¹⁰ This is one of the reasons why this scheme does not generally apply to lyotropic phases. But it is valid for all thermotropic mesophases unless such a phase with a three-dimensional lattice order is discovered.

⁸ G. W. Gray, "Molecular Structure and the Properties of Liquid Crystals," Academic Press, London & New York, 1962, p. 41; G. Friedel, *Ann Phys (Paris)* 18, 273, 387 (1922).

⁹ J. L. W. Pohlmann, *Mol Cryst Liq Cryst* 2, 1 (1966).

¹⁰ G. Friedel, *Ann Phys (Paris)* 18, 73 (1922).

In the literature, the concepts of mesomorphic and liquid crystal states are not always clearly defined partly because Friedel's original definition is disregarded. An attempt to find a general and more useful structural classification of these phases was made by C. Hermann who introduced statistical concepts of order to bridge the gap between the strictly ordered crystalline and the random, gaseous state.¹¹ In this connection, the extension of crystalline to paracrystalline lattice order which was proposed by Hosemann would be mentioned.¹² As valuable as these concepts may be for the special case, they are not sufficient to cover the more general ordering principles which are realized in nature. A notable example for this may be the plane texture of the cholesteric phase. Although its structure is not known, certain of its dominant features are evident. These are the repeat distances of an unknown structural property of the magnitude of thousands of angstroms required to explain the Bragg-like diffraction of light and a special molecular arrangement with electrical features to account for the unusually high optical activity. Proposed structural models meeting both conditions are insufficiently described by either one of the two ordering concepts.

2. Types of Mesophases. So far, only two classes of thermotropic mesophases can be definitely distinguished by characteristic textures: (1) the smectic (slippery or soap-like) mesophases in which the long molecules are arranged side-to-side in a parallel manner in layers so that the molecules are perpendicular to the plane of each layer, and (2) the nematic mesophases in which the molecules are in a strong end-to-end (string-like) configuration.¹³ The former is observed in three or possibly seven distinct variations, while the latter is either a conventional nematic phase (called a nematic mesophase) or a twisted nematic phase (called a cholesteric mesophase) in which the nematic structure is twisted with a handedness characteristic of the particular compound. This twist commonly occurs if the molecules are chiral (i.e., helical molecules and molecules having asymmetry centers). In mixtures, at least one component has to be chiral; and it can even be the component which does not by itself form a nematic mesophase. The complexity of the molecular interaction responsible for the creation of the twisted structure is implied by the fact that the handedness of the molecular, optical activity or helix alone does not determine the handedness of the helical structure.

Nematic compounds exhibited some very interesting effects under the microscope. For example, when near the clearing point while using dark field illumination, 3 β -acetoxy-26-norcholest-5-en-25-one showed focal conic type structures into which grooves or ridges were seen forming (like a needle scratching a groove into a soft surface) until the whole field was etched, resulting in a very unusual three-dimensional effect somewhat resembling the Grand Canyon. Colors, apparently due to diffraction, could be seen with the naked eye.

¹¹ C. Hermann, *Z. Kristallogr.* 79, 186 (1931); c.f., A. Mabis, *Acta Crystallogr.* 15, 1152 (1962).

¹² R. Hosemann and S. N. Bagchi, "Direct Analysis of Diffraction by Matter," Interscience Publ, New York, NY (1962).

¹³ P. G. de Gennes, "The Physics of Liquid Crystals," Clarendon Press, Oxford, 1974.

When subjected to a temperature gradient by opening the lid of the Mettler FP-2 hot stage, 4-n-butoxybenzylidene-4'-aminopropiophenone displayed, just outside the cover glass, a continuous vigorous rolling motion resembling churning, boiling, agitation, and even solar storms. All appeared to be quiet above the clearing point.

Some other nematic compounds exhibited what might be called the "scratchy movie" effect. Under the microscope, things looked similar to how a gray portion of a black and white motion picture might appear when viewed very close to a large screen, i.e., numerous specks jumping around continuously and everywhere.

3. Relation Between Mesophases and Other Phases. A transition between cholesteric and nematic mesophases has not yet been accomplished by simply changing the temperature of a pure compound. But external electric fields are capable of causing such transitions. The cholesteric helices can also be untwisted with an organic solvent such as dioxane. Furthermore, mixtures of laevo- and dextro-cholesteric phases exhibit nematic behavior at the temperature at which the mixture is racemic. However, above and below this temperature the mixture exhibits cholesteric behavior of opposite handedness. These observations indicate that the transition between cholesteric and nematic mesophases may be induced only by agencies of the proper asymmetry and not by an isotropic change in temperature.

The temperature interval of the cholesteric mesophase has an upper limit defined by a transition to the isotropic liquid and a lower limit defined by a transition to either the solid state of the smectic mesophase. The twist of the helix decreases rapidly as the temperature approaches the point of transition to the smectic state. Apparently the structure untwists before it undergoes this phase transition. It is in this pretransitional region where the cholesteric mesophase exhibits selective reflection of extremely high temperature dependence.

4. Textures of Cholesteric Mesophases. Thin films of cholesteric mesophases exhibit unexplored textures, focal conic textures, and the planar texture.

a. Unexplored Textures. These cannot be properly defined because their features are ambiguous. Most is known about the texture described by Gray as a "homeotropic condition,"¹⁴ and by others as the "blue phase."¹⁵ Apparently the term, homeotropic condition, relates to the structureless, grayish appearance under the microscope; while the term, blue phase, relates to the dull-violet appearance of the same texture observed under certain conditions. For example, the cover

¹⁴ D. Coates & G. W. Gray, *Phys Lett* 45 A, 115 (1973).

¹⁵ For example: (a) H. Kelker & R. Hatz, *Chem-Ing Techn.* 45, 1005 (1973); (b) P. M. Hareng, *Rev Techn. Thomson-CSF* 5, 319 (1973); (c) J. L. Ferguson, T. R. Taylor, & T. B. Harsch, *Electron-Technology* (NY), 85, 41 (1970); (d) B. Hampel, *Z. Werkstofftechn* 3, 149 (1972).

slip on top of a thin cholesteric film apparently collects the obliquely scattered radiation and guides it to the rim where it exists as a bluish circle. We observed that the appearance and disappearance of this bluish ring coincides with the clearing point. For many compounds, this effect is the best optical indicator of this transition to the isotropic mesophase. Below the clearing point, the focal conic texture may either grow directly into the blue phase or may be formed by coalescing birefringent batonets.^{16 17}

Furthermore, displacing the cover slide can convert this blue texture directly into the planar texture. The results of scattering experiments conducted on the blue textures of cholesteryl tetradecanoate indicate scattering centers ranging in size from 500 to 800 Å.¹⁸ However, more evidence is needed to determine whether this blue texture represents an unstable, pretransitional region just below the clearing point or whether it is a stable texture with a definable static structure. Most other effects occurring in the temperature region of the blue texture are very inconsistent. For example, we observed a second color band (which we call platelet colors) of reflected light just below the clearing point which, depending on the compound, changes colors sluggishly with temperature and some not at all.¹⁹ In certain compounds, the color regions look like ink blotches; in others, those regions are uniform and shaped like angular platelets. These domains are usually very sensitive to mechanical disturbances but comparatively insensitive to temperature changes. The color is easily destroyed by temporary mechanical pressure but usually reappears in a somewhat different pattern after a few seconds. In some cases the platelets do not reappear after being disturbed unless the temperature is significantly changed by clearing and cooling. In other cases, platelets change to regular cholesteric colors on being disturbed, but the respective colors are not generally the same at the same temperature. When a platelet is cooled, it might, for example, change from a green platelet color into a regular blue color, opposite to what one would expect when cooling a regular cholesteric color where the color will change to longer wavelengths on cooling. At the clearing point, platelet colors generally do not fade out but suddenly disappear. This property, along with the increased fluidity and fast time response of liquid crystals at higher temperature, could possibly lead to some kind of application in a thermal-imaging system. Platelets are among the least understood of all cholesteric liquid crystal phenomena.

b. Focal Conic Textures. These are well-established structures which are distinguished by their birefringence.^{20 21 22} Although the smectic and

¹⁶ G. Friedel, *Ann Phys (Paris)* 18, 273 (1922).

¹⁷ G. W. Gray, "Molecular Structure and the Properties of Liquid Crystals," Academic Press, London, NY (1962).

¹⁸ D. Coates and G. W. Gray, *Phys Lett* 45A, 115 (1973).

¹⁹ W. Elser, J. L. W. Pohlmann, and P. R. Boyd, *Mol Cryst Liq Cryst* 20, 77 (1973).

²⁰ G. Friedel, *Ann Phys (Paris)* 18, 273 (1922).

²¹ G. W. Gray, "Molecular Structure and the Properties of Liquid Crystals," Academic Press, London, NY (1962).

²² P. G. de Gennes, "The Physics of Liquid Crystals," Clarendon Press, Oxford (1974).

cholesteric focal conics incorporate the different molecular arrangements characteristic of the irrispective mesophases, the appearance of both types of textures has much in common. They can be distinguished under the polarization microscope only because of the difference of the position of the optical axis which is directly associated with the molecular arrangement.^{23 24} The application of a shear stress or of certain electrical fields can convert the focal conic texture into the planar texture whenever surface properties or other obstacles do not prevent this orientation.²⁵

The focal conic texture is essentially a planar texture whose helical axis is predominantly parallel to the surface. In most cases, cholesteric focal conics are black and white and small while the smectic focal conics show birefringent colors and are much larger. Since cholesteric focal conics generally exhibit a dark cross, they are often called banded focal conics.

When dark field illumination is used, the material does not have to be mechanically squeezed to show cholesteric colors under the microscope. Under these conditions the focal conics, which otherwise are bright and wash out the cholesteric colors, are not visible. (Smectic focal conics are also invisible under dark field illumination, but the discontinuities between them can be seen.)

When the sample is squeezed under bright field lighting, the typical white streaks appear; but, under dark field illumination, the streaks show cholesteric colors. When the temperature is raised, these colored streaks rotate like spokes in a wheel. When cooling, the streaks rotate in the opposite direction.

c. **Planar Texture.** This exhibits the building principle of cholesteric mesophases in the purest form. It consists of molecules aligned parallel to each other and generally to the substrate plane. Because of the chirality of the molecules, the direction of the preferred molecular alignment rotates about the surface normal as one progresses from the bottom to the top of the sample layer. Thus, the preferred direction of the molecules outlines a helix of a handedness which is characteristic for a given compound. This helical structure does not have physically defined layers.

The optical properties of the planar texture can be summarized as follows:

²³ G. Friedel, *Ann Phys (Paris)* 18, 273 (1922).

²⁴ R. D. Ennulat, *Mol Cryst Liq Cryst* 3, 405 (1968).

²⁵ P. G. de Gennes, "The Physics of Liquid Crystals," Clarendon Press, Oxford (1974).

- (1) It exhibits selective reflection of light.
- (2) Its optical activity is orders of magnitude larger than that of the constituent molecules.
- (3) The optical activity for wavelengths above and below the selective-reflection band has opposite signs.
- (4) *Laevo* structures reflect left-handed, circularly polarized light without reversal of handedness and transmit only right-handed, circularly polarized light. *Dextro* structures exhibit the reverse effect.

Theoretical and experimental studies have proved that these unusual optical effects have one common cause: the helical structure of the planar texture.

Although certain unexplored textures may still exist, the most stable and prevailing textures of the cholesteric mesophase have the same helical structure. It is therefore possible to clearly identify cholesteric mesophases even if selective reflection is not apparent.

5. Helix-Forming Tendency of Molecules. Although mesomorphic compounds differ widely in chemical constitution, they have certain features in common: the molecules have to be elongated or rod-shaped to be suitable for structures of predominantly orientational order; the molecules have to interact weakly enough to avoid crystallization and yet strongly enough to establish the order characteristic of the mesomorphic state. Both the lack of knowledge about the details of the molecular arrangement and the complexity of the interaction forces made it impossible to derive the mesomorphic behavior of a compound from first principles.

For smectic and nematic mesophases, Gray succeeded in correlating changes of molecular features, introduced by systematic, chemical substitutions, with variations of the mesomorphic properties.²⁶ He found that the amount of lateral attraction relative to that of the terminal attraction between neighboring molecules is significant. If the former predominates, the molecules prefer layer structures and thus the smectic mesophase. If the latter predominates, the molecules most likely form nematic phases. However, a certain amount of lateral attraction is still required to enforce short-range molecular parallelism in an environment of disordering thermal agitation. For specific classes of compounds, Gray was able to increase or decrease transition temperatures in the melt by the proper choice of substituents.

²⁶ G. W. Gray, "Molecular Structure and the Properties of Liquid Crystals," Academic Press, London, NY (1962).

Cholesteric mesophases are generally influenced by molecular modifications affecting nematic mesophases. But it is not possible to achieve useful correlations between molecular properties and cholesteric behavior without also considering changes of the helix-forming tendency of the molecules. Two empirical methods have been developed to assess this important feature: the helical twisting power,²⁷ and the effective rotary power of molecules.²⁸

The helical twisting power (HTP) of a solute²⁹ is derived from the temperature shift ΔT of the nematic temperature T_n of a compensated mixture of cholesteric liquid crystals (that is, a mixture of left- and right-handed cholesteric liquid crystals which is racemic at T_n caused by adding a solute of concentration c).

The extrapolation $\frac{1}{Z} \equiv \frac{m \Delta T_n(c)}{c} \bigg|_{c=1}$ defines the HTP of the solute (m is a constant characteristic of the solvent system). This limit process is meaningful if the relation between ΔT_n and c is linear. Under this condition, HTP is equal to the inverse of the pitch Z of the pure solute at the temperature $T_n + \Delta T_n$.

The effective rotary power^{29a} is derived from the pitch p of the mixture

$$\frac{1}{p} \equiv \sum \alpha_i \theta_i$$

where α_i and θ_i are weight percentage and effective rotary power of component i . Depending on the intent of the investigation, one usually selects a left- or a right-handed cholesteric reference material (a compound or a mixture³⁰) of desirable pitch and temperature and measures the change of the pitch caused by the addition of the test material as a function of concentration. If crystallization limits the range of concentration or if the additive is not cholesteric itself, an effective rotary power is defined by linear extrapolation of the inverse pitch to the 100% point of the additive. In the case of linear concentration dependence, both the helical twisting power and the effective rotary power are approximately equal for cholesteric compounds.³¹

The linear superposition principle of the effective rotary power expressed in the last equation is approximately valid for mixtures of similar cholesteric constituents which do not change their molecular features due to mutual interaction.

²⁷ H. Baessler and M. M. Labes, *J. Chem Phys* 52, 631 (1970).

²⁸ J. E. Adams, W. Hass, and J. J. Wysocki in "Liquid Crystals and Ordered Fluids," R. S. Porter and J. F. Johnson, Eds, Plenum Press, New York, 1970 p. 463.

²⁹ H. Baessler and M. M. Labes, *J. Chem Phys* 52, 631 (1970).

^{29a} *Ibid.*

³⁰ J. E. Adams and L. B. Leder, *Chem Phys Lett* 6, 90 (1970).

³¹ K. Ko, I. Teuscher, and M. M. Labes, *Mol Cryst Liq Cryst* 22, 202 (1973).

Using Goossens' theory,³² it can be shown that the dissimilarity of the constituents alone is sufficient to account for the nonlinear concentration dependence of the effective rotary power and its relative minimum.^{33 34} But the cholesteric matrix can also modify the helical twisting power of a solute. For example, it was observed that cholesteryl iodide³⁵ and cholesteryl 2-(2-butoxyethoxy) ethyl carbonate³⁶ can adopt the handedness of the cholesteric solvent helix. Since these compounds have a very small effective rotary power, the induction effects must be rather small.

Addition of nematogenic compounds to a cholesteric material generally increases the pitch at a given temperature with concentration.³⁷ For small concentrations of the additive, the twisting ability of the cholesteric constituent does not appear to be influenced by induction effects.³⁸

The helical twisting power of certain solute molecules depends on the molecular configuration. For example, the branched-chain cholesteryl 2-methylpentanoate (monotropic smectic) exhibits in a compensated cholesteric material different helical twisting powers for the *l*- and *d*-enantiomers.³⁹ A similar effect was observed on azobenzene dissolved in a cholesteric matrix. Photo-induced *cis-trans* and *trans-cis* isomerization resulted in a corresponding variation of the pitch.^{40 41} This effect can be used to modulate the color of selectively reflected light.

Several investigators found that the cholesteric matrix can impose a helical arrangement of achiral solute molecules.^{42 43 44 45} As a consequence, induced circular dichroism occurs in achiral compounds. However, no correlation was found between this circular dichroism and the solute and the pitch of the solvent.⁴⁶

³² W. Elser and R. D. Ennulat in "Advances in Liquid Crystals," G. E. Brown, Ed., Academic Press, New York, Vol 2, 1976, Chap 2.

³³ H. Stegemeyer and H. Finkelmann, *Chem Phys Lett* 23, 227 (1973); *Ber Bunsenges Phys Chem* 78, 860 (1974).

³⁴ J. E. Adams and W. Haas, *Mol Cryst Liq Cryst* 15, 27 (1971).

³⁵ F. D. Saeva, *J. Am Chem Soc* 94, 5135 (1972).

³⁶ L. B. Leder, *Chem Phys Lett*, 6, 285 (1970).

³⁷ J. E. Adams and W. Haas, *Mol Cryst Liq Cryst* 15, 27 (1971).

³⁸ R. Cano, *Bull Soc Franc Mineral* 90, 333 (1967).

³⁹ H. Hakemi and M. M. Labes, *J. Chem Phys* 58, 1318 (1973).

⁴⁰ E. Sackmann, *J. Am Chem Soc* 93, 7088 (1971).

⁴¹ J. Voss and E. Sackmann, *Z. Naturforsch* 28 A, 1496 (1973).

⁴² F. D. Saeva and J. J. Wysocki, *J. Am Chem Soc* 93, 5928 (1971).

⁴³ E. Sackmann and J. Voss, *Chem Phys Lett* 14, 528 (1972).

⁴⁴ F. D. Saeva, *J. Am Chem Soc* 94, 5135 (1972).

⁴⁵ K. J. Mainusch and H. Stegemeyer, *Z. Phys Chem (Frankfurt)* 77, 210 (1972).

⁴⁶ E. Sackmann and J. Voss, *Chem Phys Lett* 14, 528 (1972).

Friedel found that the addition of nonmesomorphic compounds with asymmetric carbon atoms to a nematic compound can result in a cholesteric mixture.⁴⁷ Recent investigations show that the same effect can be achieved by dissolving chiralic compounds which do not have asymmetric carbon atoms.⁴⁸ The handedness of the resulting cholesteric mesophase is determined by the chirality of the solute.

These examples demonstrate the usefulness of the empirical measures describing the molecular ability to form helical superstructures. But these results may also have significant theoretical implications because, according to Goossens' theory, the twist between the directors of adjacent molecular layers is proportional to the ratio of the asymmetric (or chiral) and the anisotropic contributions to the molecular interaction.

B. Selective Reflection

The intensity of selectively reflected, monochromatic light depends on the angles formed by the incident and observed light beams with the helical axis, on pressure and temperature, on purity and composition, and on alignment of the sample.

1. **Experimental Considerations.** The extrinsic variables are restricted primarily by experimental considerations. For example, the convergence of the incident light, the area of illumination, and the acceptance angle of the observed light have to be made small enough to ease the interpretation of the experimental results (e.g., angular resolution) and yet large enough to measure the light intensity at an acceptable signal-to-noise ratio. The experiments indicate that a useful compromise can be achieved. As expected from thermodynamic considerations,⁴⁹ high pressure increases the temperature of the transition from the cholesteric to the smectic phase and thus the temperature of the selective reflection. The latter was observed on mixtures of cholesteric compounds.⁵⁰ For materials exhibiting a strong temperature dependence of selective reflection, special precautions are necessary to achieve a sufficiently fine control of temperature and temperature uniformity.

More serious are the effects of the intrinsic parameters such as chemical stability, impurity content of the sample, and the alignment of the planar texture. We observed that an unidentified impurity,⁵¹ apparently formed by oxidation during the test, shifted the color band of cholesteryl nonanoate at a rate of about 0.1° per

⁴⁷ G. Friedel, *Ann Phys (Paris)* 18, 273 (1922).

⁴⁸ H. Stegemeyer and K. J. Mainusch, *Naturwissenschaften* 58, 599 (1971).

⁴⁹ P. H. Keyes, H. T. Weston, and W. B. Daniels, *Phys Rev Lett*, 31, 628 (1973).

⁵⁰ P. Pollmann and H. Stegemeyer, *Ber Bunsenges, Phys Chem* 78, 843 (1974).

⁵¹ R. D. Ennulat, *Mol Cryst Liq Cryst* 13, 337 (1971).

day to lower temperatures.⁵² Furthermore, the intensity peak obtained for a given wavelength occurred at slightly different temperatures for heating and cooling. Removal of the impurity eliminated this hysteresis effect and moved the color band back to its original temperature range. We believe that the impurity depressed the phase transition, thus shifting the pretransitional color band and increasing the tendency toward undercooling. It should be considered that dilute gases in contact with the sample may shift the color band significantly in a reversible or irreversible manner or even suppress the color band permanently.⁵³ Furthermore, the composition of mixtures exhibiting cholesteric mesophases has a significant influence on the temperature and temperature interval of the visible selective reflection.

The sample should consist of a uniformly aligned planar texture characterized by one helical axis normal to the surface. In addition, the sample should be thick enough to exhibit a selective reflectivity close to unity. In spite of careful sample preparation, one usually obtains a mosaic of uniform planar texture domains ranging in lateral dimensions from 10 μ m to 50 μ m. In poorly aligned samples, the individual domains exhibit different colors because of the angular dependence of the selective reflection.⁵⁴ However, even extremely temperature-sensitive samples can be aligned to such a degree that for normal illumination all individual domains selectively reflect monochromatic light within a narrow cone normal to the surface.⁵⁵ Under this condition we can estimate the range of the angular deviation between the helical axes and the common surface normal. Considering that single domain selectively reflect at specular angles,⁵⁶ we obtain from Figure 1 the relation

$$\epsilon = \frac{1}{2} \left\{ \sin^{-1} \left(\frac{\sin \phi_s}{\underline{n}} \right) - \sin^{-1} \left(\frac{\sin \phi_i}{\underline{n}} \right) \right\} \quad (1)$$

where ϕ_i and ϕ_s are the angles of incidence and observation and \underline{n} is the average index of refraction of the liquid crystal. The largest deviation ϵ occurs if the light ray incident at the largest possible angle is parallel to the helical axis of the domain; that is, if

$$\phi_{s_{\max}} = -\phi_{i_{\max}}.$$

Using the data reported in our work (i.e., $\phi_{i_{\max}} = 7^\circ$, $n \approx 1.5$),⁵⁷ we conclude that the helical axes of the domains in our sample were aligned at least to within 4.7° of the

⁵² F. J. Kahn, *Appl Phys Lett* 18, 231 (1971).

⁵³ J. L. Fergason, *US Nat Tech Inform Serv Rep No. AD 741898* (1971); see also: W. H. Toliver, J. L. Fergason, E. Sharpless, and P. E. Hoffman, *Aerosp Med* 41, 18 (1970), and references cited therein.

⁵⁴ C. J. Gerritsma and P. Van Zanten, *Phys Lett* 42A, 329 (1972).

⁵⁵ R. D. Ennulat, *Mol Cryst Liq Cryst* 13, 337 (1971).

⁵⁶ R. Dreher, *Dissertation*, Freiburg, 1971.

⁵⁷ R. D. Ennulat, *Mol Cryst Liq Cryst* 13, 337 (1971).

DISPERSIVE REFLECTION

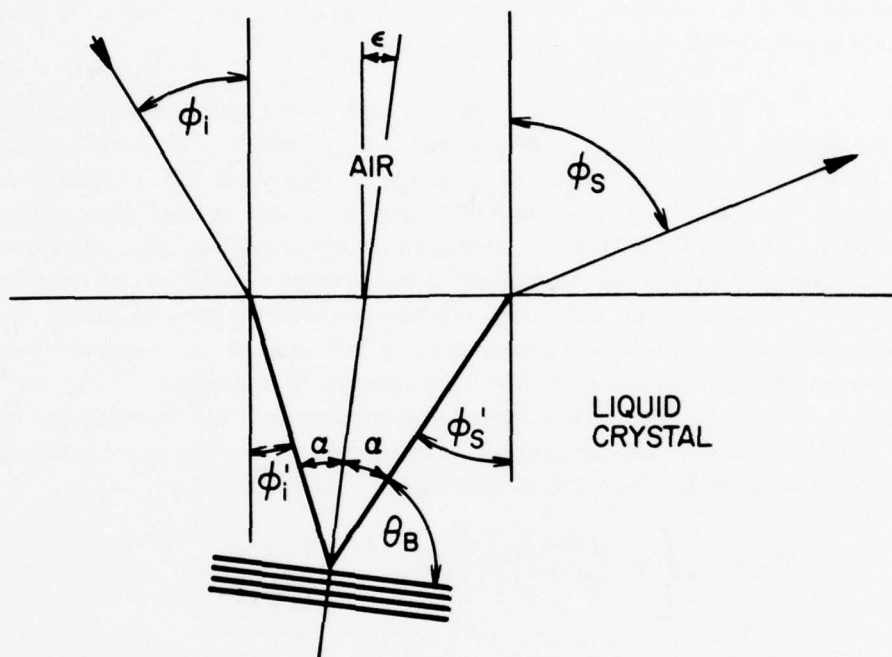


Figure 1. Geometry for selective reflection in planar texture. Stack of parallel lines indicates planes of Bragg scattering sites. [Modified from J. E. Adams, W. Haas, and J. Wysocki, *J. Chem. Phys.* 50, 2458 (1969) Permission to use this figure has been granted by the authors.]

surface normal. Adams, Haas, and Wysocki conclude from their measurement of the angular dependence of the selectively reflected light intensity that the helical axes are close to the normal of the surface.⁵⁸ As we will see, this small misalignment already washes out those features of the spectral selective reflectance which are characteristic of single domains.

A few investigators succeeded in preparing large, single-domain samples suitable for the experimental test of the theory of selective reflection. They avoided many problems by using materials exhibiting an extremely low temperature dependence of the pitch. Berreman and Scheffer prepared their samples by mixing a nematic and an optically active material,⁵⁹ while Dreher, Meier, and Saupe used room-temperature mixtures of cholesteryl derivatives.⁶⁰ The latter group of investigators sandwiched a 21 μ m-thick liquid crystal between two parallel glass plates. Since parallelism of the surface contacting the liquid crystals resulted in the best alignment, they used thick plates to avoid warping and polished the glass surfaces to a flatness of a quarter wavelength over an area of several square centimeters. Apparently, uniform sample thickness diminished the occurrence of pitch distortions observed in Cano wedges.⁶¹ The best samples were obtained by cleaning the surfaces with an organic solvent (and not with chromic acid) and by rubbing them in one direction. As pointed out by Chatelain for nematic phases,⁶² this procedure may produce a thin film of fatty acid impurities in which the molecules are parallel to the substrate in the direction of the rubbing. It is interesting to note that the aligning action of this dirt film was affected neither by moderate heating nor by slight wiping with a cloth wetted by a solvent. The liquid crystal was heated above the clearing point, applied to one of the glass substrates, and subsequently covered by the other one. (It was found that insertion of the liquid crystal by capillary action into the gap between the glass plates did not render good samples.) The residual focal conic texture was eliminated by mechanical shearing of the liquid crystal. This procedure did not affect focal conic bands (i.e., oily streaks) caused by dust particles or by surface imperfections of the substrates. But these effects were avoided by careful preparation techniques. Reasonable agreement between experiment and theory was achieved only with samples which had been stored for at least one day. Both the long equilibration time implied by the latter and the strong influence of the preparation procedure on the sample quality indicate that the preparation of single-domain samples is still an art rather than a science.

⁵⁸ J. E. Adams, W. Haas, and J. Wysocki, *J. Chem Phys* 50, 2458 (1969).

⁵⁹ D. W. Berreman and T. J. Scheffer, *Phys Rev Lett* 25, 577 (1970); *Mol Cryst Liq Cryst* 11, 395 (1970).

⁶⁰ R. Dreher, G. Meier, and A. Saupe, *Mol Cryst Liq Cryst* 13, 17 (1971).

⁶¹ P. Kassubek, G. Meier, *Mol Cryst Liq Cryst* 8, 305 (1969).

⁶² P. Chatelain, *Bull Soc Franc Mineral* 66, 105 (1943).

2. Typical Experimental Results. Figure 2 shows the spectral selective reflectance obtained with a single-domain sample. Notice the good agreement with the theoretical curve with respect to the nearly rectangular shape of the main maximum and the positions of the secondary maxima and minima. As the comparison with Figure 3 shows, polydomain samples do not exhibit any of these characteristic features. Apparently the misalignment of the domains by only a few degrees is sufficient to wash out the side maxima and to distort the main reflection band into a bell-shaped curve. Since the sample quality could not be assessed by microscopic inspection, Dreher considered the square shape of the main maximum and the existence of the side maxima as the essential criteria of a well-aligned sample.⁶³

To date, the temperature dependence of the selective reflection has been determined only for polydomain samples. Figure 4 depicts the schematic dependence of reflected intensity versus temperature and wavelength for light traveling approximately parallel to the sample normal. Notice that the intensity dependence on temperature at constant wavelength also forms a bell-shaped curve and that the projection of the intensity maximum onto the wavelength-temperature plane results in a hyperbolic-like curve.

Figures 3, 5, and 6 represent results of measurements.⁶⁴ The samples were illuminated by a 14° cone of monochromatic light of 12Å bandwidth which was perpendicular to the sample surface. The intensity of the selectively reflected light was measured over the same solid angle. As already discussed, we estimated a maximum angle of misalignment of 4.7° . The illuminated region of the sample contained several thousand domains, all of which selectively reflected light within the solid angle of observation.

Figure 5 shows the dependence of the wavelength at peak intensity (hereinafter called "peak wavelength") on the temperature. A single-domain sample should exhibit the same results because, as we will see, the angular dependence of the selective reflection is negligible under the measurement conditions stated above. Figure 3 shows the spectral response associated with various temperatures. Although the shapes of these curves deviate significantly from those obtained from single-domain samples, their halfwidths are approximately equal to the halfwidth of the reflection band of a single domain.⁶⁵ Again, this agrees with the fact that the polydomain samples were very well aligned. Figure 6 indicated the high temperature dependence of the selectively reflected monochromatic light. For example, at the wavelength of $0.650\mu\text{m}$ the halfwidth of the intensity curve amounts to only 0.025° .

⁶³ R. Dreher, *Dissertation*, Freiburg, 1971.

⁶⁴ R. D. Ennulat, *Mol Cryst Liq Cryst* 13, 337 (1971).

⁶⁵ R. D. Ennulat, L. E. Garn, and J. D. White, *Mol Cryst Liq Cryst*, 26, 245 (1974).

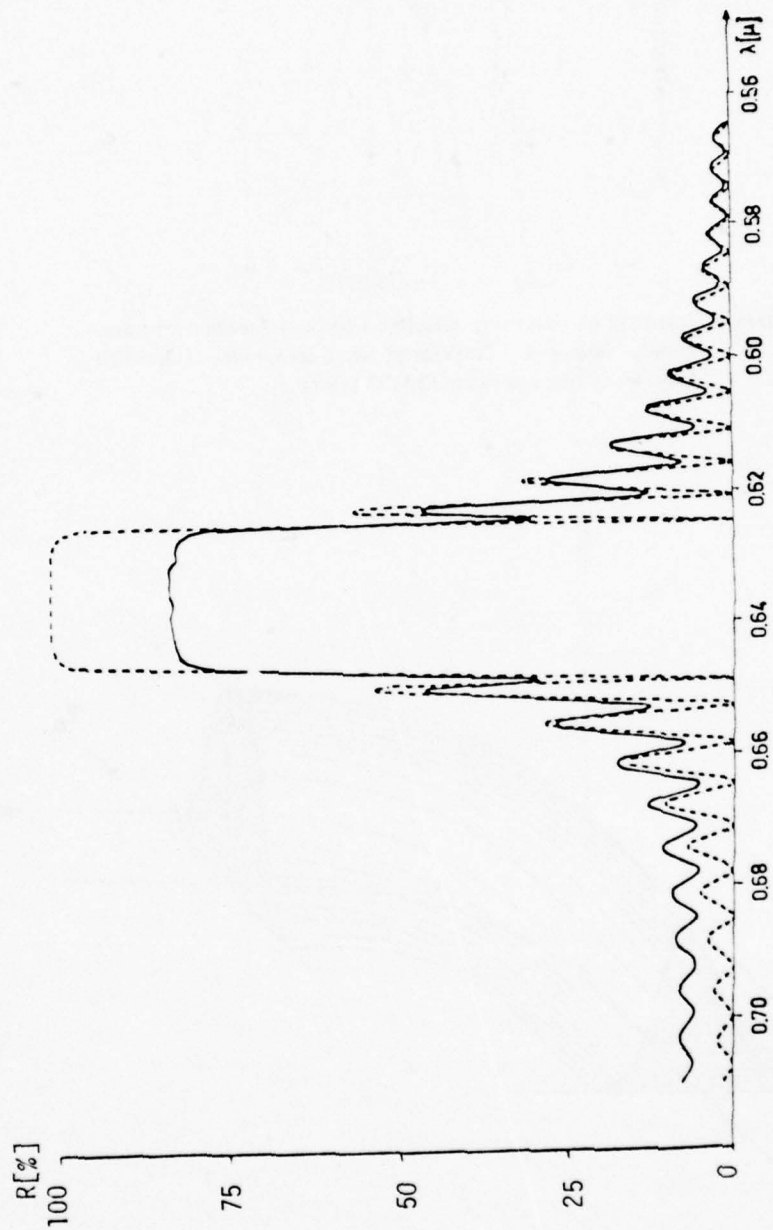


Figure 2. Reflection spectrum of a mixture of cholesteryl acetate, chloride, and nonanoate (weight ratio 6:15:20) at 24° at normal incidence. Dashed curve: computed spectrum with pitch $p = 0.4273 \mu\text{m}$ and thickness of layer of $21.0 \mu\text{m}$. Solid curve: experimental spectrum. Intensity in arbitrary units. [Modified from Mol Cryst Liq Cryst 13, 17 (1971). Permission to use this figure has been granted by the authors.]

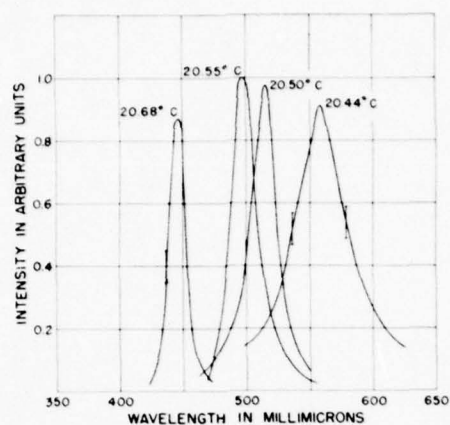


Figure 3. Intensity of selectively reflected light as a function of wavelength. Material: Cholesteryl oleyl carbonate. [Modified from *Mol Cryst Liq Cryst* 13, 337 (1971).]

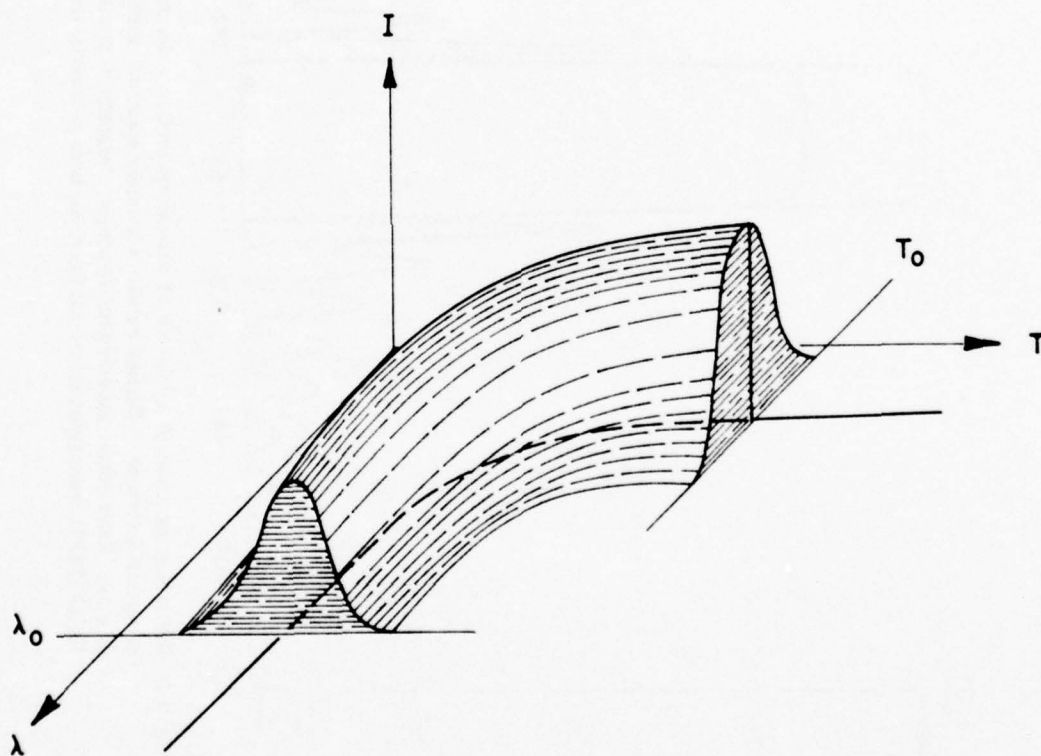


Figure 4. Intensity of light selectively reflected by the planar texture as a function of wavelength and temperature [Modified from *Mol Cryst Liq Cryst* 13, 337 (1971).]

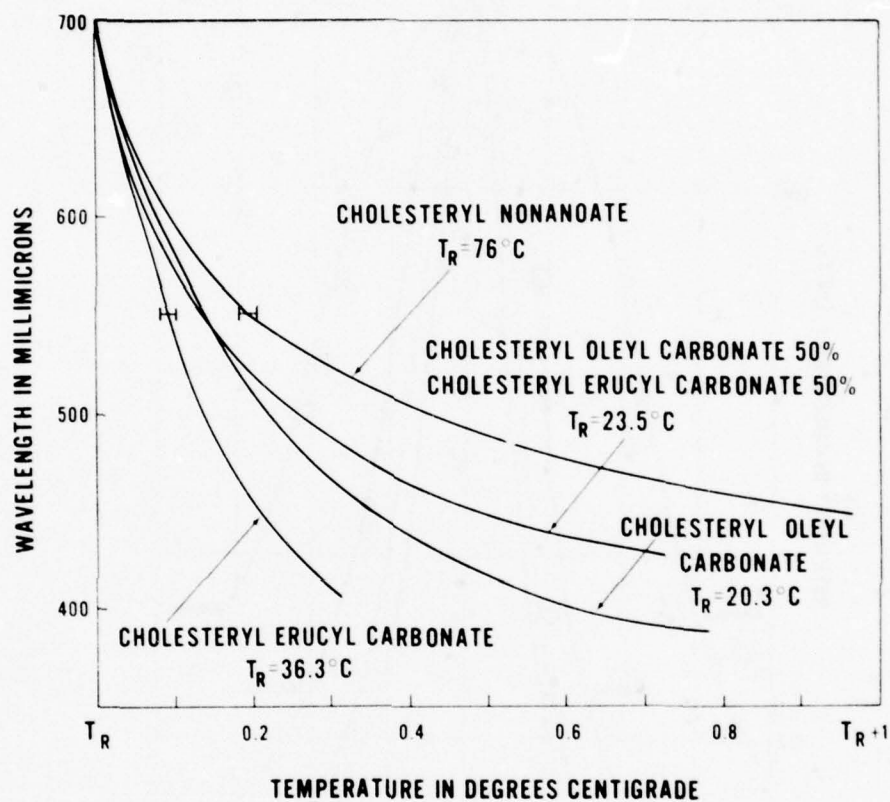


Figure 5. Wavelength of maximum selective reflection as a function of temperature. [Reproduced from *Mol Cryst Liq Cryst* 13, 337 (1971).]

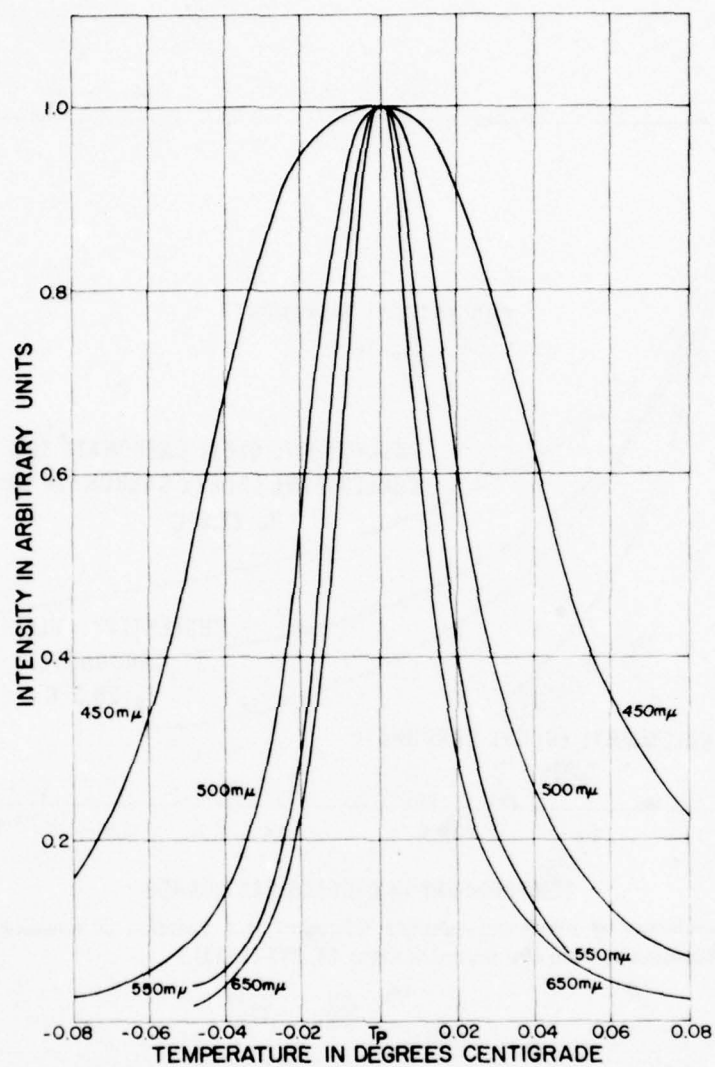


Figure 6. Normalized intensity of selectively reflected light as a function of temperature. [Reproduced from *Mol Cryst Liq Cryst* 13, 337 (1971).]

Ferguson measured and calculated the angular dependence of the peak wavelength.^{66 67} (See also Magne⁶⁸ and Böttcher.⁶⁹) Ferguson assumed that a stack of fictitious planes separated by the pitch of the helix furnishes Bragg reflection sites that are imbedded in a medium having the average index of refraction \bar{n} of the liquid crystal. As shown in Figure 1, a simple geometry consideration based on that model gives the relation

$$\lambda_p = \lambda_n \cos \frac{1}{2} \left\{ \sin^{-1} \left(\frac{\sin \phi_i}{\bar{n}} \right) + \sin^{-1} \left(\frac{\sin \phi_s}{\bar{n}} \right) \right\} \quad (2)$$

where λ_n is the peak wavelength obtained from light traveling along the helical axis and ϕ_i and ϕ_s are angles of incidence and observation, respectively. This formula agrees well with the measurements except for very large angles of incidence.⁷⁰ The experimental results in Figure 7 indicate that for increasing angles of incidence the peak wavelength is shifted toward the blue.

Equation (2) allows the determination of the wavelength shift caused by the maximum misalignment ϵ of the domains in the sample. Using the data reported in our work, ($\phi_i = \phi_s = 7^\circ$),⁷¹ we obtained a shift of

$$\lambda_p - \lambda_n = -23 \text{ \AA}$$

which is about twice as large as the spectral bandwidth of the light used.

Adams, Haas, and Wysocki observed selectively diffracted light transmission in samples deposited on a partially reflective substrate.⁷² They also observed that both this selective transmission and the selective reflection exhibit the same angular dependence of the peak wavelength. Much more fundamental is their finding that focal conic textures display selective reflection when a mirror substrate is used. This effect can be explained by assuming that the focal conic texture consists of a polydomain planar texture whose helical axes lie predominantly in the same plane. The selective transmission observed under certain conditions can be explained by the same structure. The latter is also compatible with the fact that birefringent patterns are observed with the microscope when transmitting or absorbing substrates are used. These effects support Friedel's hypothesis of the molecular arrangement

⁶⁶ J. L. Ferguson, *Mol Cryst Liq Cryst*, **1**, 293 (1966).

⁶⁷ J. L. Ferguson, *Appl Opt* **7**, 1729 (1968).

⁶⁸ M. Magne and P. Pinard, *J. Phys (Paris)* **30**, Coloq C4, 117 (1969).

⁶⁹ B. Böttcher, *Chem-Ztg, Chem-Techn* **1**, 195 (1972).

⁷⁰ R. Dreher, *Dissertation*, Freiburg, 1971.

⁷¹ R. Cano, *Bull Soc Franc Mineral*, **90**, 333 (1967).

⁷² J. E. Adams, W. Haas, and J. Wysocki, *J. Chem Phys*, **50**, 2458 (1969).

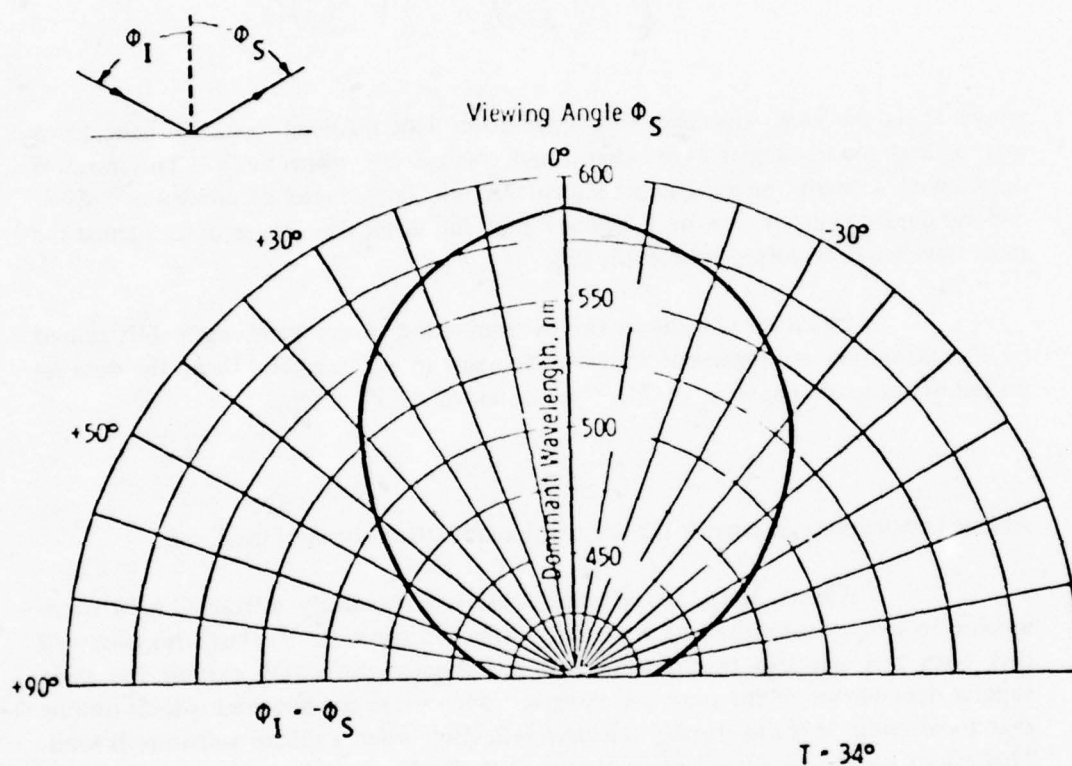


Figure 7. Wavelength of maximum scattering as a function of viewing angle. [Modified from *Mol Cryst Liq Cryst* 1, 293 (1966). Permission to use this figure has been granted by the author.]

in cholesteric focal conics.⁷³ He concluded from his observations that the layers required to explain the focal conic properties should consist of planar texture elements which have their helical axes parallel to the local normal of the Dupin cyclides comprising the focal conic structure. In such a molecular arrangement, the helical axes of a large number of domains would make a small angle with the sample plane. The results prove that the focal conic textures are embodiments of essentially the same molecular building principle, namely, the helical arrangement of the molecules.

III. EXPERIMENTAL: CHARACTERIZATION OF LIQUID CRYSTALS

A. Hot-Stage Microscopy. Microscopic studies of hundreds of liquid crystals were conducted with a Leitz Ortholux polarizing microscope combined with a Mettler FP-2 hot stage for the heating and cooling of the samples. The normal total, visual magnification of the microscope was 70X. Zone-refined materials with accurately known melting points were used to calibrate the hot stage. Figure 8 shows a typical calibration curve. Materials which proved to be very suitable for calibration included 2-methylnaphthalene, bibenzyl, cyclododecane, biphenyl, naphthalene, p-dibromobenzene, xanthene, acetanilide, benzoic acid, adipic acid, and 2-chloroanthraquinone. The melting temperatures of these compounds range from 35° to 210°. For convenience and accuracy of measurements, transition temperatures were recorded at an equilibrium or near-equilibrium temperature condition where approximately 50% of the liquid crystal in the observable microscopic field was in the lower temperature phase or mesophase and the other 50% of the observable liquid crystal co-existed in the higher temperature phase or mesophase. This co-existence often appeared as a well-defined cooler circular "disc" surrounded by a warmer "ring," each portion having the same area.

The sample was prepared for observation by putting several milligrams of the liquid crystal between thin cover glasses and positioning them in the hot stage so that the field of view would be at the center of the cover glass. The temperature of the hot stage was then raised at a rate of 10°/min until signs of melting were observed; whereupon the scan rate was reduced to 2°/min, then to 0.2°/min, and finally stopped altogether near the appropriate equilibrium point. The temperature was then raised or lowered in 0.05° increments (the smallest increments of which the FP-2 was capable) until the final equilibrium melting temperature was determined. This first melting point determination, however, was always too high because the two cover glasses were not in virtual contact with each other until the sample was completely melted; whereupon, the heat-transfer characteristics improved. Once the sample was melted, however, all readings were valid because conditions were then virtually identical between cover glasses. The correct melting temperature was determined,

⁷³ G. Friedel, *Ann Phys (Paris)* 18, 273 (1922).

DEVIATION OF MEASURED MELTING POINT
FROM ACTUAL MELTING POINT (°C)

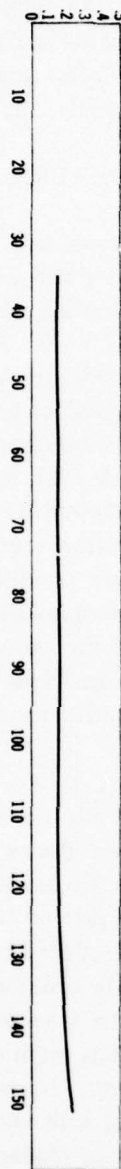


Figure 8. Typical calibration curve for Mettler FP-2 Microscope Hot Stage. Actual temperature was determined by subtracting value of ordinate from measured temperature. The following zone refined materials were used, reading from left to right: α -methylnaphthalene, bibenzyl, cyclododecane, biphenyl, naphthalene, p-dibromobenzene, xanthene, acetanilide, benzoic acid, and adipic acid.

after the initial melting, by freezing the sample (lowering the hot-stage temperature is generally sufficient to do this) and then reheating. Freezing temperatures were determined by cooling at a constant rate — generally $10^{\circ}/\text{min}$. In some cases it was necessary to cool very rapidly by removing the liquid crystal from the hot stage and placing it on top of the stage in order to detect cholesteric colors and the smectic mesophase. Occasionally the sample crystallized at such a high temperature that it had to be plunged into ice water to detect the colors.

In order to attain low temperatures, the FP-2 stage was cooled with nitrogen gas which was first passed through a helical copper coil immersed in liquid nitrogen. This allowed us to reach a temperature of -5° .

In addition to the three basic scanning rates of $0.2^{\circ}/\text{min}$, $2^{\circ}/\text{min}$, and $10^{\circ}/\text{min}$, scanning rates of $0.4^{\circ}/\text{min}$, $0.5^{\circ}/\text{min}$, $1.1^{\circ}/\text{min}$, $2.5^{\circ}/\text{min}$, $2.75^{\circ}/\text{min}$, $4^{\circ}/\text{min}$, and $12^{\circ}/\text{min}$ could be obtained by depressing the three scanning buttons either half-way or all the way in and in different combinations. This allows for a time-saving flexibility which is not apparent from the Mettler FP-2 manual.

It also proved advantageous to install an on-off switch for the cooling fan in the hot stage because its vibration could cause blurring of the microscopic image.

B. Differential Thermal Analysis.⁷⁴ A modified Perkin-Elmer DSC-1 differential scanning calorimeter was used to determine heats of transition and transition temperatures. The instrument consisted of a sample holder assembly, an analyzer unit, and a control unit. It was modified to obtain a tenfold increase of sensitivity, amounting to 0.0038 millicalories per second per unit of deflection (0.38 mcal/s full scale). In order to achieve this increase in sensitivity, a voltage divider was connected to the voltage output of the control unit. A ten-turn zero potentiometer was also installed in order to have a finer control in zeroing the recorder pen.

The noise level was reduced by using a constant-temperature environment for the sample. Ice water was pumped through a cooling jacket surrounding the sample holder assembly to enable cooling to 29° , when scanning at a rate of $10^{\circ}/\text{min}$. This allowed for reversible scanning at lower temperatures, enabling the observation of lower melting, freezing, and mesophase transitions. For cooling to even lower temperatures, a methanol-dry ice mixture was used.

Careful attention was paid to insure that the new electrical connections were securely made, so as not to introduce noise. This included the use of silicon rubber or epoxy where needed to immobilize wires, and twisting the wires from the sample holder to the analyzer to reduce noise.

⁷⁴ R. D. Ennulat in "Analytical Calorimetry," R. S. Porter and J. F. Johnson, Eds, Plenum Press, New York, NY, 1968, p. 219.

The liquid crystal samples, usually weighing around 5 mg, were sealed in aluminum capsules and inserted into the sample holder with an empty reference capsule in the other sample holder. The sample holder assembly and cooling jacket were mounted inside a plexiglass enclosure and purged with dry air or nitrogen gas in order to minimize moisture condensation in the sample-holder assembly and on the cooling jacket.

Zone-refined materials were used to calibrate the instrument at our normal scan rate of $10^{\circ}/\text{min}$. A typical calibration curve is shown in Figure 9. The transition temperature of a highly purified material was taken to be the temperature corresponding to the point where a projection of the straightest portion of the leading edge of the melting curve crossed the baseline of the melting curve. The purer the material, the straighter the leading edge and the less it will deviate from an ideal straight line from the peak to the baseline. Care had to be taken to use samples which were not too large, because larger samples indicated a higher transition temperature due to the delayed formation of a peak. It turned out that very tiny samples of zone-refined materials gave the most reliable melting temperature indications because they melted very quickly and had small peaks and narrow baselines and therefore allowed less room for error.

IV. RESULTS

A. Physical Properties* of Liquid Crystals

1. **Homologous Series.** Eleven homologous series of alkanoates, co-phenylalkanoates, alkyl carbonates, and S-alkyl thiocarbonates of cholesterol, cholest-5-en-3 β -thiol, and 5-cholestan-3 β -ol were prepared and their mesomorphic properties investigated. More specifically, the following series were prepared:

- I Cholesteryl alkanoates
- II S-Cholesteryl alkanethioates
- III Cholesteryl ω -phenylalkanoates
- IV S-Cholesteryl ω -phenylalkanethioates
- V Cholesteryl alkyl carbonates
- VI Cholesteryl S-alkyl thiocarbonates
- VII S-Cholesteryl alkyl thiocarbonates
- VIII 5 α -Cholestan-3 β -yl alkanoates
- IX 5 α -Cholestan-3 β -yl ω -phenylalkanoates
- X 5 α -Cholestan-3 β -yl alkyl carbonates
- XI 5 α -Cholestan-3 β -yl S-alkyl thiocarbonates

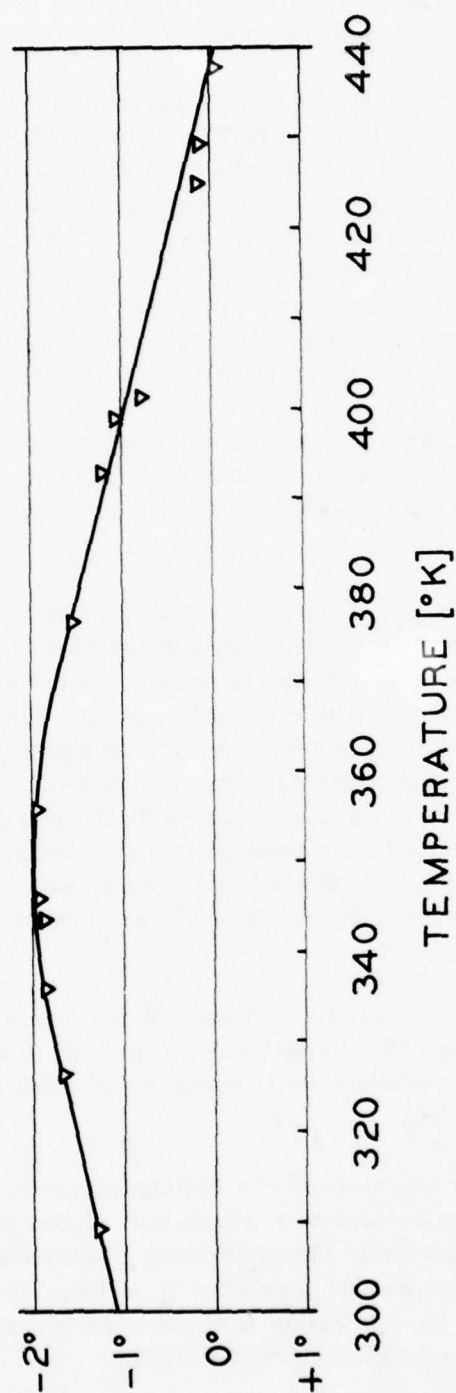


Figure 9. Calibration curve for differential scanning calorimeter. Temperature is corrected by adding value of ordinate to instrument reading. The following zone-refined materials were used — with increasing melting points: 2-methylnaphthalene; 4-nitrotoluene; cyclododecane; biphenyl; 1, 4-diethoxybenzene; naphthalene; xanthene; 4, 4'-azoxyanisole; *trans*-stilbene; benzamide; adipic acid; indium; benzanilide.

The stigmasteryl carbonates and thiocarbonates were also synthesized but exhibited no cholesteric mesophases. In all thirteen series, no impurities could be detected by thin-layer chromatography. This implies a purity of at least 99 mole percent.

In most of the mesomorphic compounds, the transition temperatures in the melt are reproducible to within about 1° , partly because of the high purity attained by modern methods of preparation and partly because of better test equipment. Although temperature-programmable microscope stages increased the accuracy of the optical determination of the transition temperatures, differential scanning calorimetry (DSC) was used to thermodynamically certify the phase transition and to measure the transition enthalpies. For our purpose, it is expedient to characterize the mesomorphic behavior primarily in terms of types of mesophases, transition temperatures in the melt, and existence of color bands in planar textures.

2. Transition Temperatures. The temperatures of the cholesteric-isotropic and smectic-cholesteric transitions are shown in Figures 10 through 13. Figure 10 shows the transition temperatures of the alkanoates; Figure 11 the ω -phenylalkanoates; and Figures 12 and 13, the carbonates.

3. Multiple Melting Points. An interesting phenomenon was observed with 5 α -cholestan-3 β -yl 9-phenylnonanoate and 5 α -cholestan-3 β -yl 10-phenyldecanoate. Both compounds have five distinct melting temperatures; whereas we found no other liquid crystal with more than two different melting points, although many compounds were found to have two melting points. In general, the higher-temperature melting crystals have a different appearance than the lower-temperature melting crystals when a given compound is observed with the microscope. Both compounds with the five melting points have at least three different observable crystal formations. For a given compound, the particular type of crystal which is formed depends on the temperature at which it crystallizes — the lower the freezing temperature, the more unstable the crystal and thus a lower melting point.

4. Heats of Transition. The heats of transition for nine homologous series are shown in Figures 14 through 35. The heats were calculated from the areas of the corresponding transition curves which were plotted by the DSC-1 recorder. All curves were plotted from right to left.

Figure 36 shows the typical shape of a melting transition curve. Figure 37 shows a typical melting curve preceded by the melting of another crystal form and then recrystallization into another form. Figure 38 shows a solid-solid transition where one crystal form readjusts into another form prior to melting. In each case, melting (endothermic) is indicated by a deviation above the baseline and crystallization (exothermic) is indicated by a deviation below the baseline.

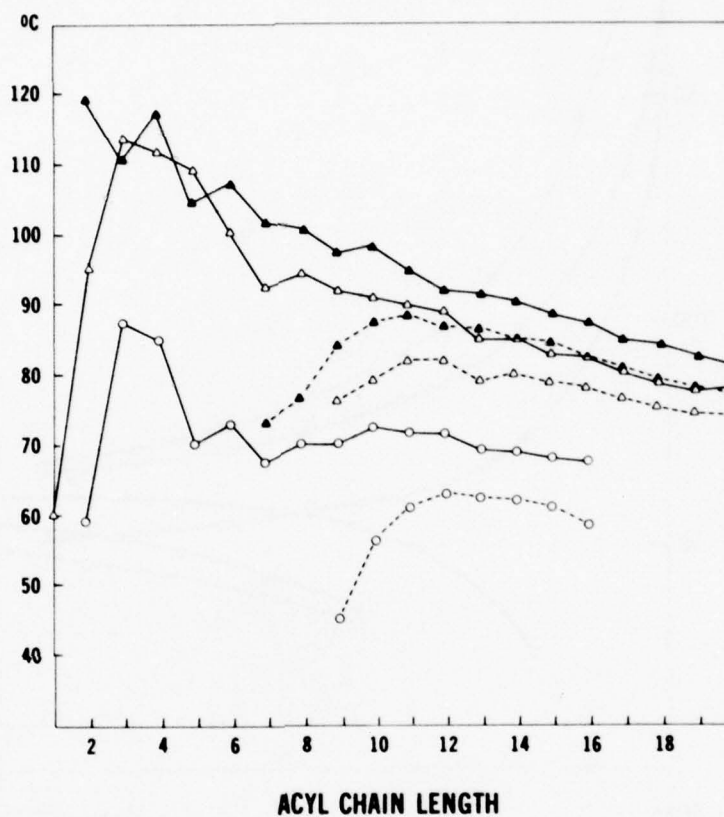


Figure 10. Transition temperatures of alkanoates. Solid lines: cholesteric-isotropic phase transitions; broken lines: smectic-cholesteric phase transitions.

- △ cholesteryl alkanoates
- ▲ S-cholesteryl alkanethioates
- 5α-cholestan-3β-yl alkanoates

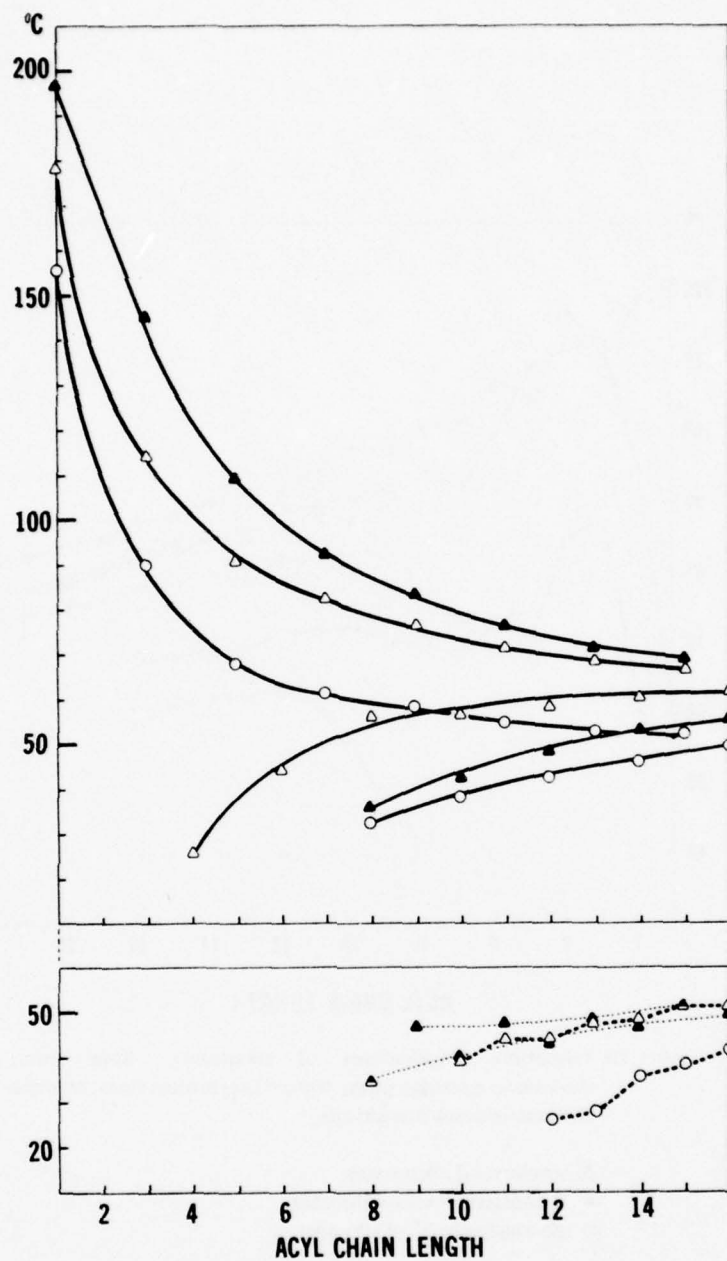


Figure 11. Transition temperatures of ω -phenylalkanoates (transitions as defined in Figure 10).

- \triangle cholesteryl ω -phenylalkanoates
- \blacktriangle S-cholesteryl ω -phenylalkanethioates
- \circ 5 α -cholestan-3 β -yl ω -phenylalkanoates

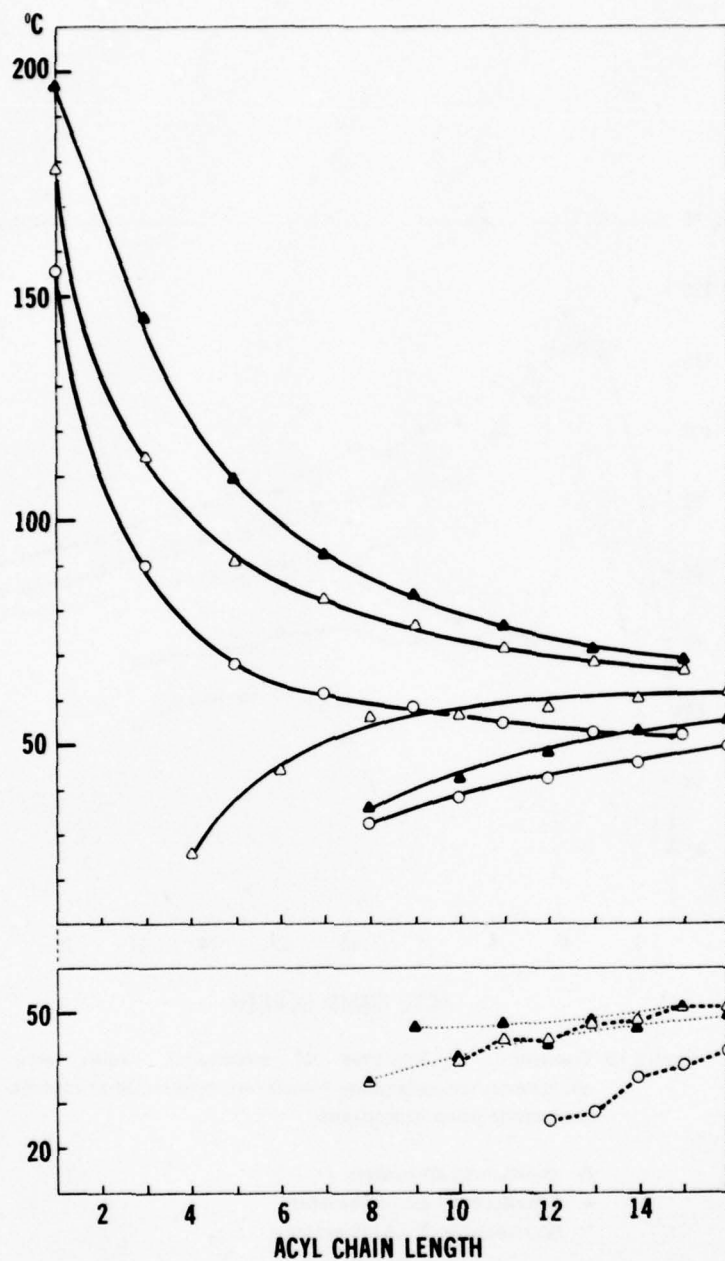


Figure 11. Transition temperatures of ω -phenylalkanoates (transitions as defined in Figure 10).

- △ cholesteryl ω -phenylalkanoates
- ▲ S-cholesteryl ω -phenylalkanethioates
- 5 α -cholestan-3 β -yl ω -phenylalkanoates

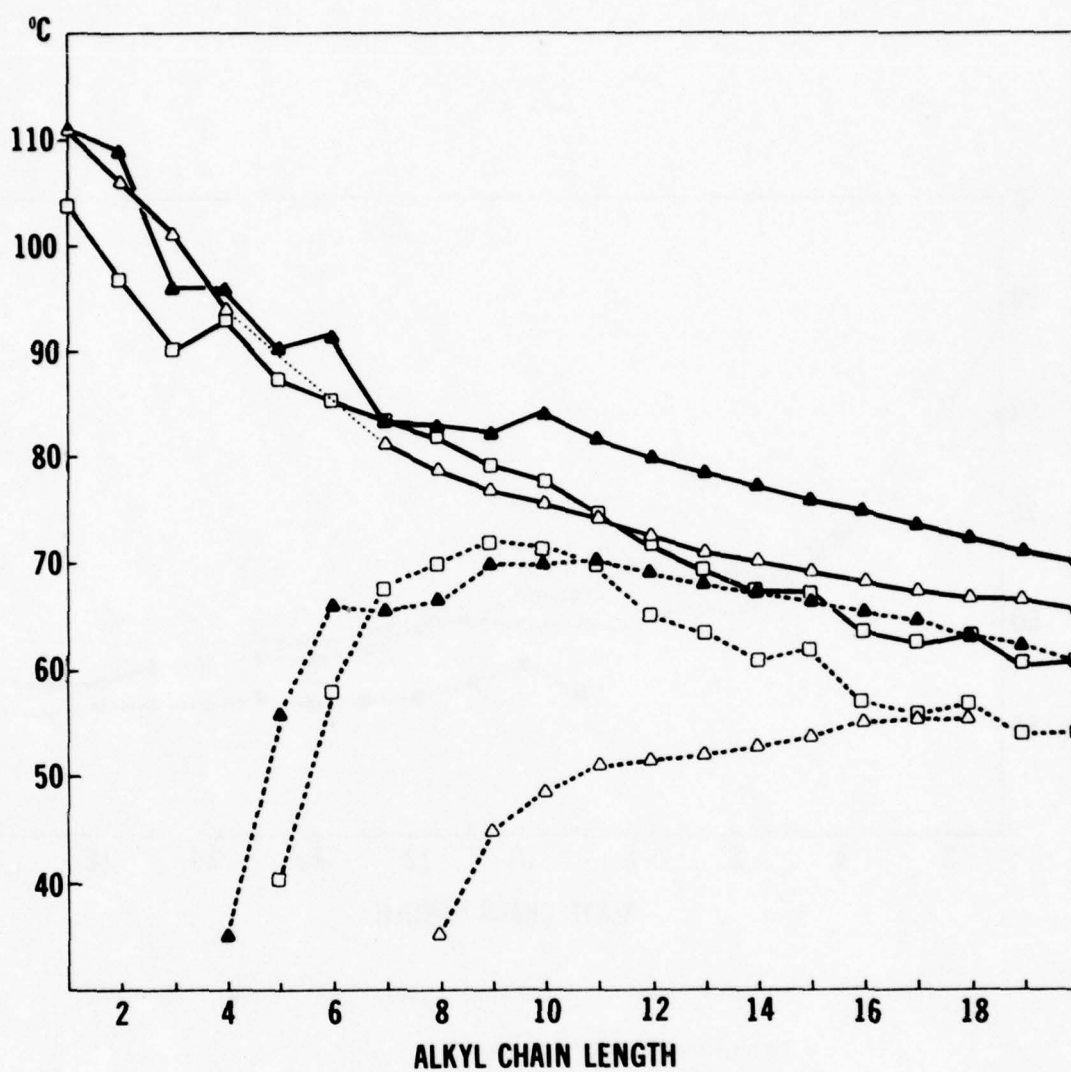


Figure 12. Transition temperatures of carbonates (transitions as defined in Figure 10).

- △ cholesteryl alkyl carbonates
- cholesteryl S-alkyl thiocarbonates
- ▲ S-cholesteryl alkyl thiocarbonates

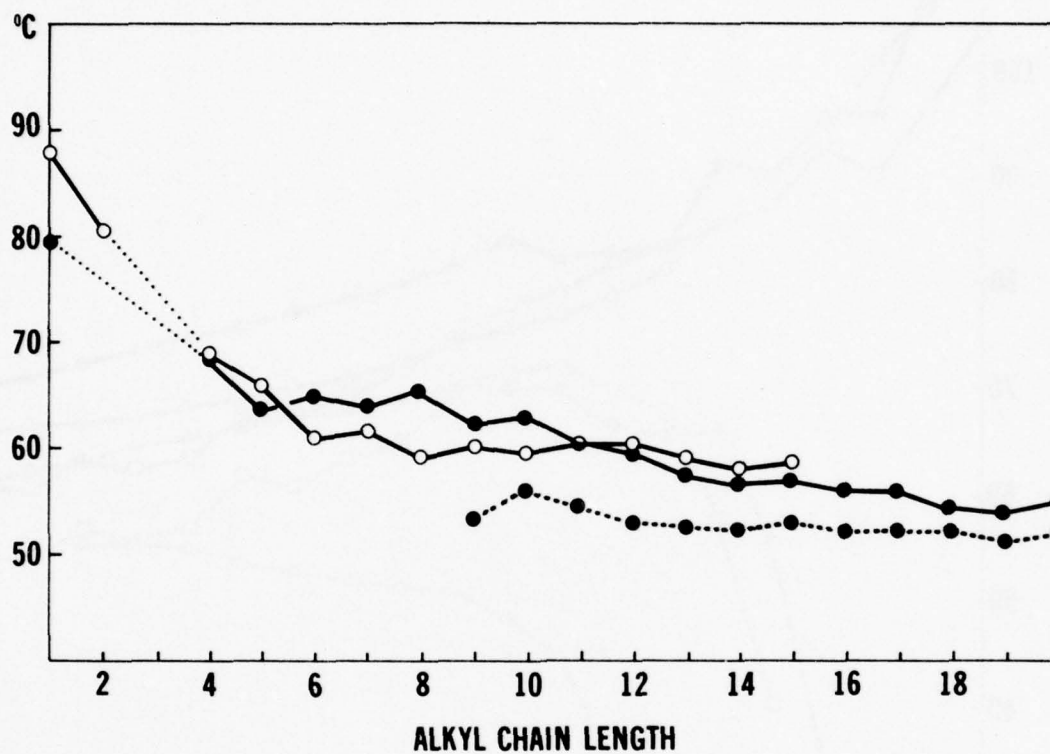


Figure 13. Transition temperatures of carbonates (transitions as defined in Figure 10).

- 5α-cholestan-3β-yl alkyl carbonates
- 5α-cholestan-3β-yl S-alkyl thiocarbonates

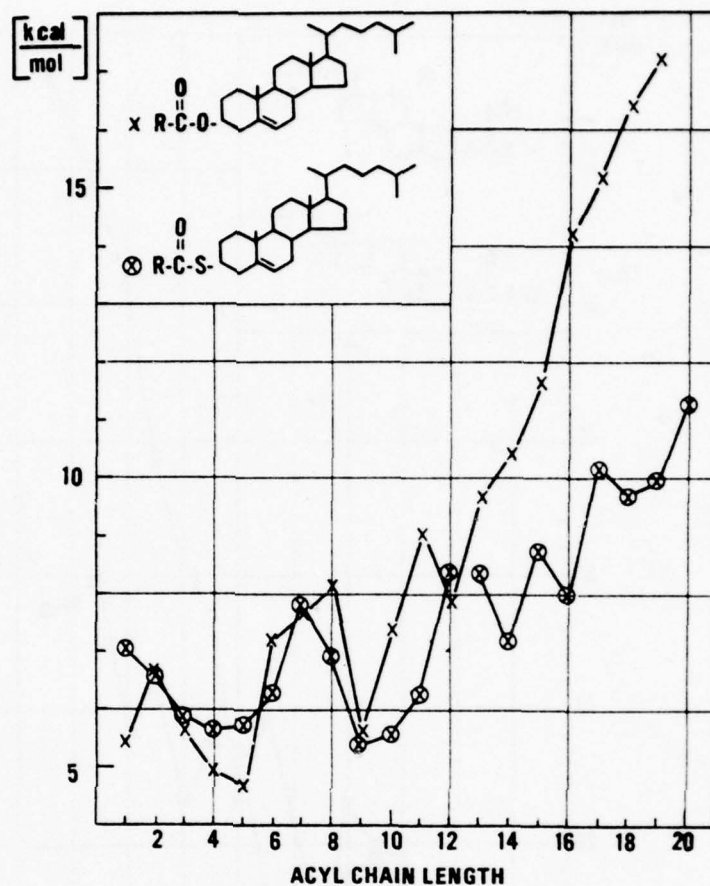


Figure 14. Enthalpy of fusion of the alkanoates of cholesterol and thiocholesterol.

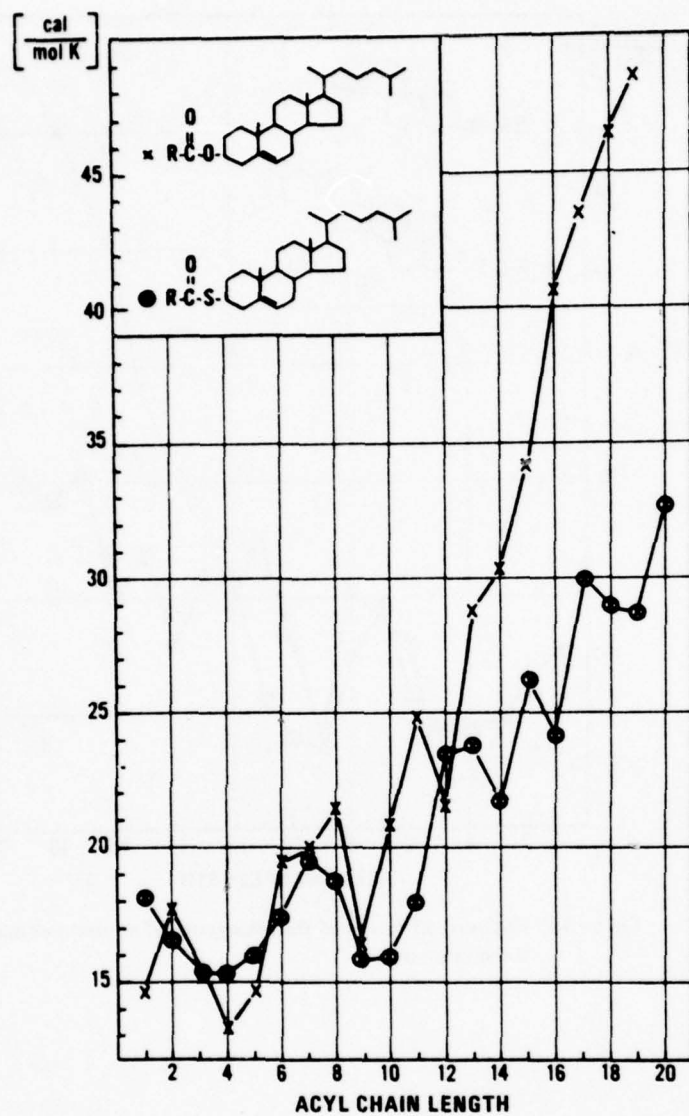


Figure 15. Entropy of fusion of the alkanoates of cholesterol and thiocholesterol.

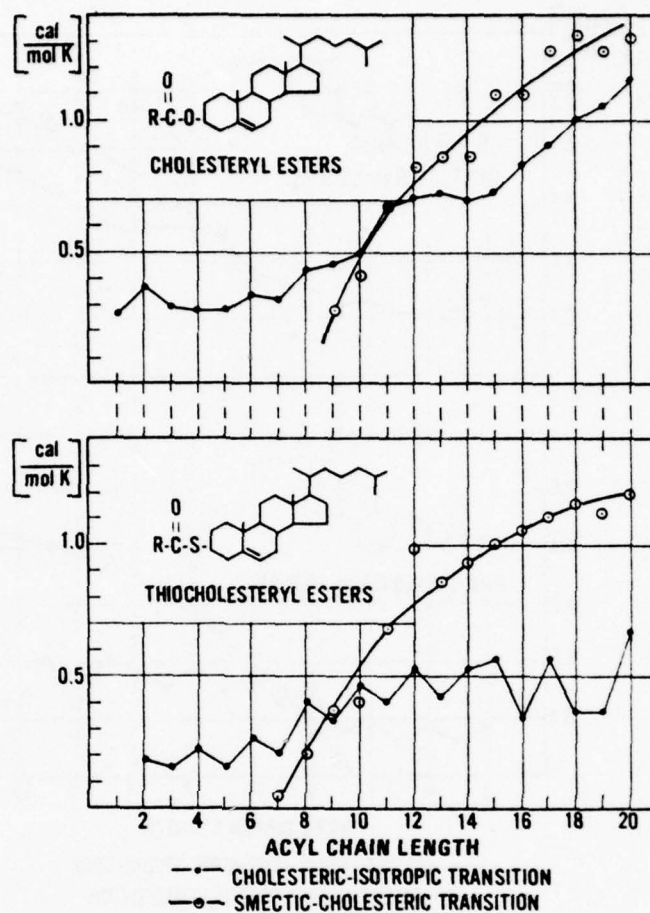


Figure 16. Enthalpy changes at transitions in the melt of the alkanoates cholesterol and thiocholesterol.

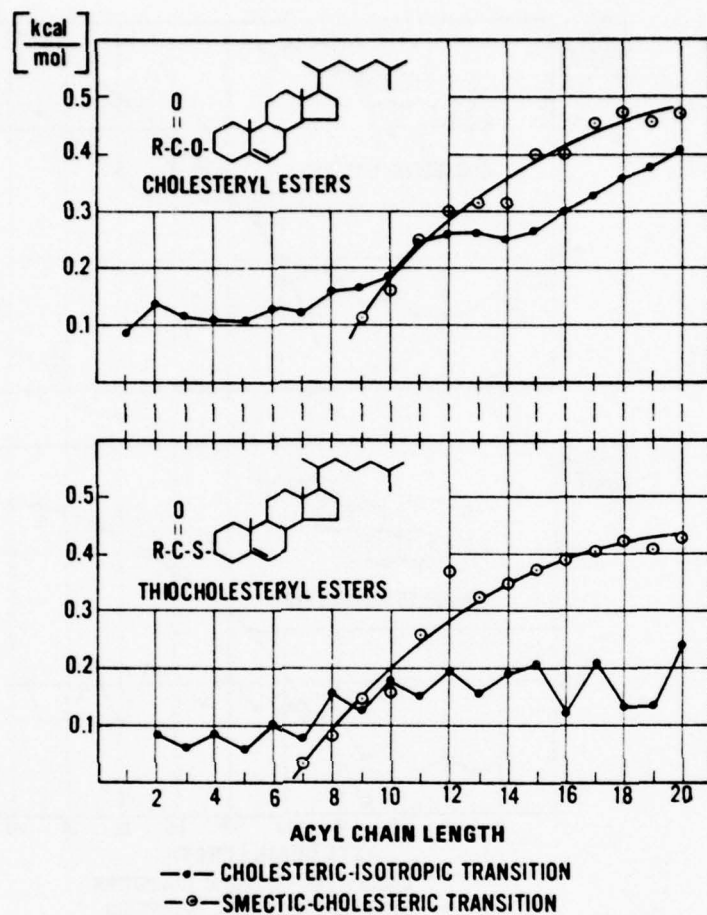
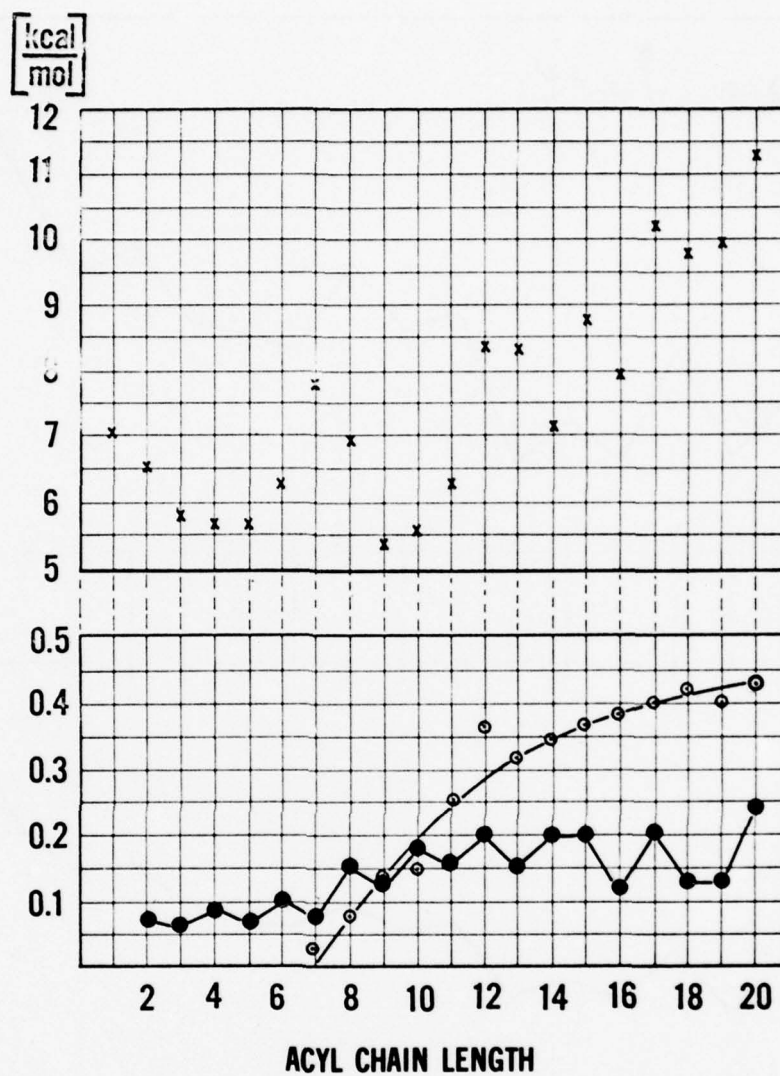


Figure 17. Entropy changes at transitions in the melt of the alkanoates of cholesterol and thiocholesterol.



- × MELTING POINT
- CLEARING POINT
- ⊙ SMECTIC-CHOLESTERIC TRANSITION

Figure 18. Heats of transition of the thiocholesteryl alkanoates.

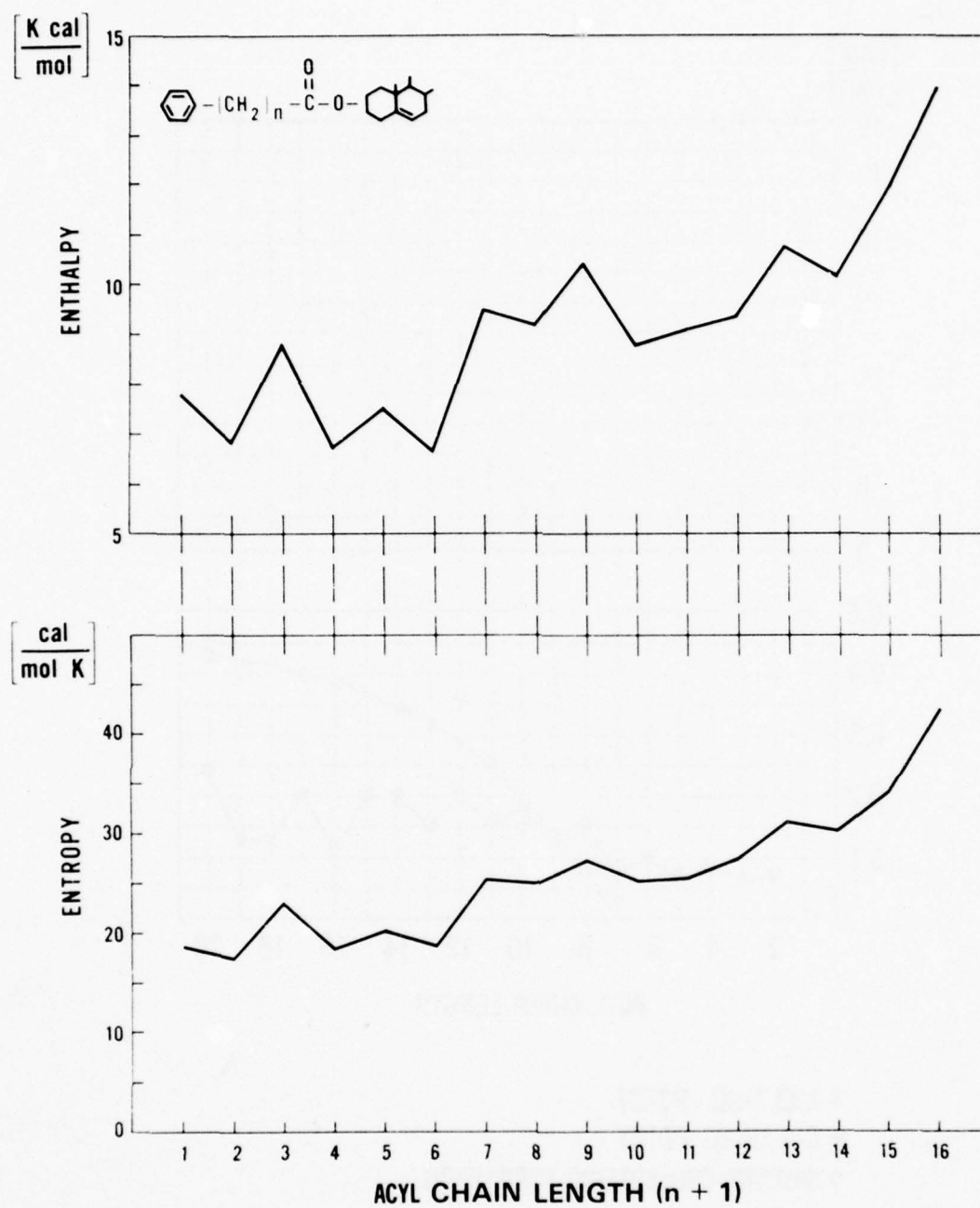


Figure 19. Enthalpies and entropies of fusion of cholesteryl ω -phenylalkanoates.

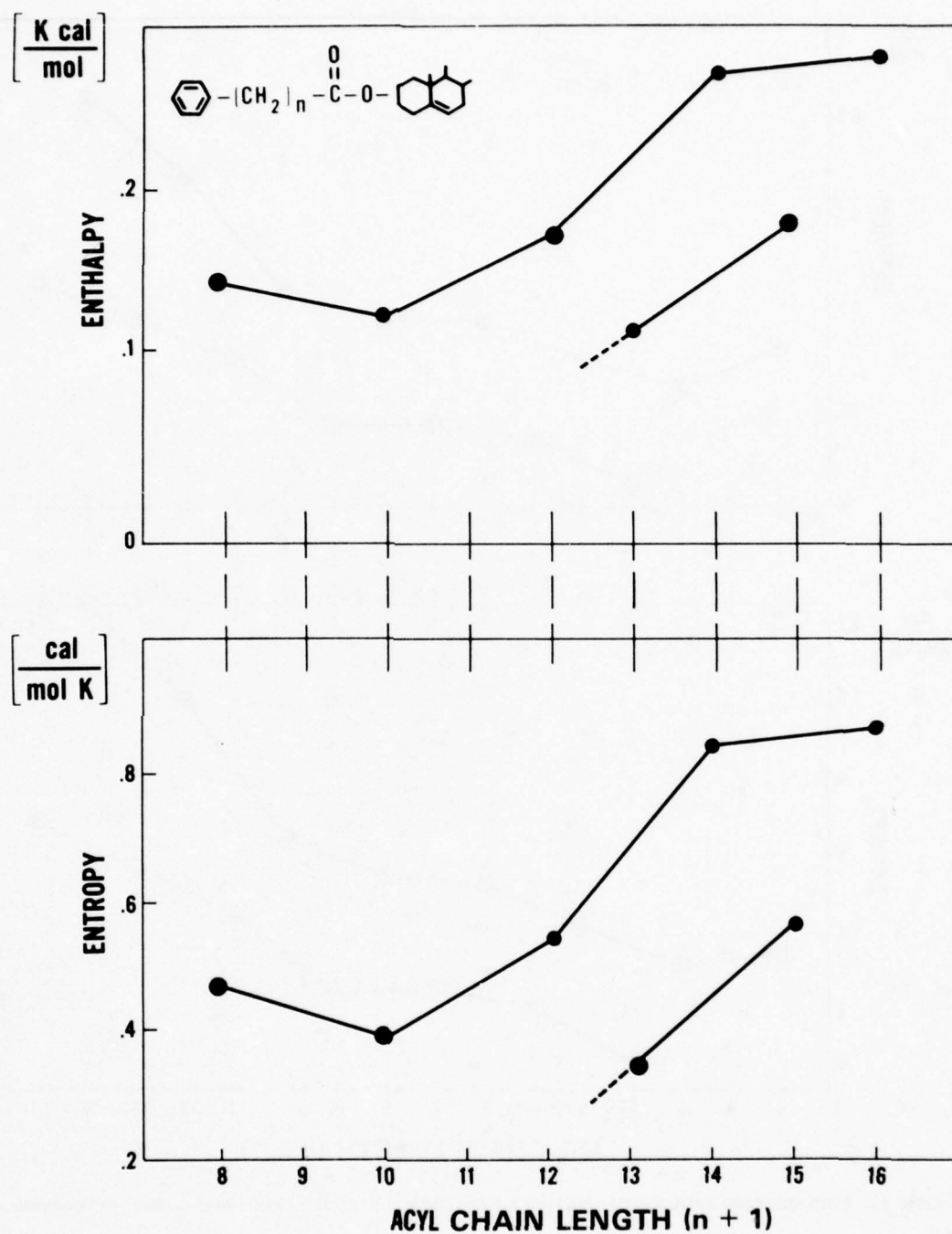


Figure 20. Enthalpies and entropies of smectic-cholesteric transitions of cholesteryl ω -phenylalkanoates.

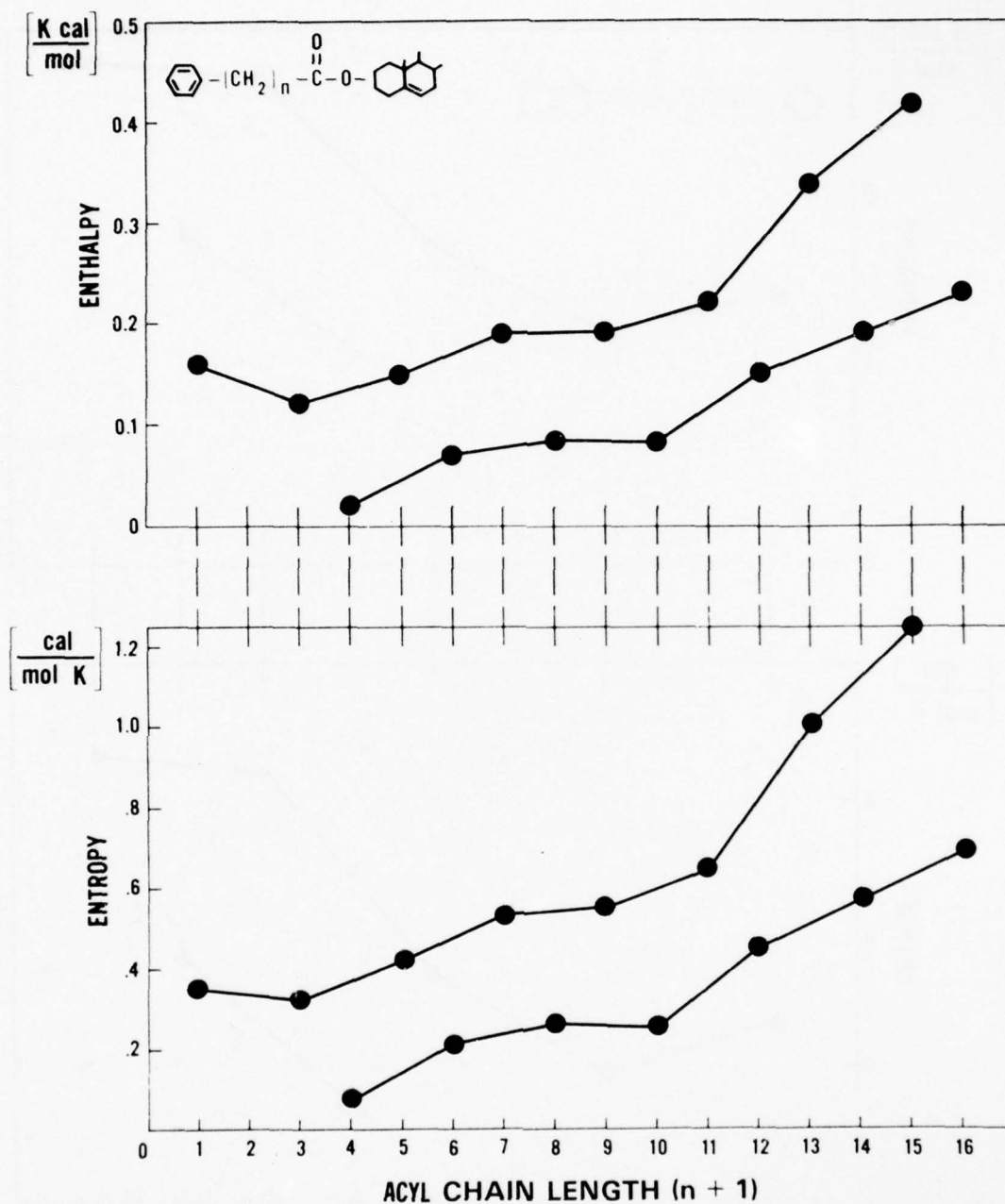


Figure 21. Enthalpies and entropies of cholesteric-isotropic transitions of cholesteryl ω -phenylalkanoates.

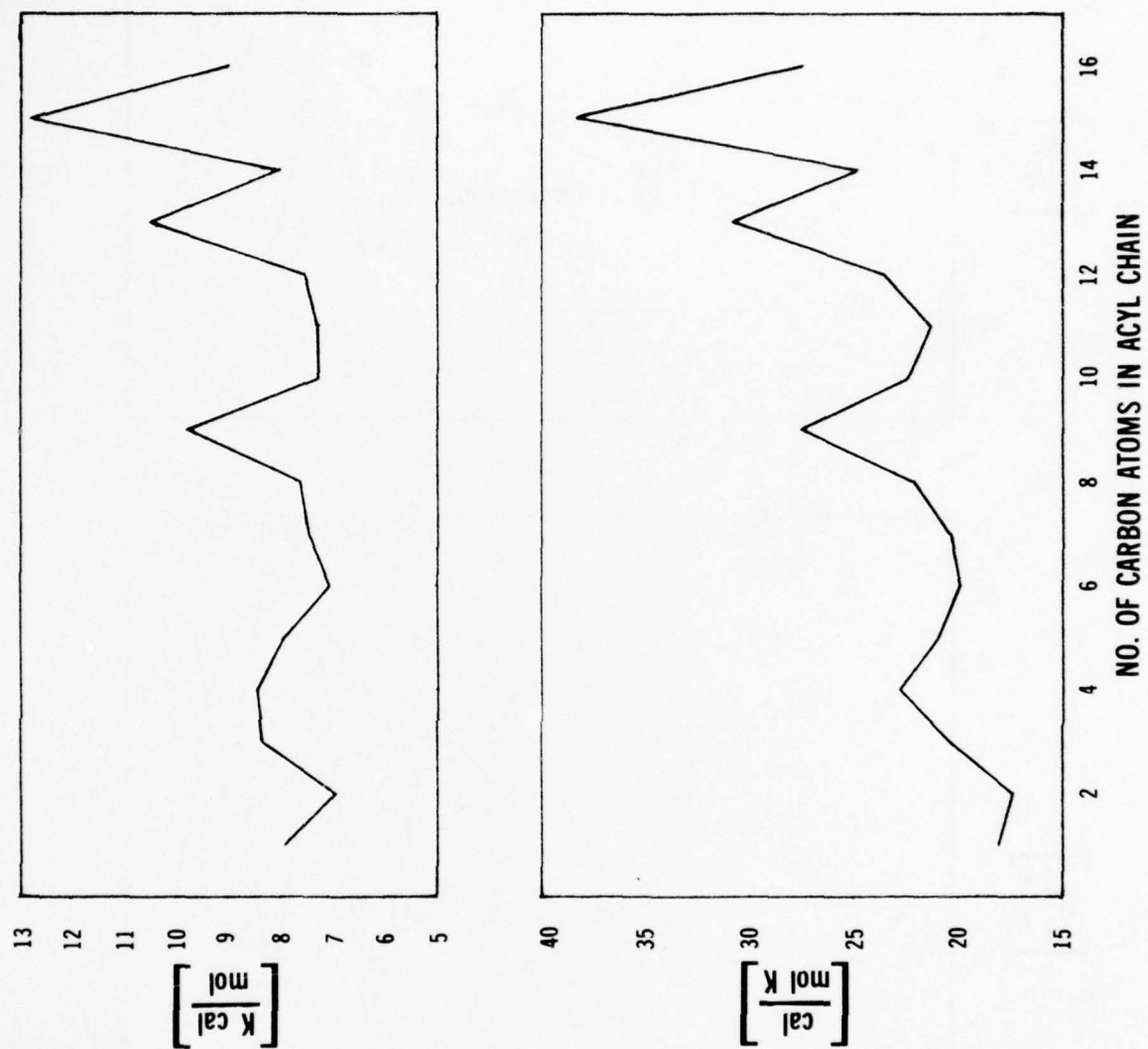


Figure 22. Enthalpies and entropies of fusion for S-cholesteryl ω -phenylalkanethioates.

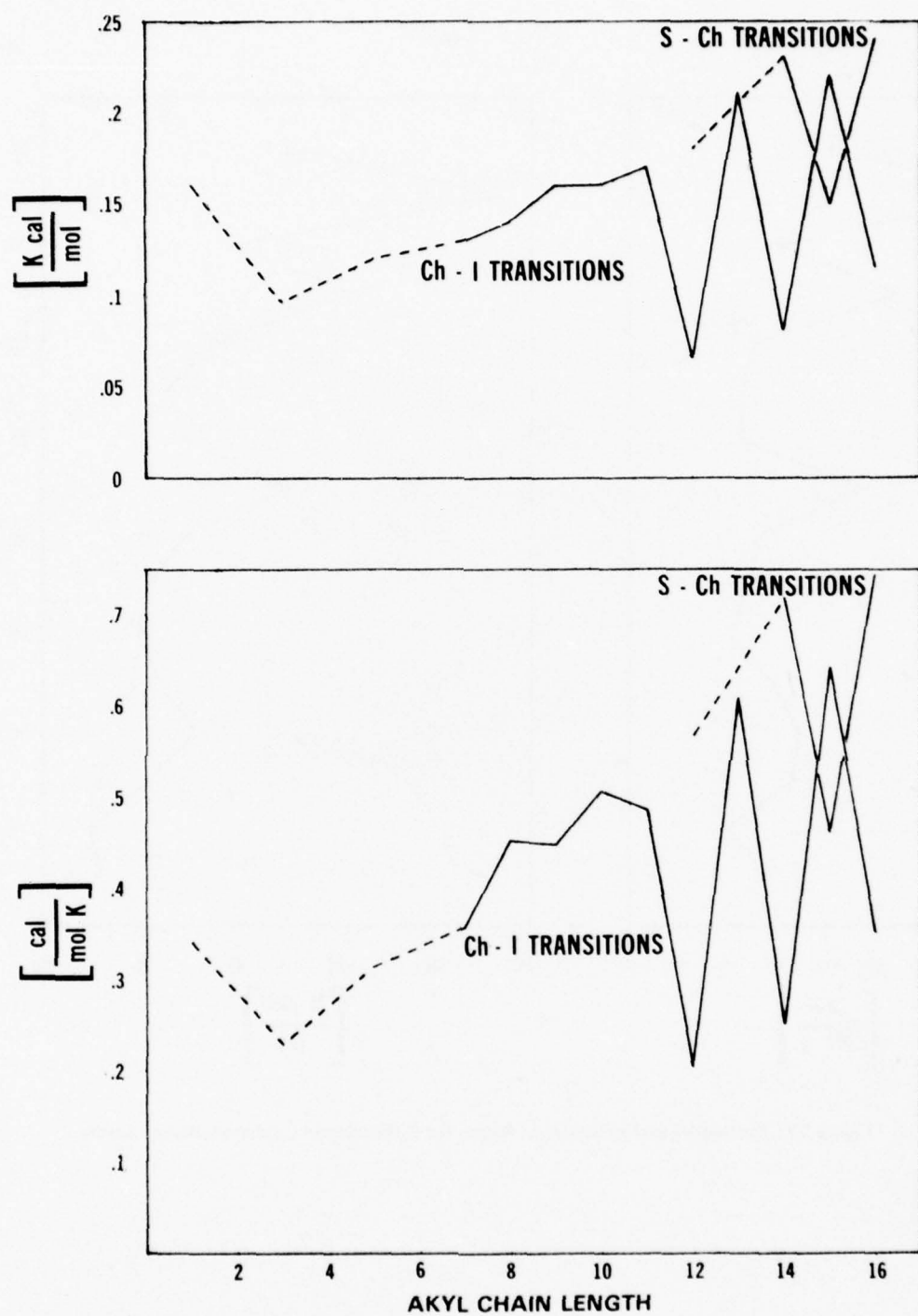
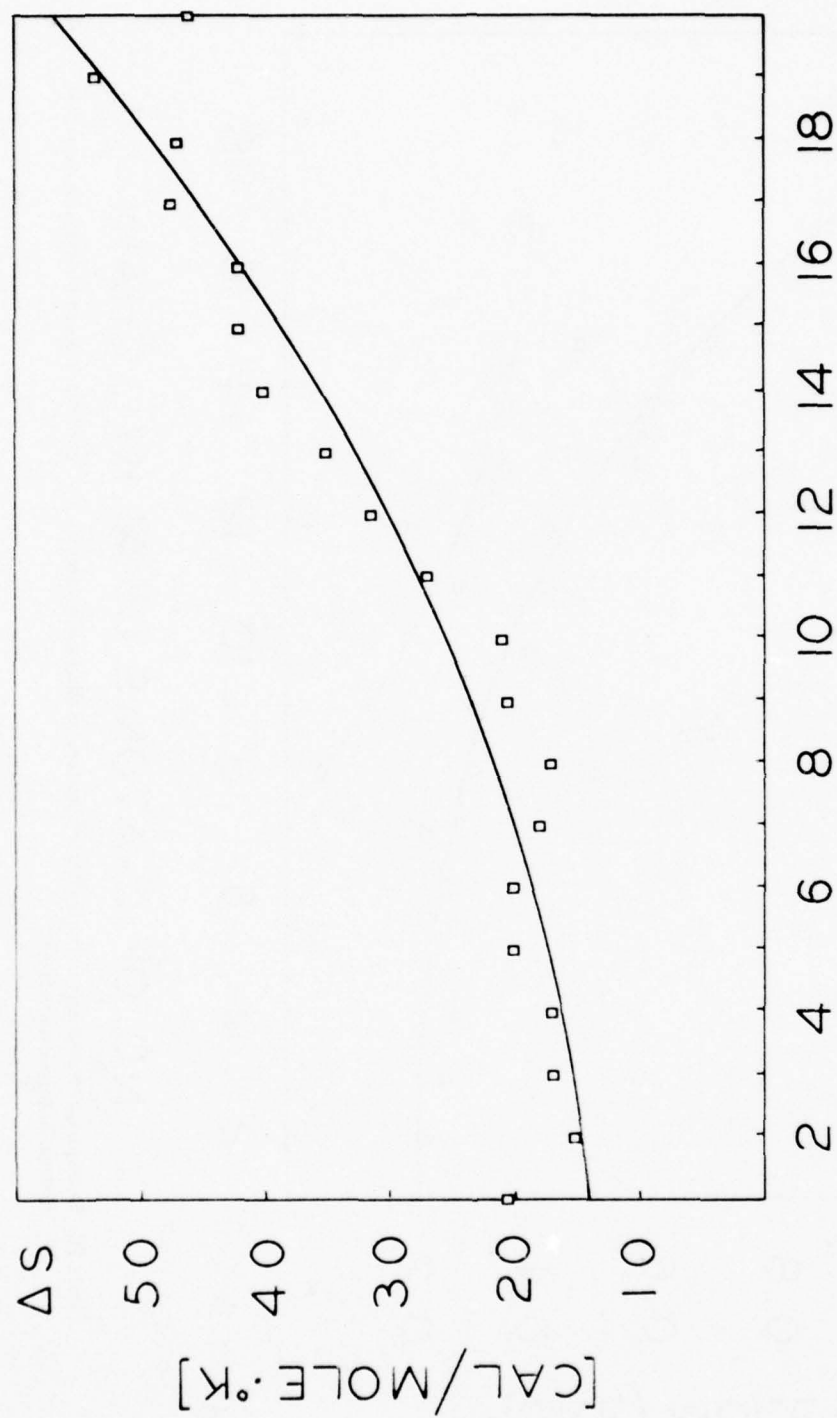
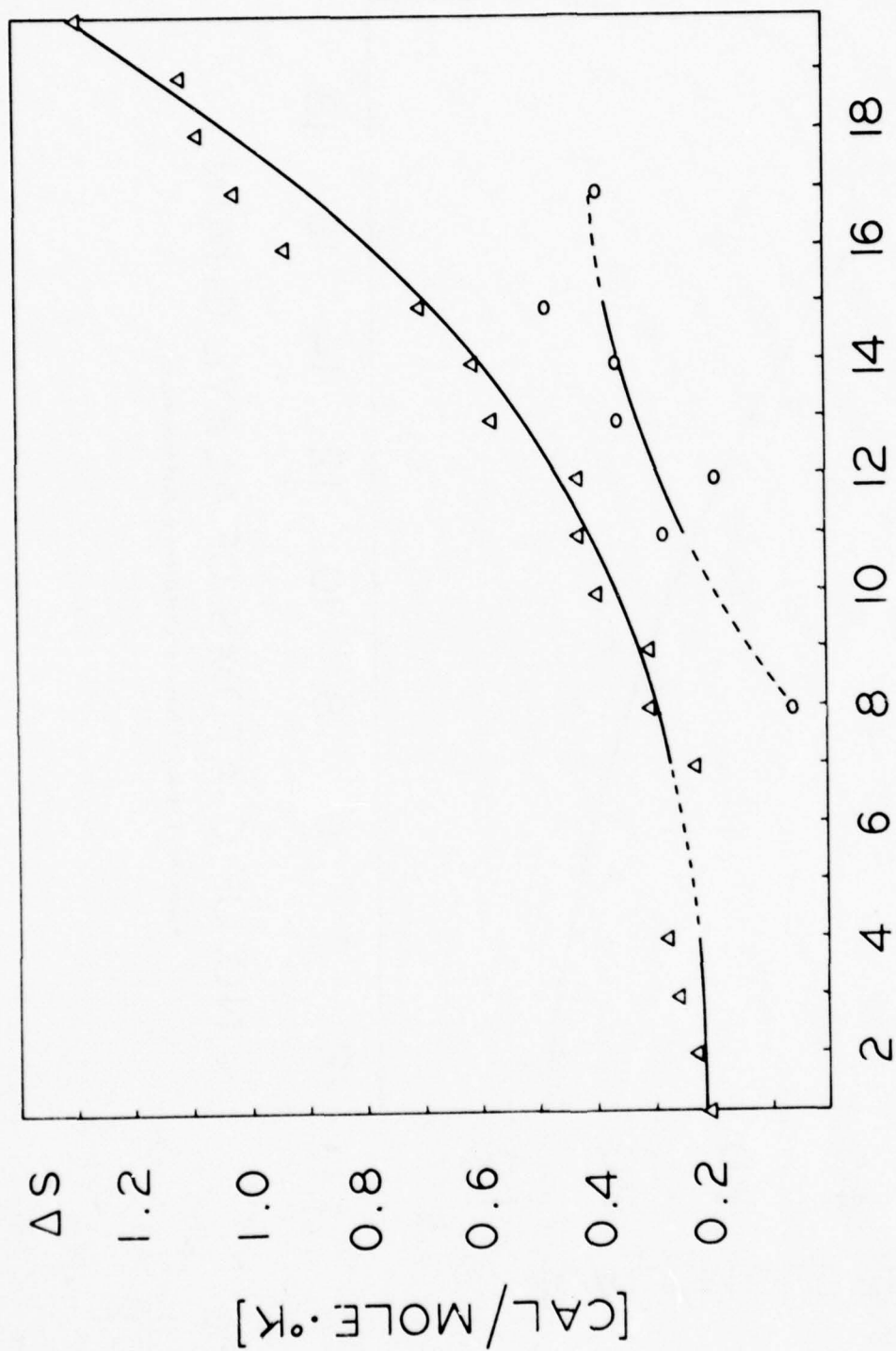


Figure 23. Enthalpies and entropies of cholesteric-isotropic transitions and smectic cholesteric transitions for S-cholesteryl ω -phenylalkanethioates.



NO. OF C-ATOMS OF ALKYL CHAIN

Figure 24. Entropy of fusion of cholesteryl n-alkyl carbonates.



NO. OF C-ATOMS OF ALKYL CHAIN

Figure 25. Entropies of transitions in the melt of cholesteryl n-alkyl carbonates: Δ —, cholesteric-isotropic transitions; \circ —, smectic-isotropic transitions.

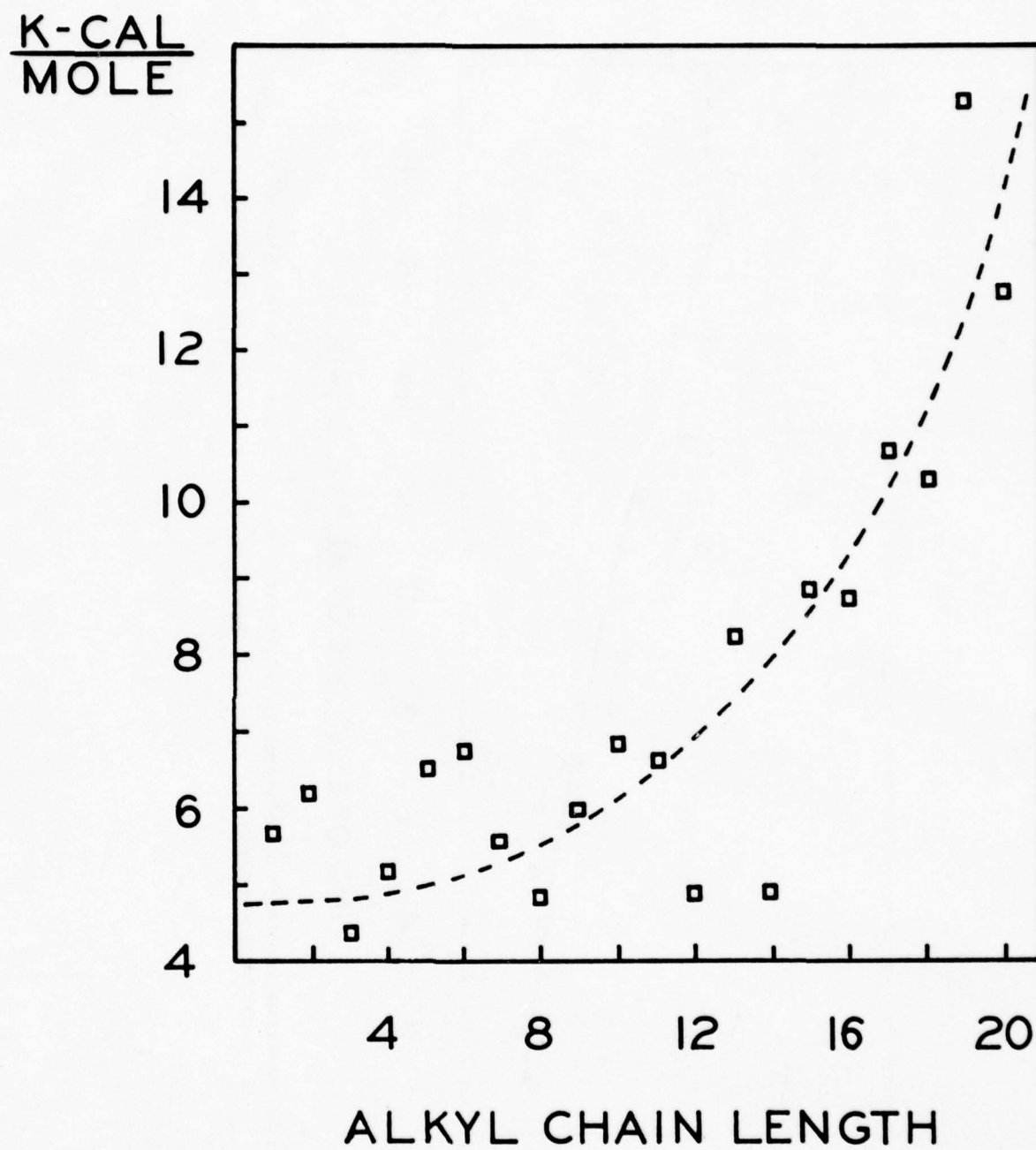


Figure 26. Heats of fusion of cholesteryl S-alkyl thiocarbonates.

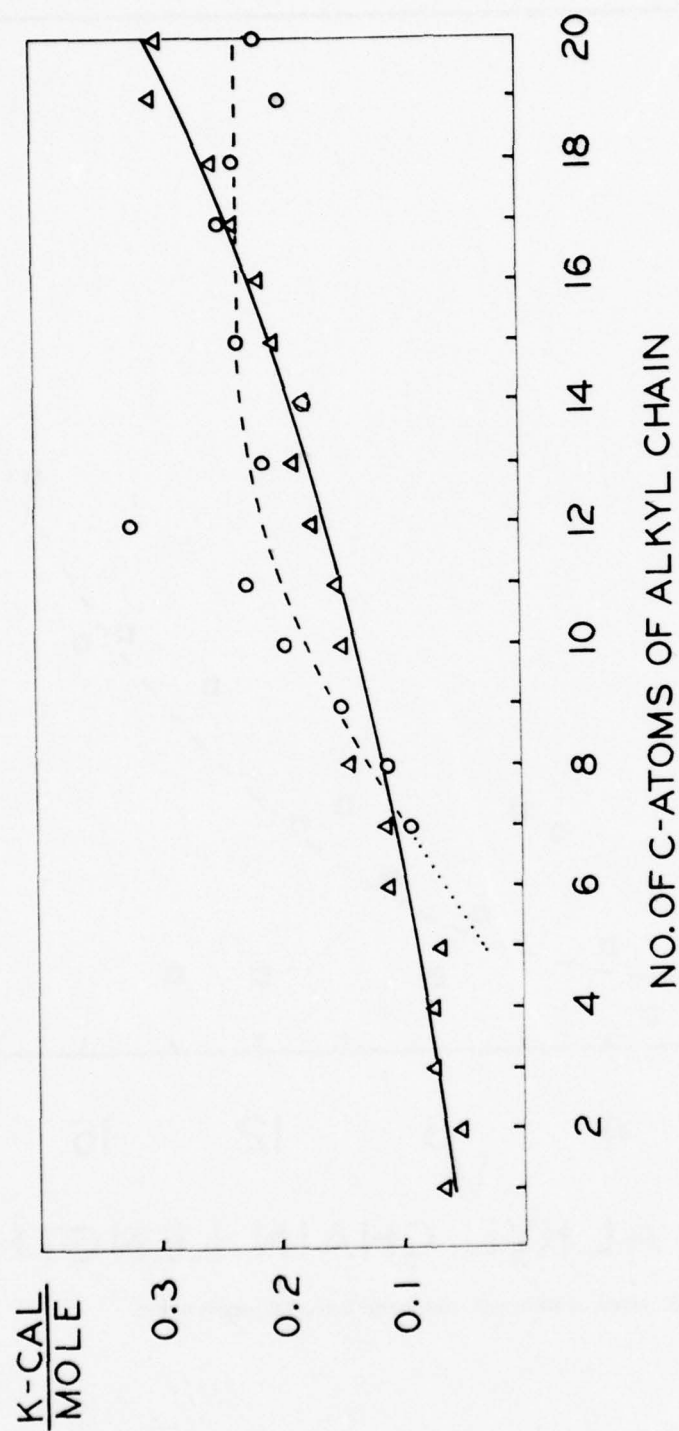
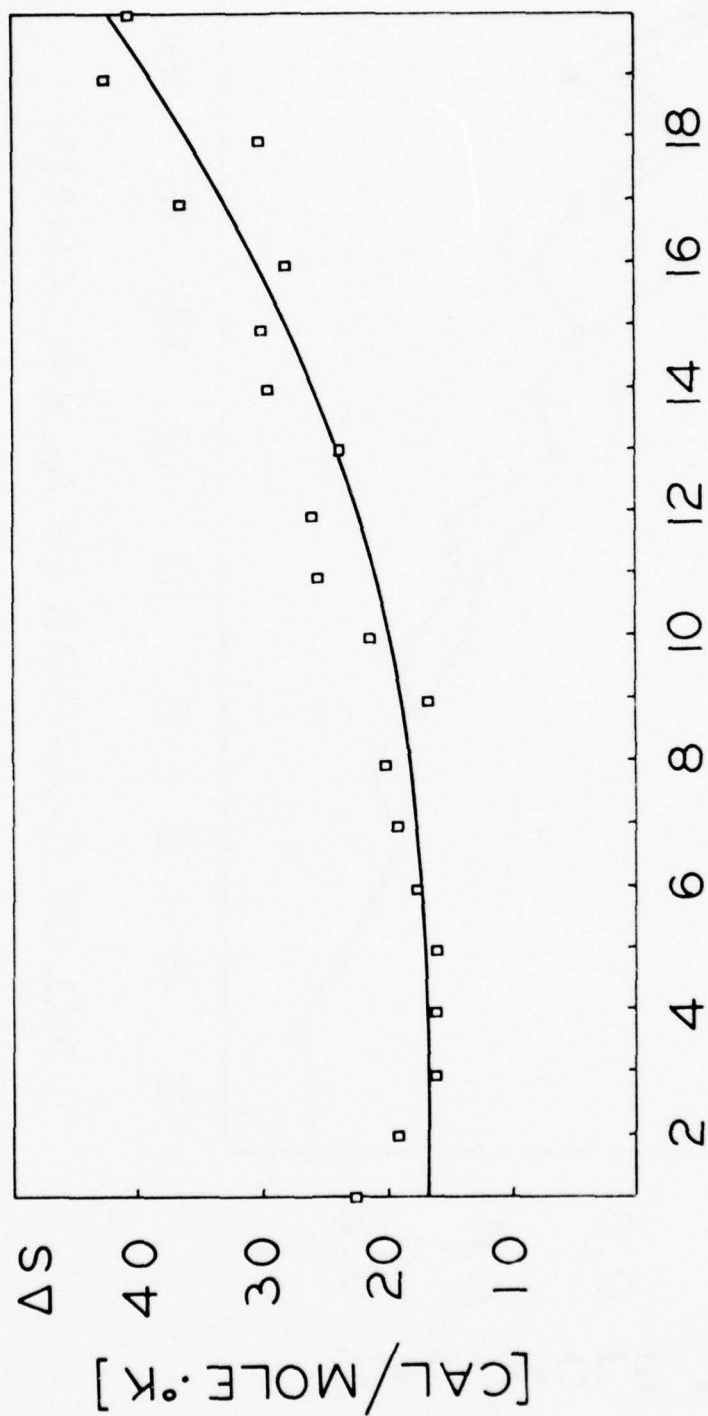


Figure 27. Heats of transitions in the melt of cholesteryl S-alkyl thiocarbonates: Δ —, cholesteric-isotropic transitions; \circ —, smectic-cholesteric transitions.



NO. OF C-ATOMS OF ALKYL CHAIN

Figure 28. Entropy of fusion of S-cholesteryl alkyl thiocarbonates.

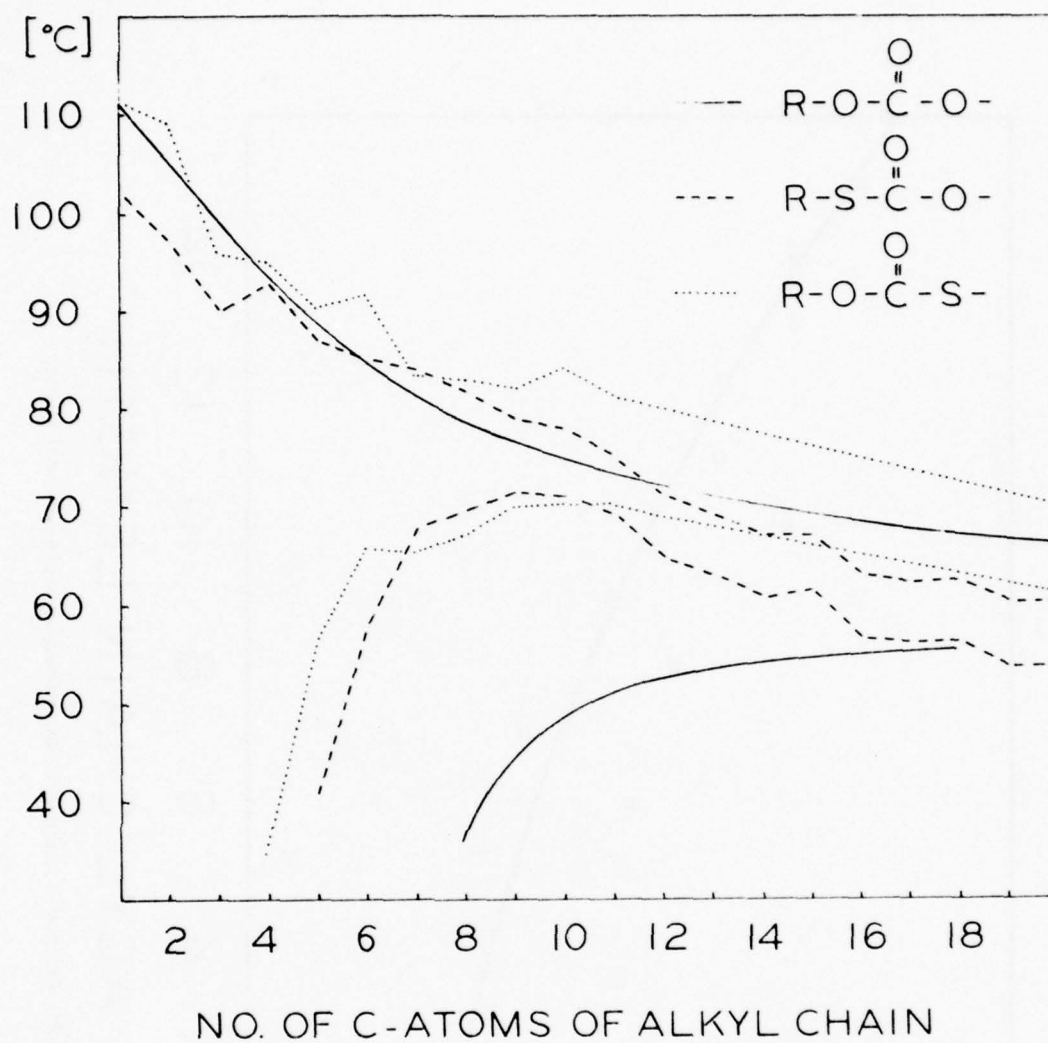


Figure 30. Smectic-cholesteric and cholesteric-isotropic transitions of —, cholesteryl alkyl carbonates; —, cholesteryl S-alkyl thiocarbonates; . . . , S-cholesteryl alkyl thiocarbonates.

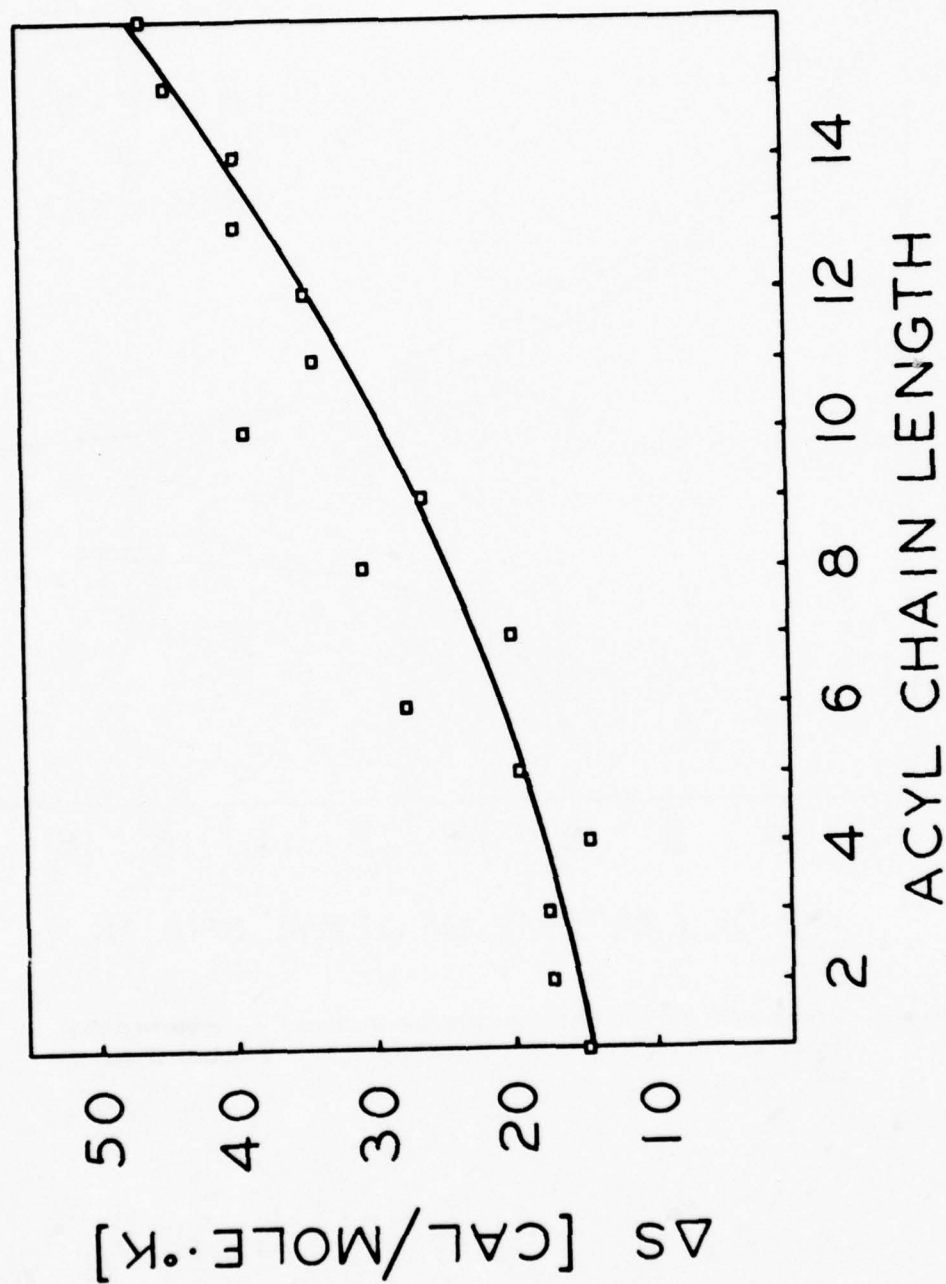


Figure 31. Entropy of fusion of 5 α -cholestan-3 β -yl ω -phenylalkanethioates.

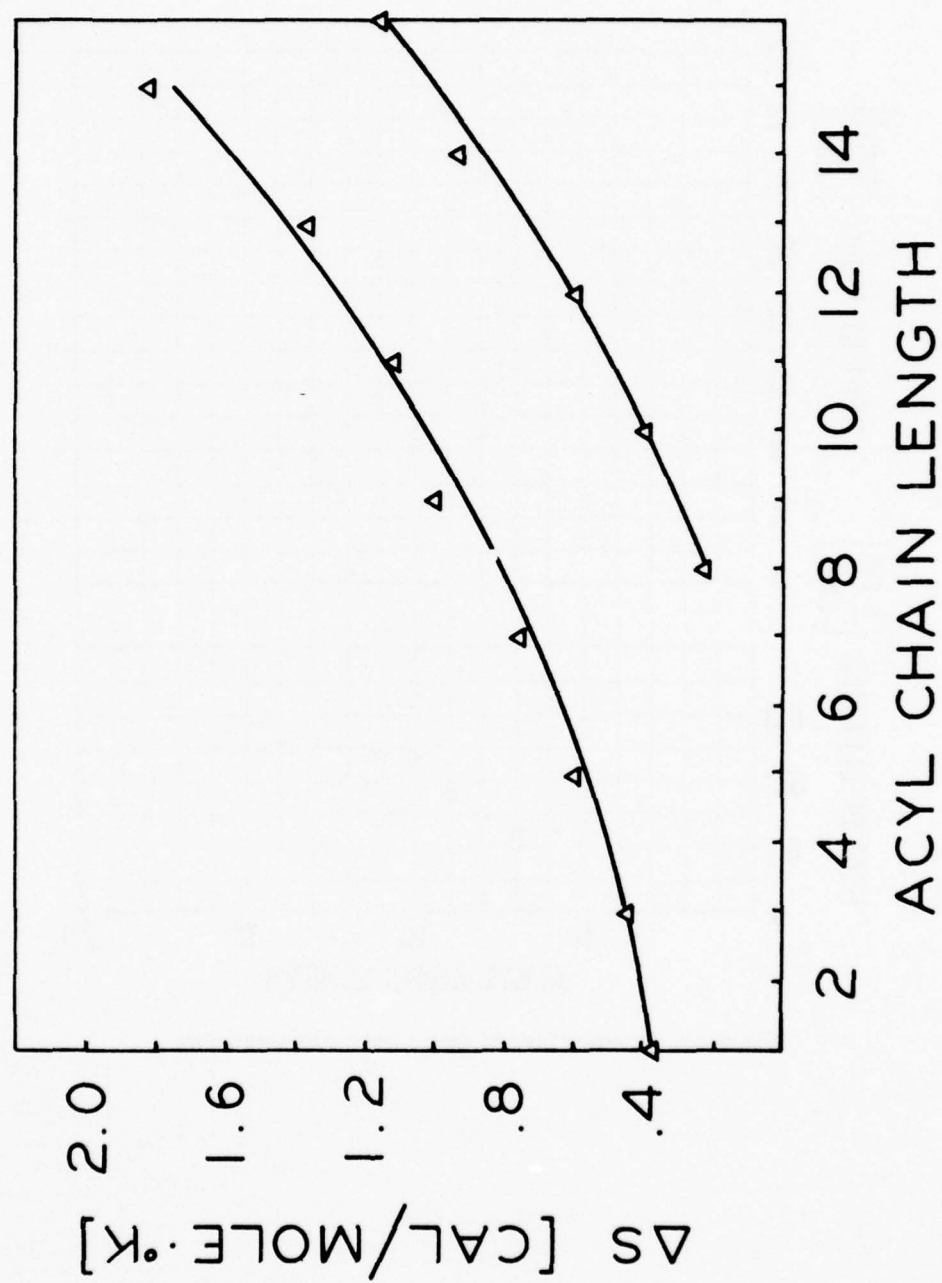


Figure 32. Entropy of the cholesteric-isotropic phase transitions.

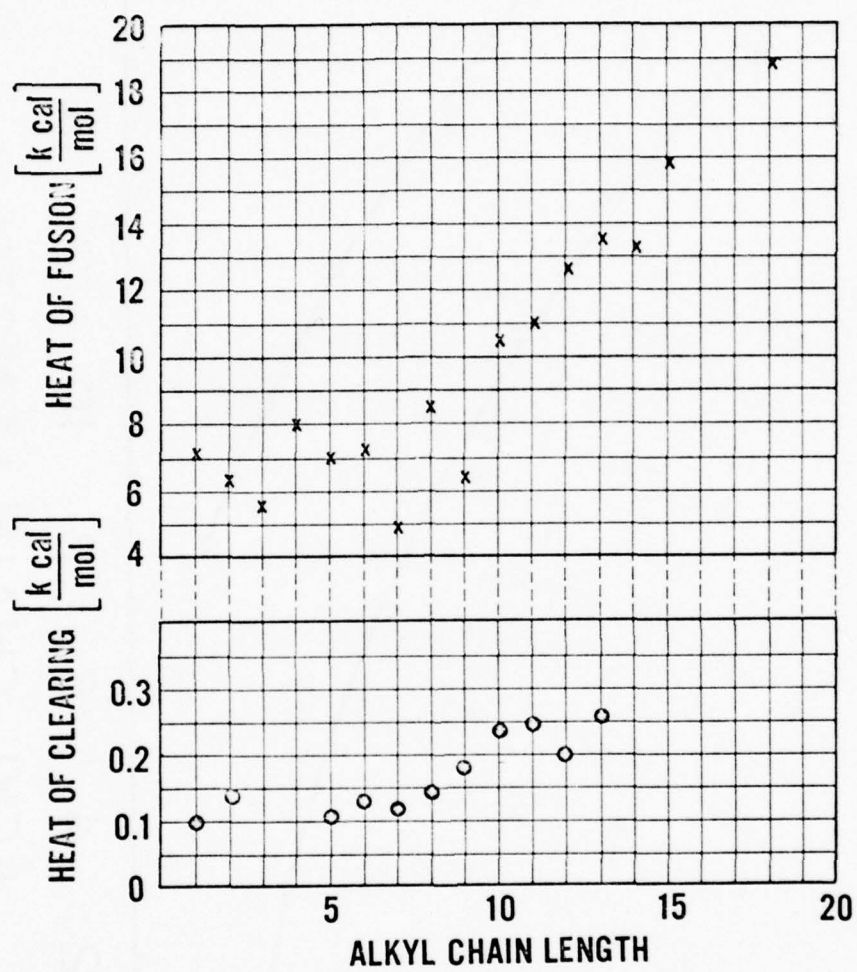


Figure 33. Transition heats of cholestanyl n-alkyl carbonates.

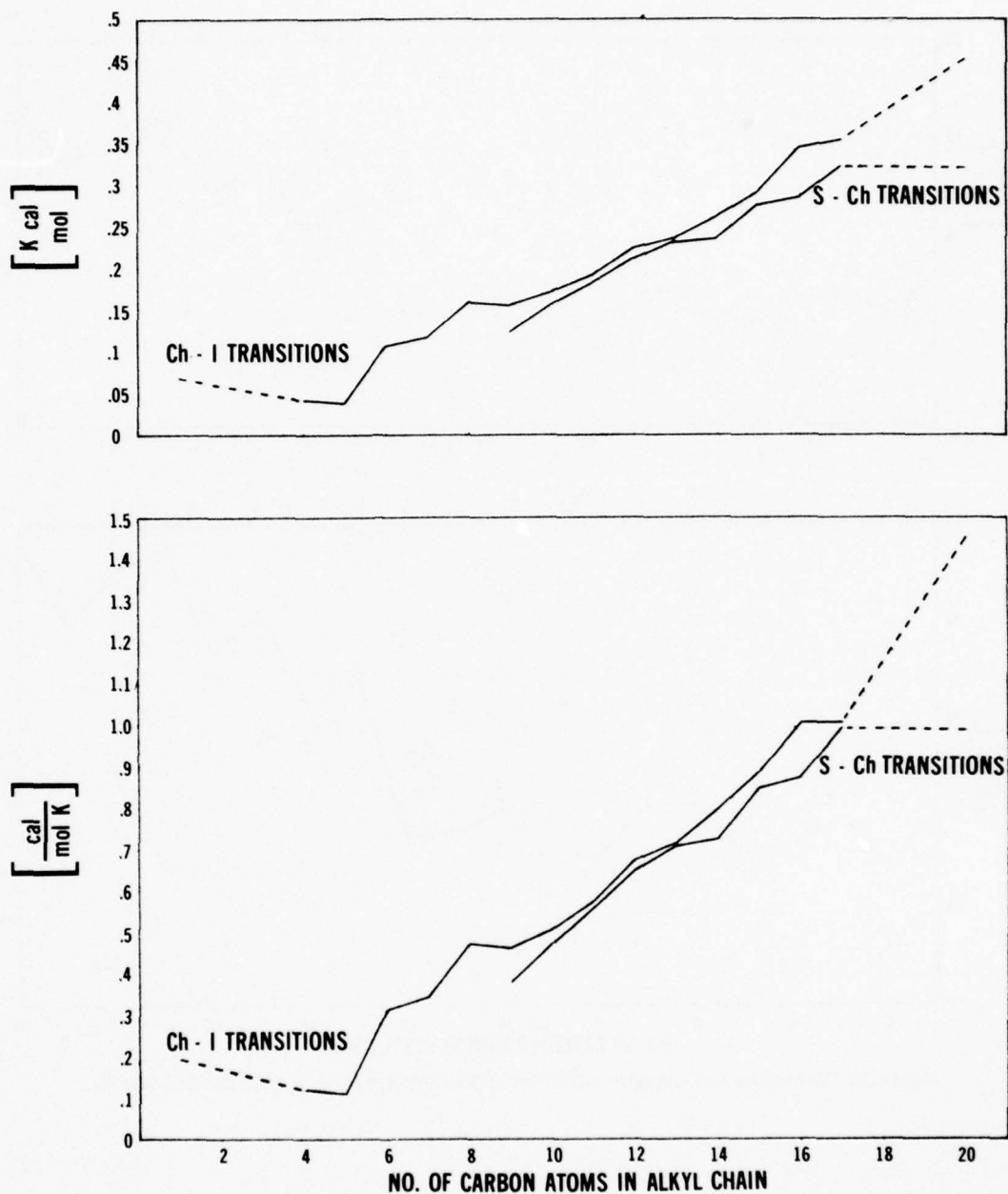


Figure 34. Enthalpies and entropies of cholesteric-isotropic transitions and smectic-cholesteric transitions for 5α -cholestan- 3β -yl S-alkyl thiocarbonates.

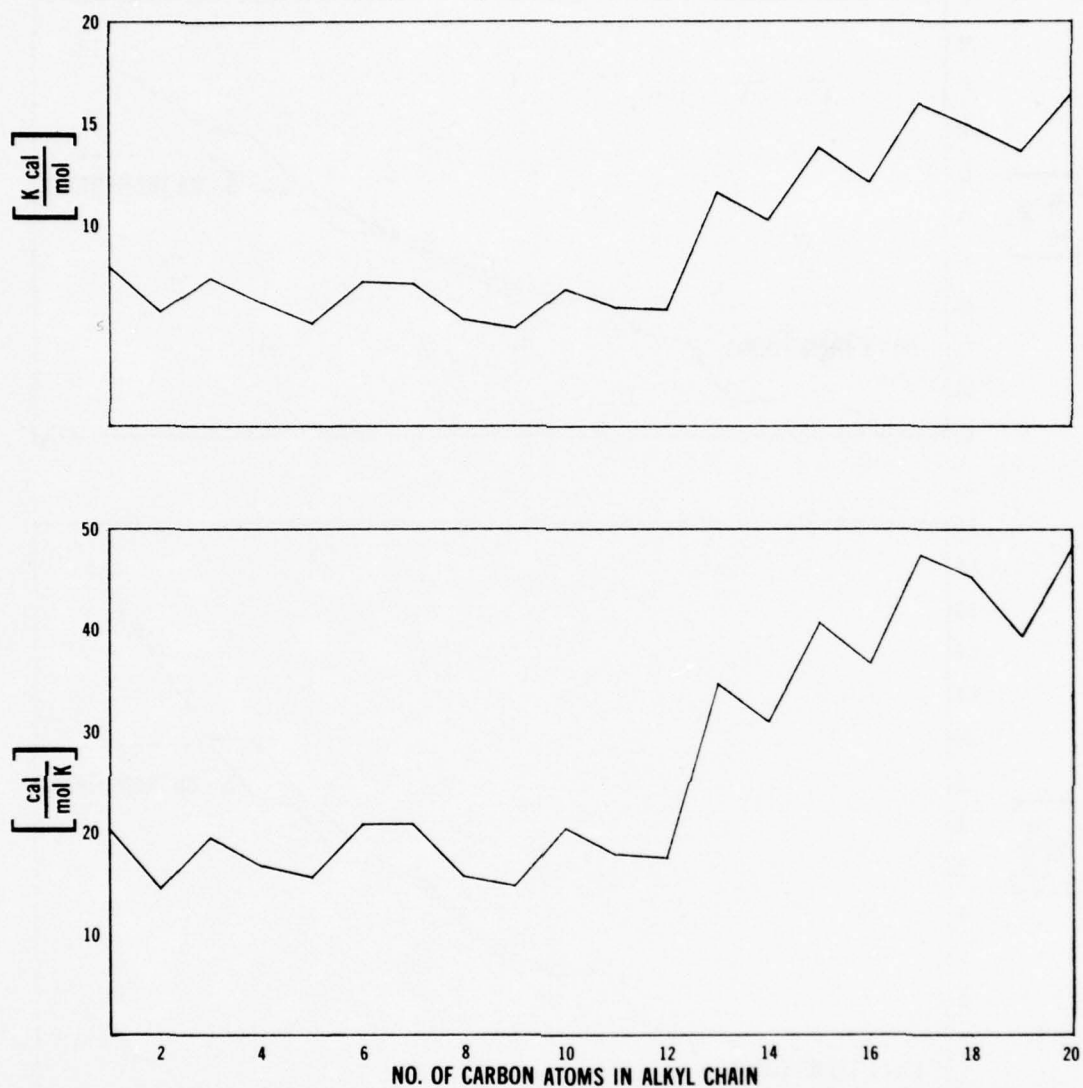


Figure 35. Enthalpies and entropies of fusion of 5 α -cholestan-3 β -yl S-alkyl thiocarbonates.

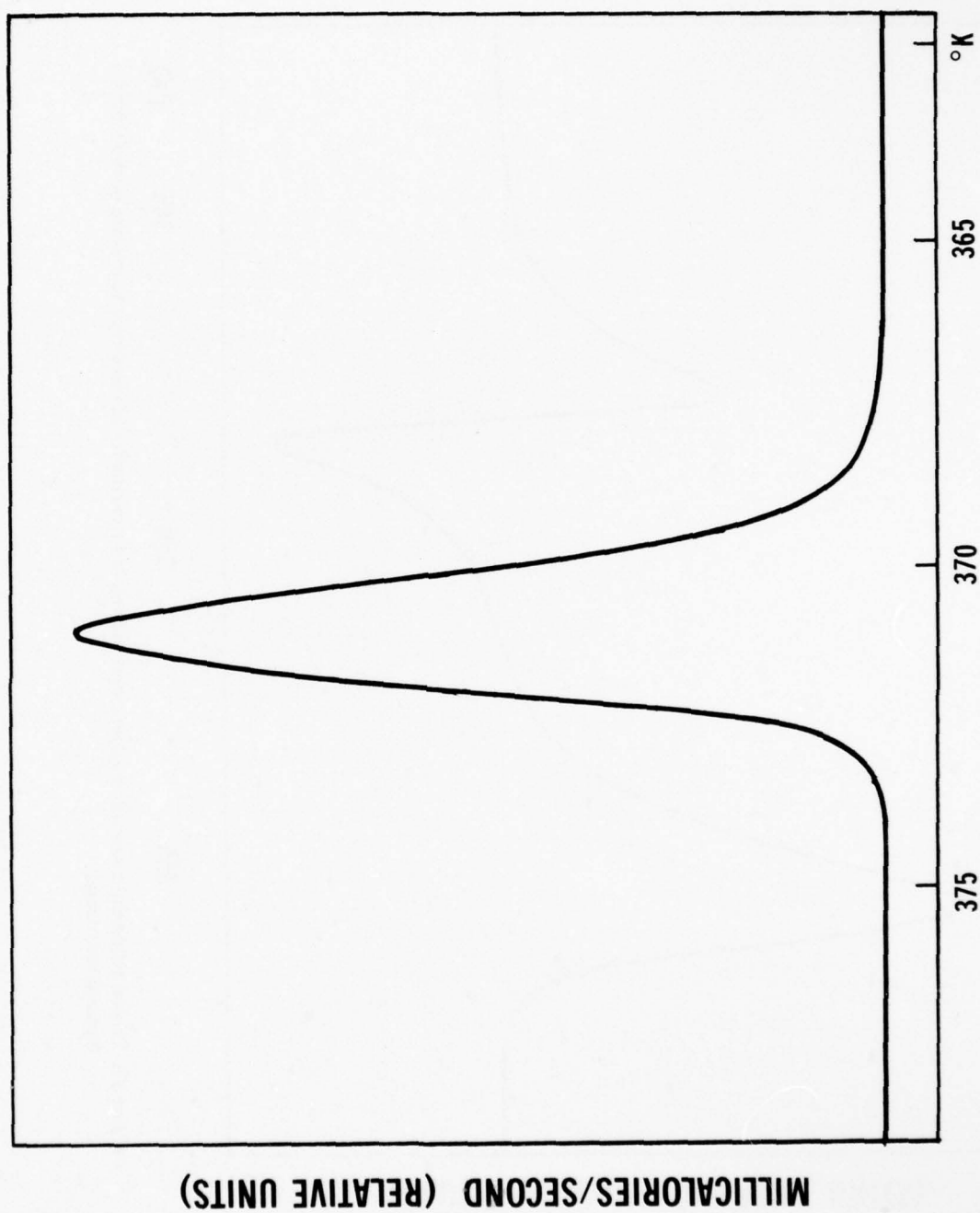


Figure 36. Typical shape of a melting transition curve (S-cholesteryl 8-phenyloctanoate).

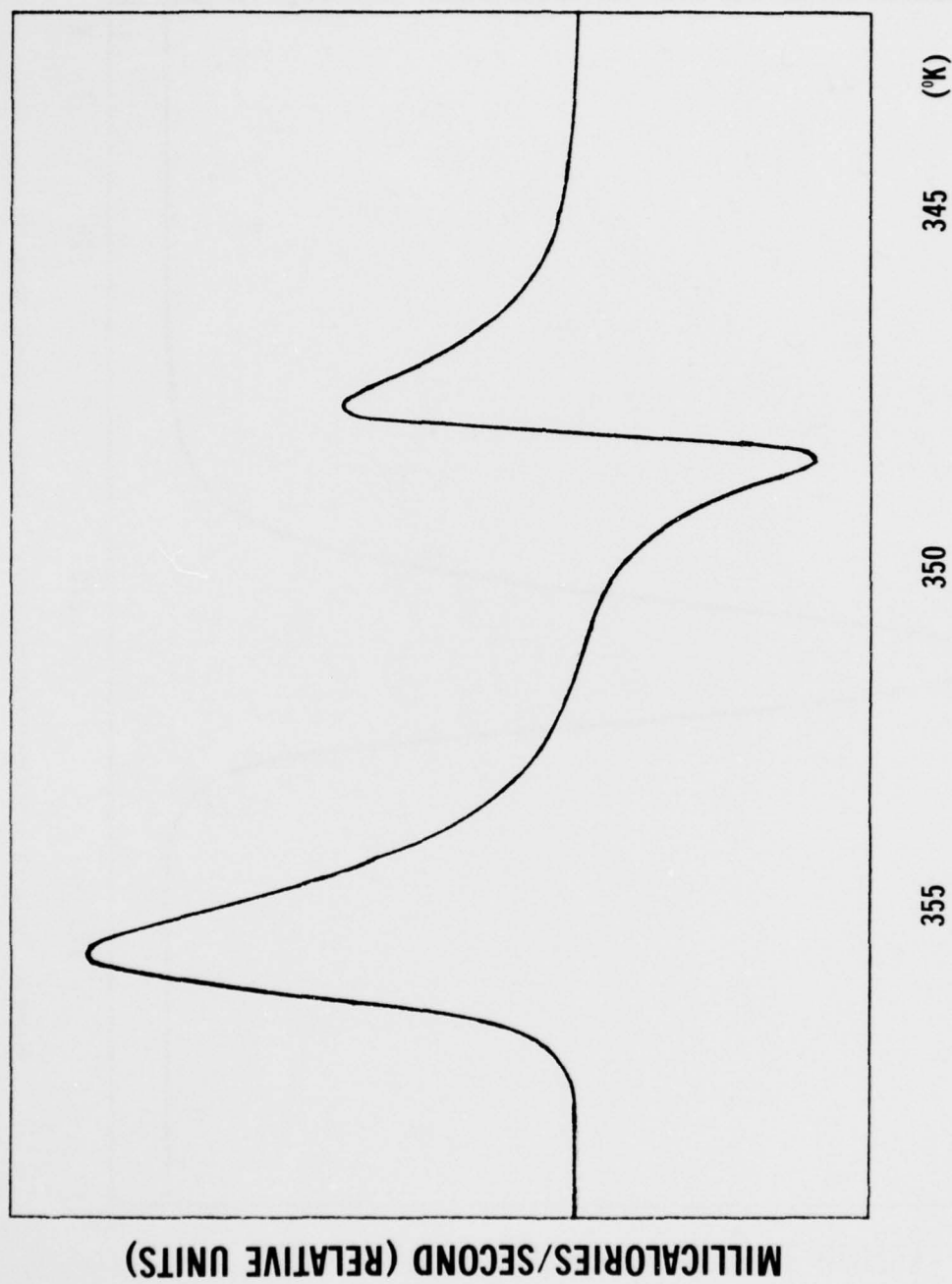


Figure 37. Typical solid-solid transition involving some melting and recrystallization just prior to melting (S-cholesteryl 6-phenylhexanoate).

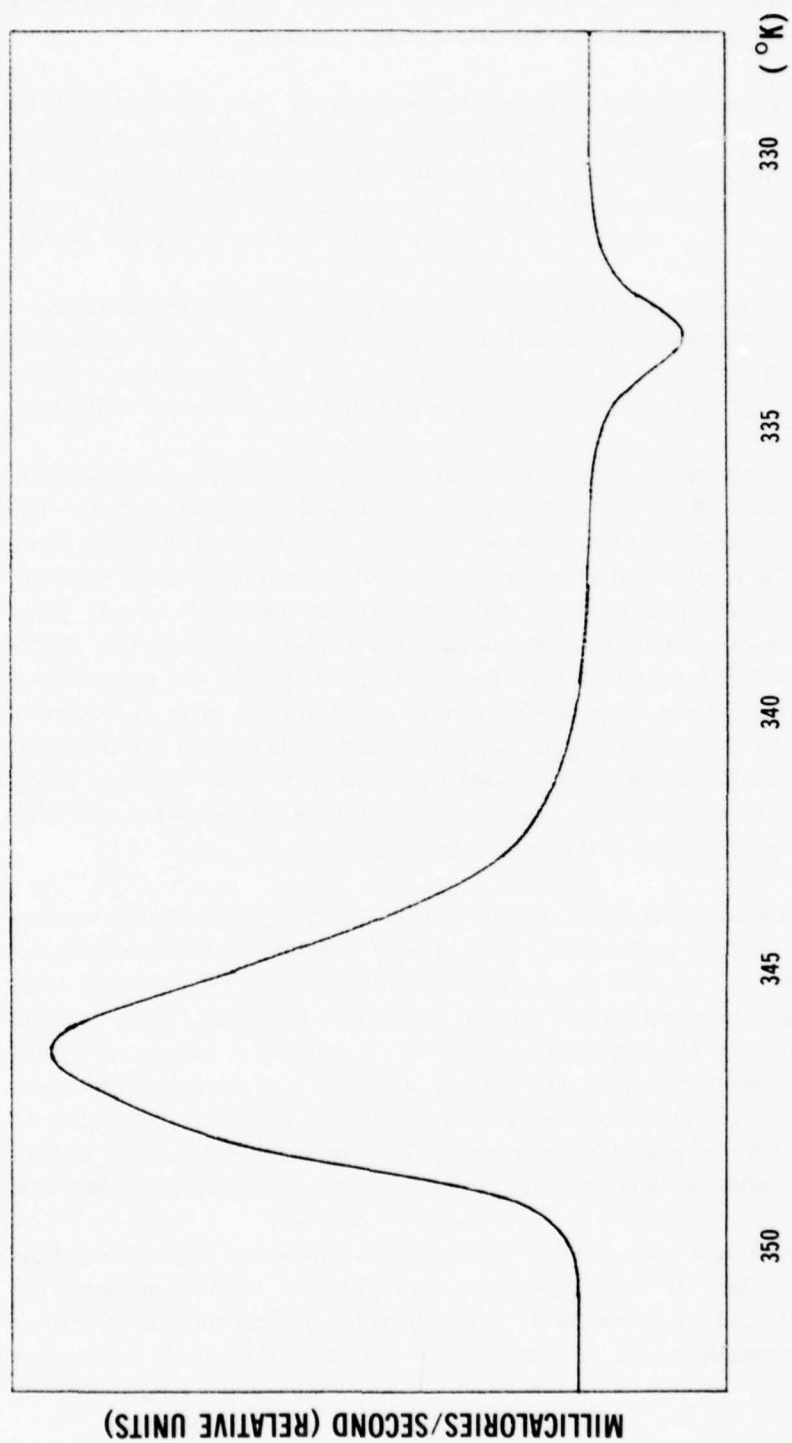


Figure 38. Solid-solid transition occurring just prior to melting (5 α -cholestan 3 β -yl eicosyl thiocarbonate).

Figure 39 shows a typical cooling curve of an isotropic-cholesteric transition on the right followed by a cholesteric-smectic transition.

An interesting and unexplained phenomenon was observed with 84 out of 87 of those thio compounds which exhibit cholesteric-isotropic transitions. Thio compounds have an atom of sulfur substituted for the oxygen atom in the 3 β -position of the various cholesteryl derivatives. These sulfur-containing liquid crystals belong to the homologous series II, IV, VI, VII, and XI listed in Section IV.A.1.

When run on the Perkin-Elmer DSC-1, these compounds exhibited a very small extra endothermic peak located anywhere from 1° to 3.6° below the peak of the clearing-point curve — the average being 2.1°. The heats involved are on the order of 1% to 10% of the heats of the corresponding cholesteric-isotropic transitions.

The only thio compounds which did not show this extra peak were members 10, 12, and 14 of the S-cholesteryl ω -phenylalkanethioate series. The hexadecanethioate showed the extra peak on only one run. In all probability, members 10, 12, and 14 would have shown the peak if it were not for baseline noise. Apparently the heats involved in these instances were just too small to see. None of the numerous non-thio compounds were observed to display this extra peak. Microscopic examination failed to reveal any changes in appearance at the temperatures where the tiny peak appeared. Figure 40 shows a typical heating curve of this small, unexplained peak occurring between the smectic-cholesteric transition (on the right) and the cholesteric-isotropic curve. Figure 41 shows an extra peak occurring during cooling. Figure 42 shows two extra peaks occurring during heating; while in Figure 43 one of the extra peaks occurs in the smectic mesophase.

5. Temperature of Color Bands. Table 2 lists the temperature regions associated with the platelet and regular color bands of various members of the homologous series which were purified by chromatographic methods. The platelet band has a higher average temperature and appears just above the regular color band in the table. The colors are abbreviated as follows: V = violet, I = indigo, B = blue, A = aqua, G = green, Y = yellow, O = orange, and R = red. An asterisk indicates crystalline cholesteric colors; a dash indicates no observable cholesteric color; and an "X" indicates that the compound was not made. In some cases only a faint or very faint violet or blue color could be observed — generally over a wide temperature range.

One should expect some inaccuracies which are larger than those implied by the last digit of the temperature values, because in most instances the width of the color band was subjectively determined by the human eye. Although most of the compounds listed are cholesteric, we reported only relatively stable color

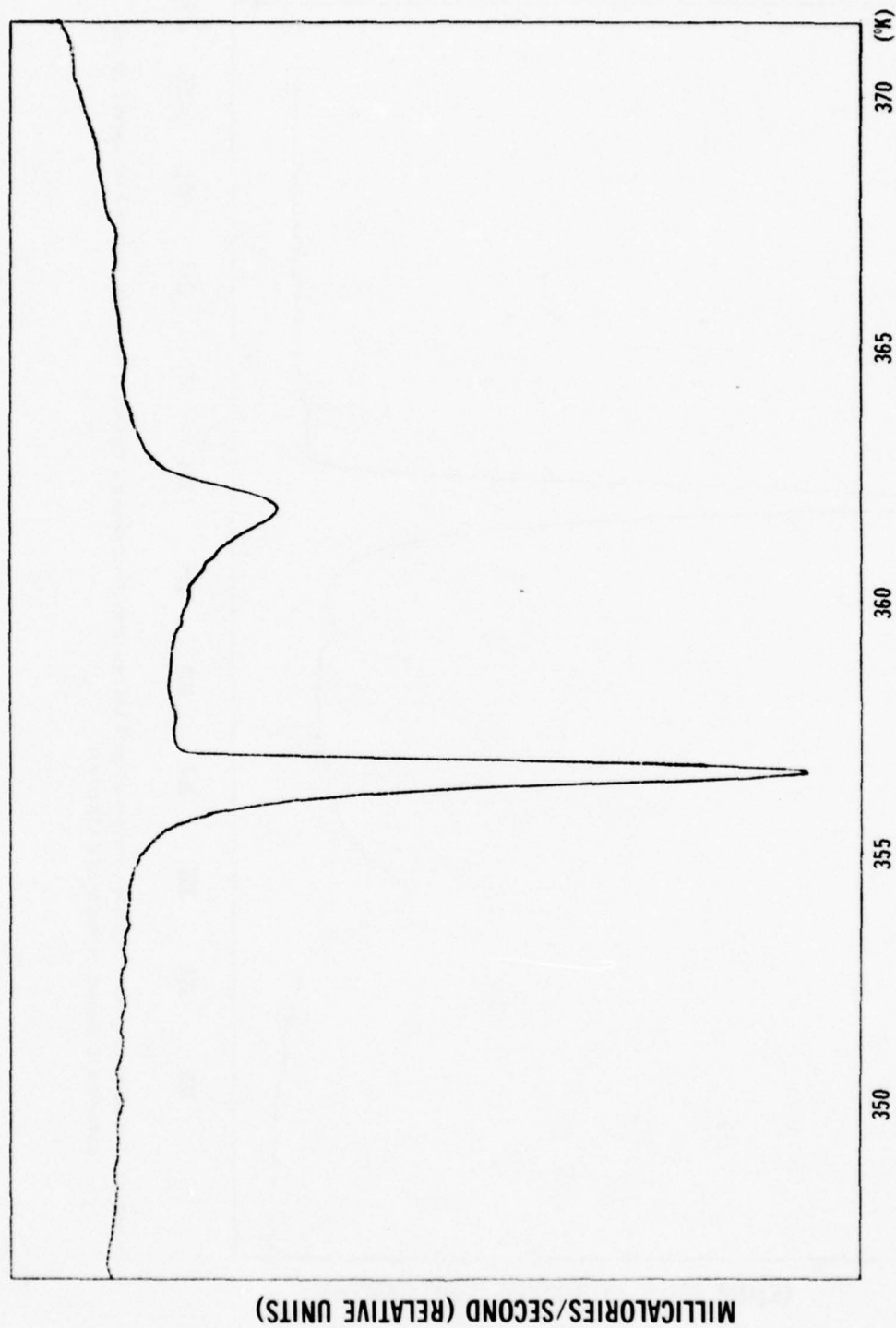


Figure 39. Typical cooling curve showing isotropic-cholesteric transition (on right) and cholesteric-smectic transition (S-cholestery) tridecanethioate).

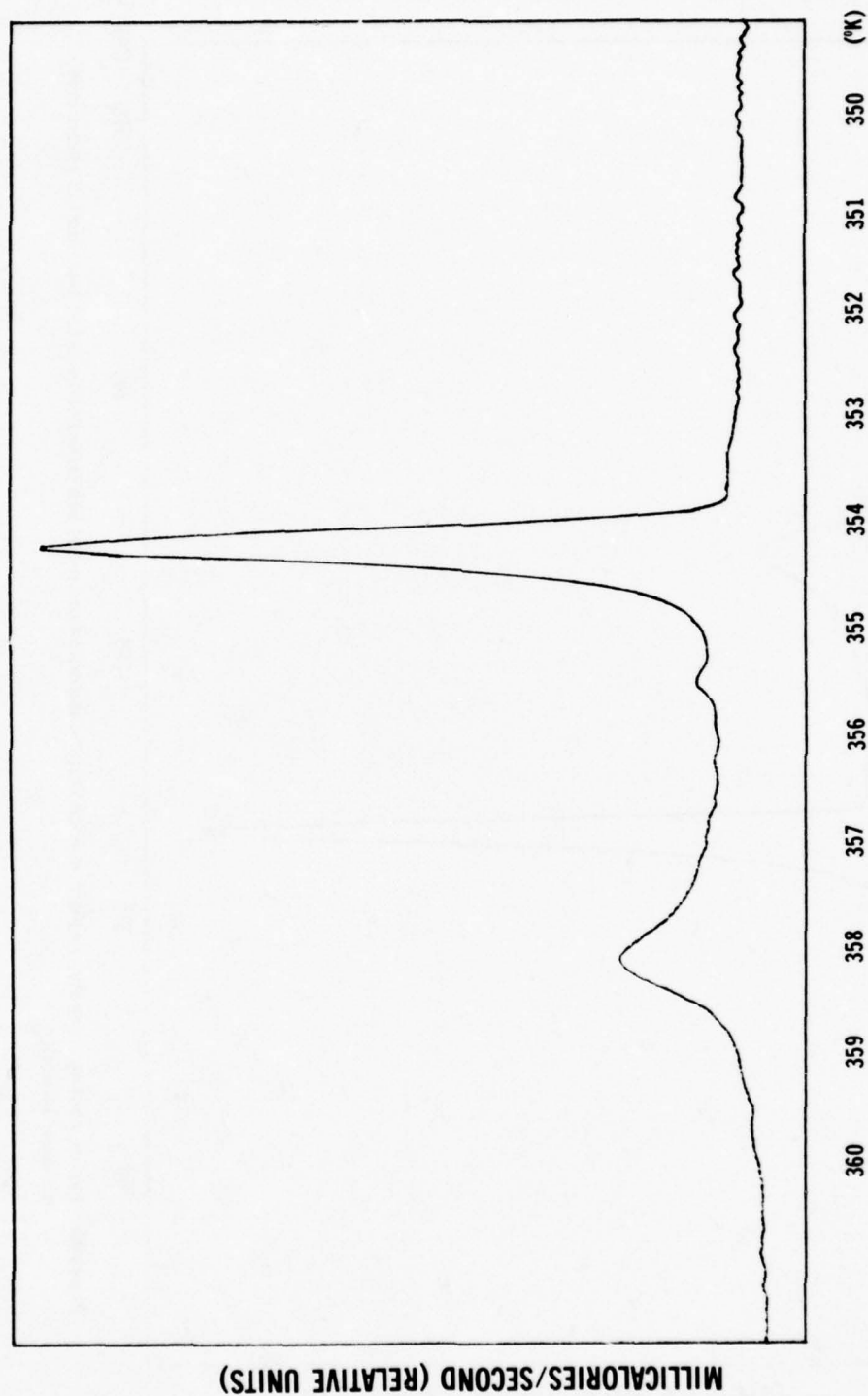


Figure 40. Typical heating curve showing unexplained peak between smectic-cholesteric transition (on right) and the cholesteric-isotropic transition (S-cholesteryl heptadecanethioate).

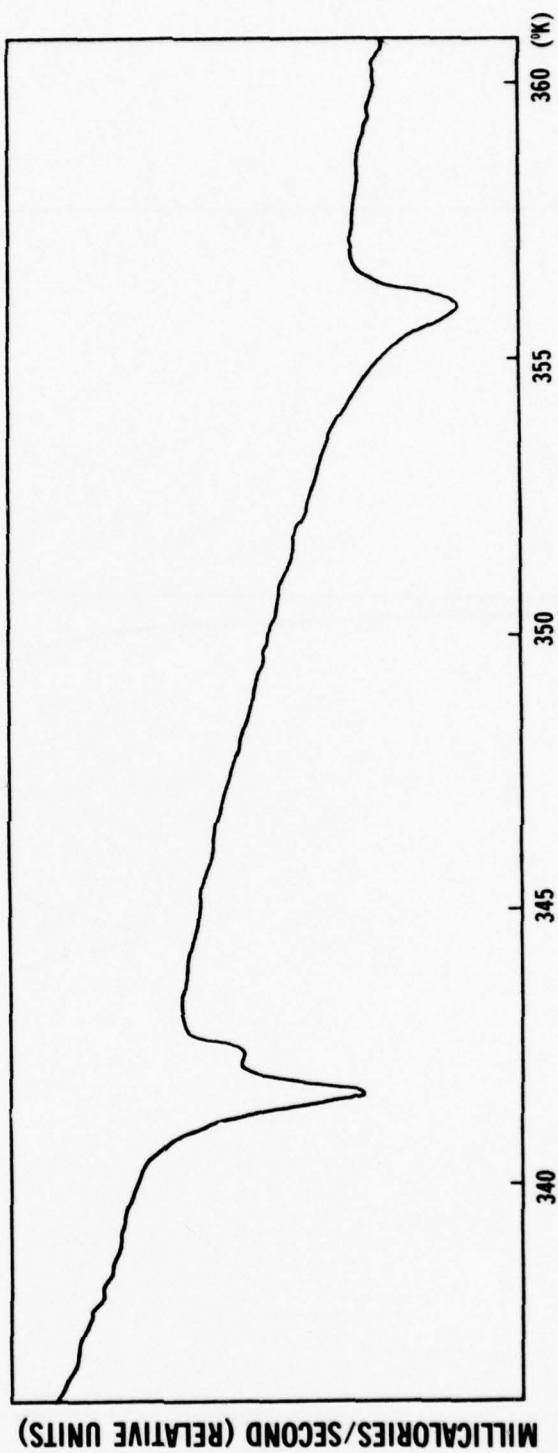


Figure 41. Cooling curve showing unexplained peak between isotropic-cholesteric transition (on right) and cholesteric-smectic transition (S-cholesteryl nonyl thiocarbonate).

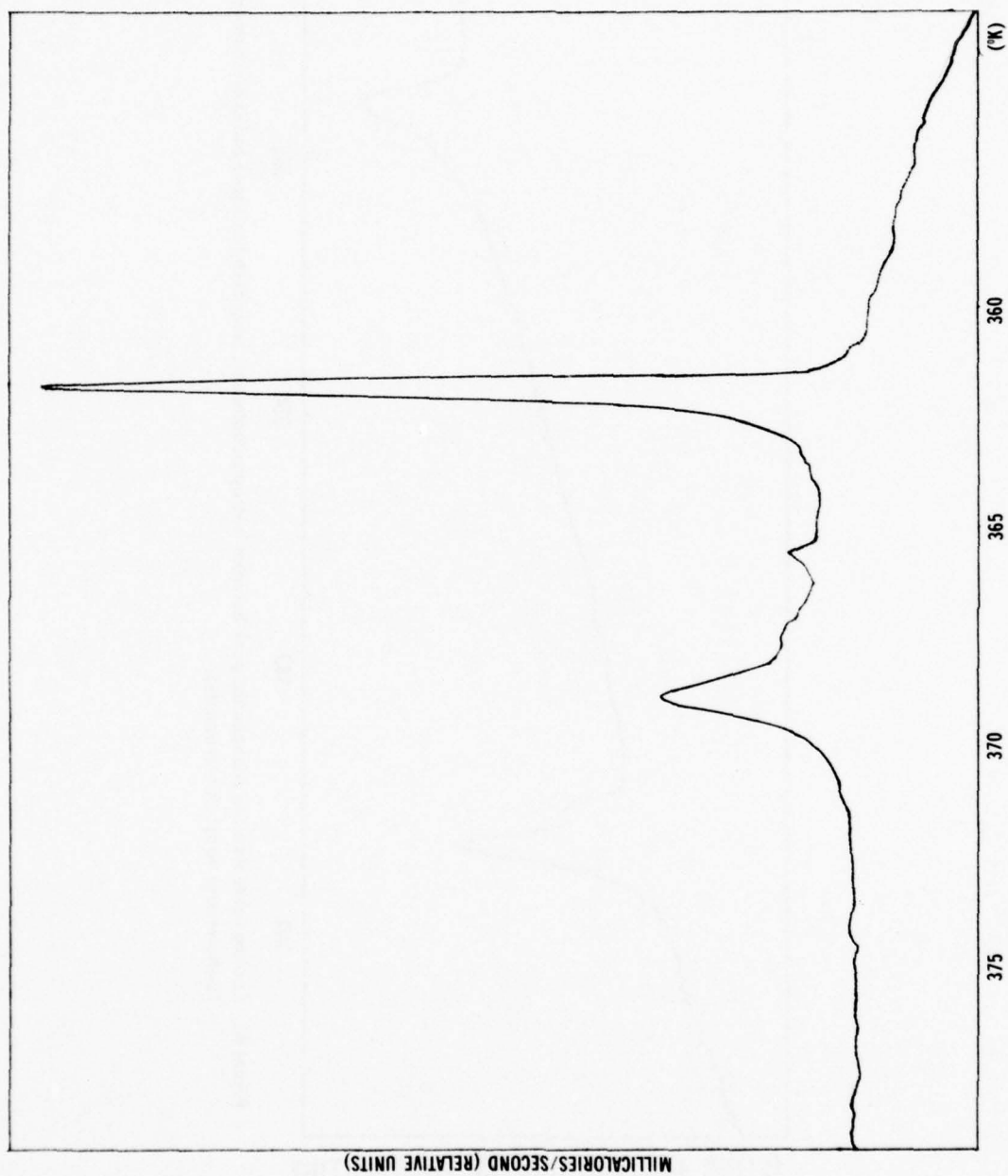


Figure 42. Heating curve showing two reproducible unexplained peaks between the smectic-cholesteric transition (on right) and the cholesteric-isotropic transition (S-cholesteryl undecanethioate).

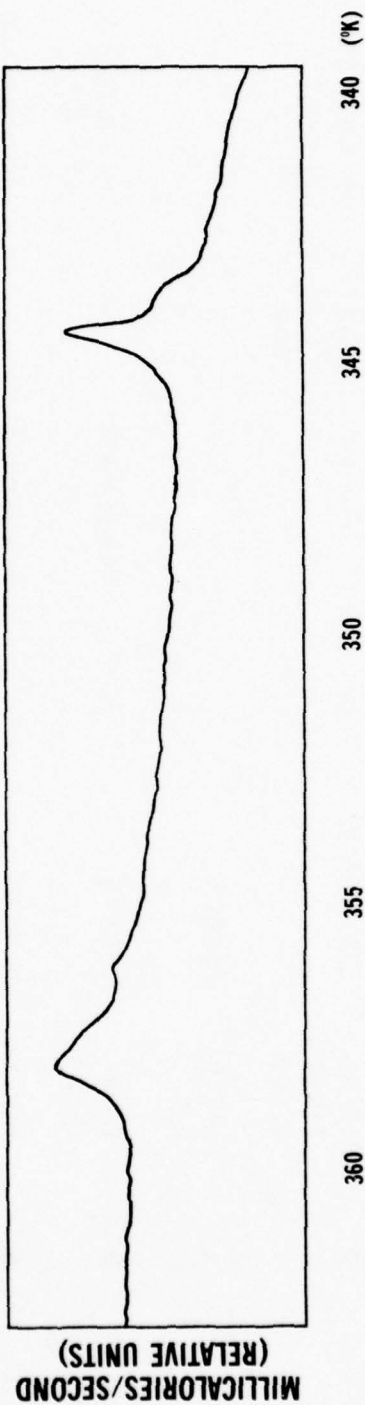


Figure 43. Heating curve showing unexplained peaks just prior to the smectic-cholesteric transition (on right) and the cholesteric-isotropic transition (S-cholesteryl decyl thiocarbonate).

Table 2. Temperature Ranges (°C) of Platelet and Regular Cholesteric Colors for Eleven Homologous Series

Member	Cholesteryl Alkanoates		S-Cholesteryl		Cholesteryl	
	Platelets	Regular Colors	Platelets	Regular Colors	Platelets	Regular Colors
1	—	—	—	On fast cooling V-R	178.7-?	—
2	—	94.6-46 G-R FP = 77	—	—	—	—
3	114.62- 114.57 V, G, R	113.6-40 V-R	—	—	114.5- 114.2 G-R	95.6-69.7 GY-Y FP = 69.7
4	111-108 B-G	107-92 V	—	—	—	—
5	108.8- 107.2 V-G	105-85 V	—	44.8-36.9 V-R	—	61.2-R.T. A-GY FP ~ R.T.
6	100.2-90+ V-G	97-70 V	—	44.8-34.9 V-R	—	28.7-<R.T. V-R
7	—	~ 89 B	—	72.7-71.6 V-R	83.1 G-Y FP = CP	82.5-<R.T. FP = 72
8	—	On fast cooling V-R	—	74-73 V-R	—	On fast cooling V-R
9	92.9- 75.8 V-G	77.9-76.5 V-R	—	—	76.65- 74.5 V-Y	—

Table 2. Temperature Ranges (°C) of Platelet and Regular Cholesteric Colors for Eleven Homologous Series (Cont'd)

Member	Cholesteryl Alkanoates			S-Cholesteryl			Cholesteryl		
	Platelets	Regular Colors		Platelets	Alkanethioates		Platelets	ω -Phenylalkanoates	
		87.9-? V-G	76.8-76.1 not all colors		Regular Colors	Platelets		Regular Colors	Platelets
10									
11									
12									
13									
14									
15									
16									
17									
18									
19									
20									
21									
22									

Table 2. Temperature Ranges (°C) of Platelet and Regular Cholesteric Colors for Eleven Homologous Series (Cont'd)

Member	S-Cholesteryl		Cholesteryl		Cholesteryl S-Alkyl	
	ω -Phenylalkanethioates		Alkyl Carbonates		Thiocarbonates	
	Platelets	Regular Colors	Platelets	Regular Colors	Platelets	Regular Colors
1	—	—	110.95- 110.8 V, G	—	102.2- 101.2 V-G	—
2	—	—	105.8- 105.5 V, G	60-R, T, V faint	—	—
3	—	—	101-93.7 V, G, O	85-50 B FP = 50	—	—
4	—	—	94-92.7 V-O	—	—	—
5	—	—	—	On fast cooling V-G	—	—
6	—	—	—	On fast cooling V-R	—	56-53 V-R
7	92.4-91.9 Grey	43.5-34 V-R	81.3-80.3 G-R	On fast cooling V-R	—	67.9-67.82 V-R
8	—	—	78-70 G-R	41-37.4 V-R	—	~ 71.5 flash spectrum
9	—	50.3-48.1 V-R	77.2-63.5 A-Y	50-45.5 V-R	—	—
10	—	—	75.9-73.5 B-G	51-49.4 V-R	—	—

Table 2. Temperature Ranges (°C) of Platelet and Regular Cholesteric Colors for Eleven Homologous Series (Cont'd)

Member	S-Cholesteryl		Cholesteryl		Cholesteryl S-Alkyl	
	ω -Phenylalkanethioates		Alkyl Carbonates		Thiocarbonates	
	Platelets	Regular Colors	Platelets	Regular Colors	Platelets	Regular Colors
11	—	49.9-48.5 V-R	74.4-71.3 V-G	52.3-51.5 V-R	—	—
12	—	—	72.5-68.6 V-G	53-52.1 V-R	—	—
13	—	51.1-49.8 V-R	69.8-68.9 V-G	53.1-52.6 V-R	—	—
14	—	47.37-47.3 V-R	70.4-69.1 V-G	53.9-53.1 V-R	—	—
15	—	52.4-51.6 V-R	69.7-69.35 V-G	54.9-54.1 V-R	—*	—
16	—	49.6-49.5 V-R	69.2-68.95 V-G	55.7-55 V-R	—	—
17	X	X	68.65-68.4 V-G	56.2-55.7 V-R	—*	—
18	X	X	67.4-62 V	56.4-55.9 V-R	—	57.7-57.4
19	X	X	67.15-65 V, G, R	~ 56 width unk V-R FP = 60	—*	~ 52 fast cooling V-R
20	X	X	65.9-? V	—	—	~ 56.4~ 56.2 V-R
21	X	X	X	X	X	X
22	X	X	X	X	X	X

Table 2. Temperature Ranges (°C) of Platelet and Regular Cholesteric Colors for Eleven Homologous Series (Cont'd)

Member	S-Cholesteryl Alkyl		5 α -Cholestan-3 β -yl		5 α -Cholestan-3 β -yl		ω -Phenylalkanoates	
	Thiocarbonates		Alkanoates		Alkanoates		Alkanoates	
	Platelets	Regular Colors	Platelets	Regular Colors	Platelets	Regular Colors	Platelets	Regular Colors
1	111-109 V (CAP)	—	—	—	—	—	—	—
2	105-102 B Haze	—	X	X	—	—	—	—
3	96-85 B Haze	—	—	≤ 87.6 G	89.95-62 V-R	—	—	—
4	93-65 B Haze	On fast cooling V-R	—	84.95-25 V-G FP = 77	—	—	—	—
5	86-61 V Haze	57.9-56.5 V-R	—	70-25 V FP = 78	67.9~67 V-G	67-40 YG-R	—	—
6	85-57 B Haze	66.8-66 V-R	—	73.2-25 V FP = 70	—	—	—	—
7	79-65 B Haze	65.9-65.65 V-R	—	67.3-25 V-A	—	60-32 YG-R	—	—
8	80-68 B Haze	67.4-66.9 V-R	—	66-25 B-G FP = 58	32.5 B-G FP = 40	—	—	—
9	—	70.25-70.2 V	—	64-46.4 V-R	—	58.4-30 A-YO	—	—
10	82-71.5 B Turbid	70.2-70.1 V-R	—	72.6-56.4 V-R FP = 58	—	—	—	—
11	81-71 B Turbid	70.03-70.0 V-G	—	61.9-61.1 V-R	—	53.5-36 B-G FP = 36	—	—

Table 2. Temperature Ranges (°C) of Platelet and Regular Cholesteric Colors for Eleven Homologous Series (Cont'd)

Member	S-Cholesteryl Alkyl		5 α -Cholestan-3 β -yl		5 α -Cholestan-3 β -yl	
	Platelets	Regular Colors	Alkanoates	Regular Colors	Platelets	Regular Colors
Thiocarbonates						
12	80-70.5 B	70.45-70.40 V-R	—	63.6-63.1 V-R	42.25-41.8 BG	26.6-26.1 V-R
13	74-69 Bluish	68.8-68.76 V-G FP = 68	—	62.55-62.45 V-A FP = 69	—	52-30 B-R FP = 34
14	76-68.5 Bluish Turbid	67.8-67.72 V-R FP = 68.5	—	68.7-62.5 B-A	—	36-35.6 V-R
15	73-67 Bluish	66.5-66.42 V-R	—	66.7-61.1 V-B FP = 67	—	53.8-39.7 V-R
16	70-66 Bluish	65.2-65.0 V-R	—	64-58.7 B Faint	—	49-41.75 V-R
17	68-66 B	64.1-64 V-R FP = 64	—	~ 80 On fast cooling V Faint	X	X
18	65-63.5 B	63.14-63.0 V-R	—	On fast cooling V	X	X
19	68-62.5 Bluish	62-61.9 V-R FP = 62	—	On fast cooling V	X	X
20	65-61.5 Bluish	60.6-60.45 V-R FP = 64	—	On fast cooling V	X	X
21	X	X	X	X	X	X
22	X	X	X	X	X	X

Table 2. Temperature Ranges (°C) of Platelet and Regular Cholesteric Colors for Eleven Homologous Series (Cont'd)

Member	5 α -Cholestan-3 β -yl Alkyl Carbonates		5 α -Cholestan-3 β -yl S-Alkylthiocarbonates	
	Platelets	Regular Colors	Platelets	Regular Colors
1	86-85.5 V-Y	—	76.4 VB FP = 79	—
2	80.1-77.3 V-G	—	—	—
3	—	—	—	—
4	68.7-66.6 VG FP = 69.8	—	—	—
5	68.8-61 V-G	—	—	—
6	58.7-58.1 V-O	—	—	—
7	59.2-58.6 A-R	—	—	34.3-31.3 V-R
8	58.1-57 B-G	—	—	47.8-47 V-R
9	59.6-57 B-G	—	—	52.4-52.35 V-R
10	58.5-52.9 B-G	—	—	—
11	58.3-54.4 V-G	On fast cooling ~ 39.2	—	—
12	58-54.4 V-G	43.5-42.1 V-R	—	—
13	57.9-52.6 V-G	43.4-42.6 V-R	—	—
14	56.2-55.1 V-G	On fast cooling	—	—

Table 2. Temperature Ranges (°C) of Platelet and Regular Cholesteric Colors for Eleven Homologous Series (Cont'd)

Member	5 α -Cholestan-3 β -yl Alkyl Carbonates		5 α -Cholestan-3 β -yl S-Alkylthiocarbonates	
	Platelets	Regular Colors	Platelets	Regular Colors
15	56.8-56.4 B FP = 56.4	On fast cooling ~ 40.8 V-R	—	—
16	—	—	—	—
17	~ 55 B FP = 60.7	—	—	—
18	—	—	—	—
19	—	—	—	—
20	—	—	—	—
21	X	X	—	—
22	—	—	—	—

V - violet
I - indigo
B - blue
A - aqua
G - green
Y - yellow
O - orange
R - red

R.T. - room temperature
FP - freezing point
CAP - capillary

— no color
X not made
* cholesteric crystal colors

bands and did not give the estimated temperatures of those color regions which could only be temporarily observed on rapid undercooling. As a consequence these tables provide an overview of the compounds that might be useful for thermometric applications.

The most sensitive liquid crystal which we measured (noncrystallizing in the color range) was S-cholesteryl 14-phenyltetradecanethioate, which reflects the spectral range of 420 to 600 nm within 0.07° and thereby allows the detection of temperature variations of $2 \times 10^{-5}^\circ$.

Although S-cholesteryl dodecyl thiocarbonate had a color bandwidth of $0.065 \pm 0.005^\circ$ and cholestanyl S-nonyl thiocarbonate had a bandwidth of $0.05 \pm 0.01^\circ$, both crystallized in the color range and would therefore probably not be useful in practical application.

The most sensitive liquid crystals, having color bandwidths of 0.25° or less, are listed in Table 3. Since five compounds were too pure to exhibit a complete color spectrum, from 0.08% to 10% cholesteryl chloride had to be added, depending on the compound, to produce a color spectrum.

6. Dependence of Selective Reflectance on Temperature and Wavelength.

The temperature and wavelength dependence of the selective reflection was investigated for relatively few compounds.⁷⁵⁻⁷⁶ The samples were films about 20 μm thick which exhibited a polydomain structure of planar texture elements. It was estimated that the helical axes of the domains were aligned to within a few degrees of the surface normal (see section II.B.2). The incident and selectively reflected light rays filled a narrow cone perpendicular to the sample surface. Because of the small angular dependence of the selective reflectance for light incident and reflected close to the average direction of the helical axes (see Figure 9), the measured data should be representative of perpendicular incidence and perpendicular selective reflection.

Figures 5, 7, and 8 show the wavelength dependence of the selective reflection at various temperatures as well as the temperature dependence of the peak wavelength and of the selective reflectance of monochromatic light of cholesteryl oleyl carbonate,⁷⁷ S-Cholesteryl 14-phenyltetradecanethioate,⁷⁸ cholesteryl nonanoate, and cholesteryl erucyl carbonate (containing 5% of cholesteryl chloride to achieve wetting of the glass substrate and thus a good sample) are the only other

⁷⁵ R. D. Ennulat, *Mol Cryst Liq Cryst*, 13, 337 (1971).

⁷⁶ R. D. Ennulat, L. E. Garn, and J. D. White, *Mol Cryst Liq Cryst*, 26, 245 (1974).

⁷⁷ R. D. Ennulat, *Mol Cryst Liq Cryst*, 13, 337 (1971).

⁷⁸ R. D. Ennulat, L. E. Garn, and J. D. White, *Mol Cryst Liq Cryst*, 26, 245 (1974).

Table 3. Liquid Crystals with Cholesteric Color Bandwidths of 0.25° or Less

Liquid Crystal	Bandwidth (°C)	Average Temperature (°C)	Melting Point (°C)	Freezing Point (°C)	Comments
5 α -cholestan-3 β -yl s-nonyl thiocarbonate	.05 \pm .01	52.4	61	53	crystallizes in color range
s-cholesteryl dodecyl thiocarbonate	.06	69	93	71	can crystallize in color range
s-cholesteryl 14-phenyltetradecanethioate	.07	47.35	51	very low	
5 α -cholestan-3 β -yl s-decyl thiocarbonate with 0.8% cholesteryl chloride	.075	52	62	28	
s-cholesteryl decyl thiocarbonate	.08	70.2	77	37	
s-cholesteryl pentadecyl thiocarbonate	.08	66	84	38	
cholesteryl sheptyl thiocarbonate	.08	67.5	65	56	
s-cholesteryl tetradecyl thiocarbonate	.10	68	78.5	68.5	
s-cholesteryl hexadecyl thiocarbonate	.10	65	82	37	
s-cholesteryl heptadecyl thiocarbonate	.10	64	69.9	~ 64	crystallizes in color range
s-cholesteryl nonadecyl thiocarbonate	.10	62	75.35	~ 68	crystallizes in color range
s-cholesteryl 10-phenyldecanethioate with 10% cholesteryl chloride	.12	28	—	—	9% cholesteryl chloride may work better
s-cholesteryl octadecyl thiocarbonate	.14	63	64	48	
s-cholesteryl 12-phenyldodecanethioate with 7% cholesteryl chloride	.14	34	—	very low	
s-cholesteryl 16-phenylhexadecanethioate	.14	49.5	~54.6	very low	
s-cholesteryl eicosyl thiocarbonate	.15	60.5	70.5	~ 65	crystallizes in color range
s-cholesteryl undecyl thiocarbonate with 8% cholesteryl chloride	.18	62	—	—	
cholesteryl 10-phenyldecanoate	.20	39.4	77.25	apparently low	The only liquid crystal in this list not containing sulfur.

Table 3. Liquid Crystals with Cholesteric Color Bandwidths of 0.25° or Less (Cont'd)

Liquid Crystal	Bandwidth (°C)	Average Temperature (°C)	Melting Point (°C)	Freezing Point (°C)	Comments
cholesteryl s-eicosyl thiocarbonate	.20 ± .1	56.3	64	57	
cholesteryl s-hexadecyl thiocarbonate (old)	.20	55	53	very low	
cholesteryl s-hexadecyl thiocarbonate (new) with 0.9% cholesteryl chloride	.25	55	53	25	freezing point taken with DSC-1 at a cooling rate of 10°/minute

compounds for which a set of data has been reported.⁷⁹ As indicated by the influence of the thermal history on the selective reflectance, the degree of alignment within these polydomain samples was insufficient for the determination of the selective reflectivity. Consequently, only gross variations of the intensity observed under identical experimental conditions may be meaningful.

7. Chain-Length Dependence of the Color Band. The influence of the acyl chain length on the temperature range of the color band was investigated with cholesteryl alkanoates,⁸⁰ and S-cholesteryl ω -phenylalkanethioates.⁸¹ The former series is reported to exhibit color bands from the propionate to the hexanoate and from the nonanoate to the octadecanoate which, except for minor variations, decrease from about 30° to 3° for the octadecanoate. Considering that these materials were of unspecified origin and that in this homologous series of pure alkanoates only the nonanoate and the decanoate have well-defined color bands (see Table 2), we conclude that impurity effects must be responsible for this discrepancy. This is confirmed by Kassubek and Meier who have obtained a maximum pitch p of 0.310 μm (i.e., $\lambda_{p_{\text{max}}} = np \approx 1.5 \times 0.310 \mu\text{m} = 0.465 \mu\text{m}$) at 88° for the pure propionate and of about 0.300 μm (i.e., $\lambda_{p_{\text{max}}} \sim 0.450 \mu\text{m}$) at 86° for the pure pentanoate.⁸²

Furthermore, they found only a linear decrease of these pitches with temperatures to over 100° and did not observe the nonlinear dependence characteristic of pre-transitional effects.

In the S-cholesteryl ω -phenylalkanethioates, the relation between the temperature width of the color band and the chain length dependence indicates an odd-even effect (Figure 44). For odd acyl chain lengths, the temperature interval decreases with increasing chain length at the rate of 0.16° per methylene group, while it increases with even chain length at about half that rate. Considering the linearity of the odd branch and assuming linearity for the even branch, one should observe a crossover at about the 16-phenylhexadecanethioate and no color bands for the 19-phenylnonadecanethioate and higher odd members. By the same token, extrapolation of the even branch toward shorter chain length implies that no even member lower than 14-phenyltetradecanethioate should exhibit a color band. Experimental experience supports the latter speculation. This odd-even effect is in phase with that observed for the cholesteric-smectic and the cholesteric-isotropic transition

⁷⁹ R. D. Ennulat, *Mol Cryst Liq Cryst*, **13**, 337 (1971).

⁸⁰ S. P. Brown, *Mater Eval*, **26**, 163 (1968).

⁸¹ R. D. Ennulat, to be published.

⁸² P. Kassubek and G. Meier, *Mol Cryst Liq Cryst*, **8**, 305 (1969).

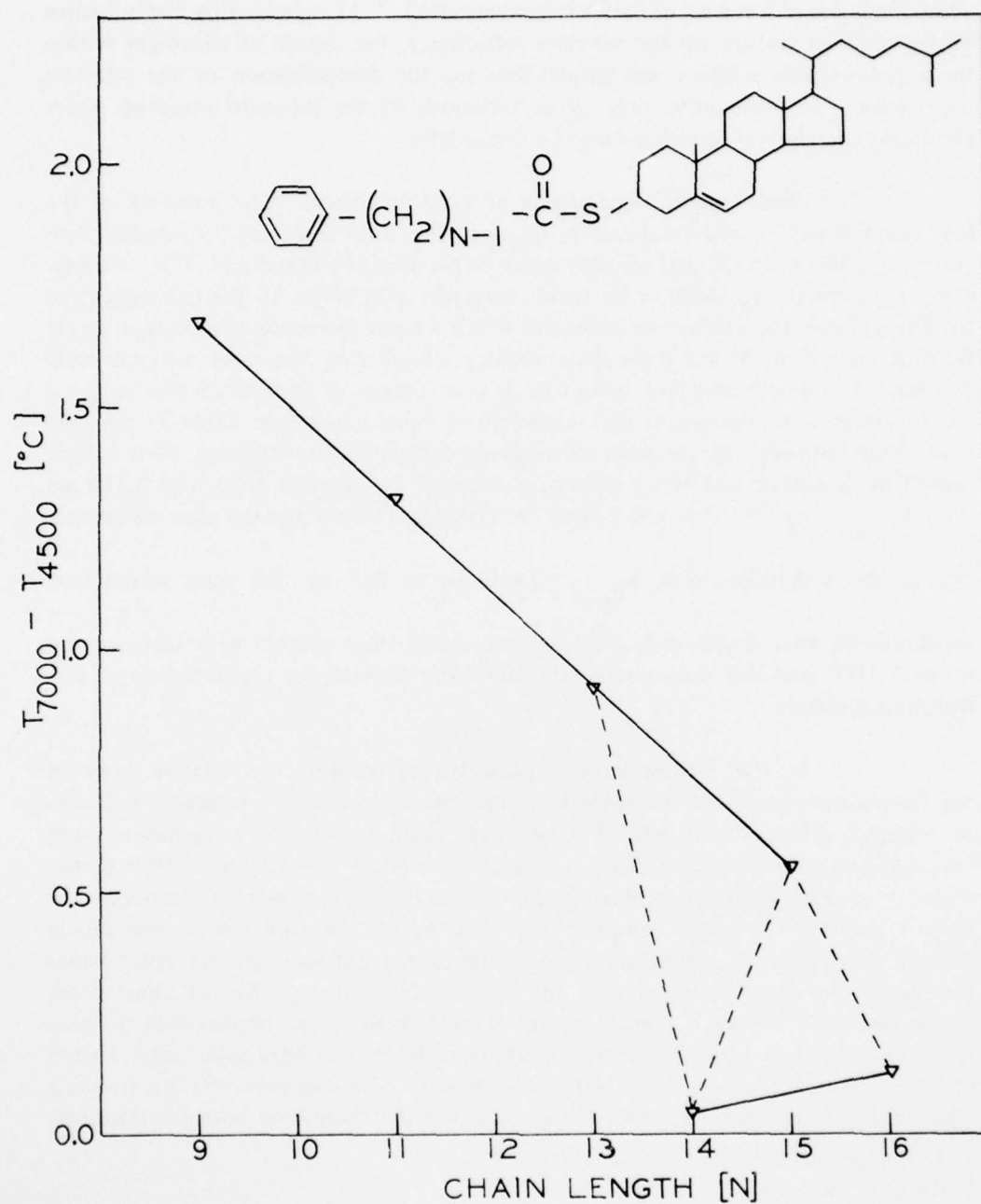


Figure 44. Width of the color band (4500 to 7000 Å) of S-cholesteryl ω -phenylalkanethioates as a function of chain length.

temperatures.⁸³ Since the addition of a methylene group to higher ω -phenylalkane-thioates does not significantly change lateral polarizability and size of the molecule, these drastic odd-even effects may be caused by differences of the molecular conformation.⁸⁴

8. Extremely Temperature-Sensitive Selective Reflectance. Of those compounds which do not crystallize in the cholesteric mesophase, S-Cholesteryl 14-phenyltetradecanethioate exhibits the highest temperature sensitivity of the selective reflection reported to date, because its color band occupies a temperature interval of 0.07°.⁸⁵ But in spite of this high dependence on temperature the measurements obtained during a given run (Figure 45) fit the theoretical relation derived by

$$\text{Keating}^{86} \quad \lambda_p = \frac{A}{T} \left(1 + \frac{B}{T - T_0} \right)^2 \quad (3) \quad \text{as well as the curve postulated by}$$

$$\text{Alben}^{87} \quad \lambda_p = \lambda_0 + \frac{A}{(T - T_0)^2} \quad (8) \quad \text{within the relative measurement}$$

uncertainty of ± 0.2 m°C. As Table 4 indicates, the characteristic temperatures T_0 differ within the test runs for each formula by less than 0.03°. Furthermore, the T_0 values of both formulas coincide within 0.03°. This can be explained by the fact

that the expansion of Keating's formula contains $\frac{1}{(T - T_0)^2}$ as the dominant term.

However, the other parameters of the equations vary strongly with the test run. We were unable to determine whether these discrepancies were caused by measurement errors or by small differences of the thermal history of the sample. Figure 46 shows the peak-wavelength curves of the other members of the series. It would be interesting to know how closely these experimental results can be represented by the above equations with the same set of parameters A , B , and λ_0 and whether or not these parameters depend on chain length. We believe that the observed unwinding of the helical structure is a pretransitional effect. Consequently, the closer the reference temperature T_0 is to the cholesteric-smectic transition temperature, the narrower is the width of the color band.

The temperature dependence of the selectively reflected light intensity at a given wavelength is another measure of the temperature sensitivity of selective reflection. The intensity curve measured at a wavelength of 0.54 μm has a halfwidth

⁸³ W. Elser, J. L. W. Pohlmann, and P. R. Boyd, *Mol Cryst Liq Cryst* 27, 325 (1974).

⁸⁴ R. D. Ennulat and A. J. Brown, *Mol Cryst Liq Cryst*, 12, 367 (1971).

⁸⁵ R. D. Ennulat, L. E. Garn, and J. D. White, *Mol Cryst Liq Cryst*, 26, 245 (1974).

⁸⁶ P. N. Keating, *Mol Cryst Liq Cryst*, 8, 315 (1969).

⁸⁷ R. Alben, *Mol Cryst Liq Cryst*, 20, 231 (1973).

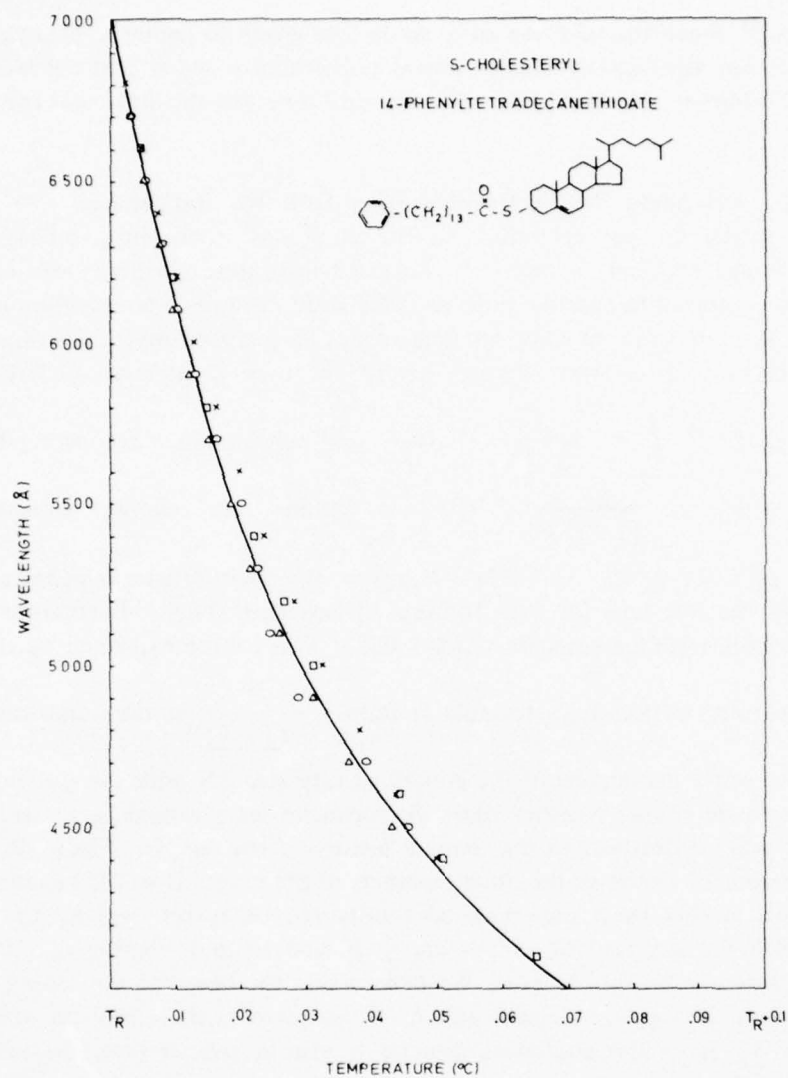


Figure 45. Wavelength of maximum selective reflection as a function of temperature.

Material: S-cholesteryl 14-phenyltetradecanethioate

- X = data set I
- = data set II, measured on same day on same sample as set I
- △ = data set III, 2nd sample, cooled at 2 m°/min, measured 8 days after set I
- = data set IV, 3rd sample, cooled at 5 m°/min, measured 9 days after set I (cf. Table 4).

[Reproduced from *Mol Cryst Liq Cryst* 26, 245 (1974).]

Table 4. Parameters of Curve Fits λ_p (I) to Figure 47

	Data Set			
	I	II	III	IV
$\lambda_p = \frac{A}{T} \left(1 + \frac{B}{(T - T_0)^2} \right)^2$	T_0 [°K]	320.070	320.093	320.097
	A [Å °K]	479319	699985	693706
	B [°K]	0.0930	0.0455	0.0422
				0.0601
$\lambda_p = \lambda_0 = + \frac{A}{(T - T_0)^2}$	T_0 [°K]	320.048	320.071	320.080
	λ_0 [Å]	2287.5	2863.4	2933.5
	A [Å °K ²]	48,903	26,112	19,970
				30,889

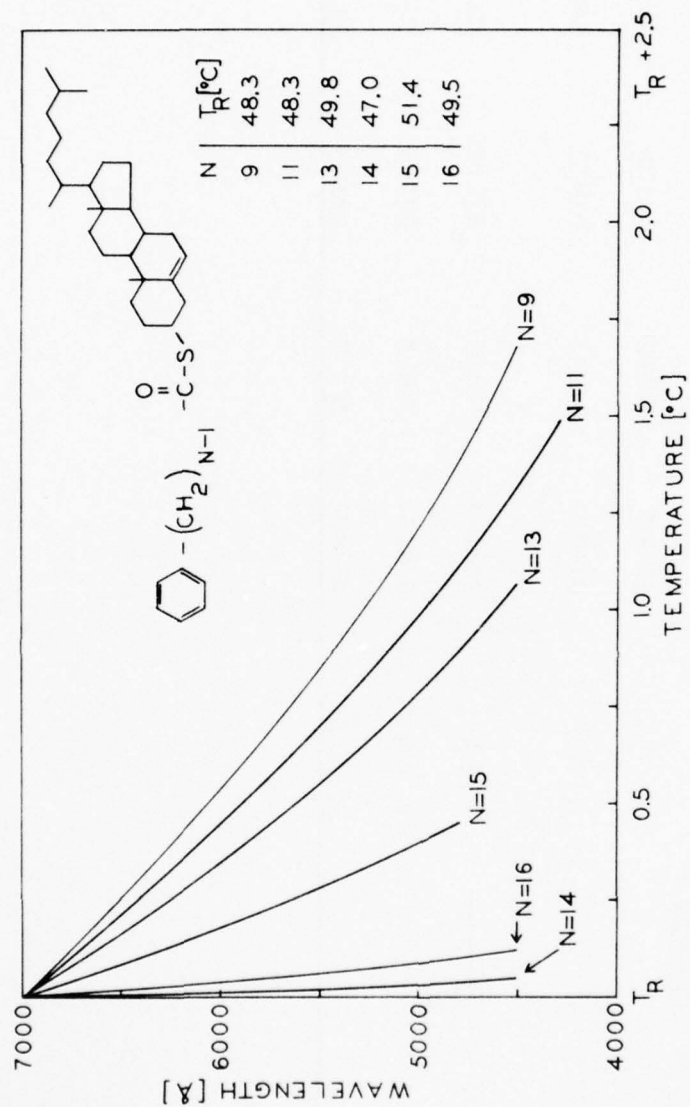


Figure 46. Wavelength of maximum selective reflection as a function of temperature.
Materials: S-cholesteryl ω -phenylalkanethioates.

of 7.6 m°C,⁸⁸ which is about one-third of that reported for cholesteryl oleyl carbonate (see Figure 8). Furthermore, we found that the maximum relative intensity change per degree (i.e., the maximum contrast per degree Celsius) amounts to about 50,000% per degree Celsius.⁸⁹ The latter exceeds previously reported data, summarized in Figure 47, by almost a factor of five.

9. Crystal Colors. Seven compounds exhibited cholesteric colors in the crystalline phase. Three are members of the cholesteryl S-alkyl thiocarbonate series and four are members of the stigmasteryl S-alkyl thiocarbonate series even though no member of the latter series exhibited a cholesteric mesophase.

In the case of stigmasteryl S-tridecyl thiocarbonate, blue cholesteric color, much of which appeared in the center of the crystals, was seen. Under the microscope, big blobs of color were also seen, especially on squeezing, and nearly solid cholesteric blue was obtained which produced the optical sign of a cholesteric mesophase when observed with a quarter-wave plate and a Bertrand lens in the optical path of the microscope. On heating, the color disappeared at approximately 65.6°, 4 degrees below the melting point of the more stable crystals which do not exhibit any cholesteric color. Crystals showing cholesteric colors, therefore, are in a metastable form and apparently crystallize in a helical manner similar to what occurs in a cholesteric mesophase.

Stigmasteryl S-pentadecyl thiocarbonate exhibits green cholesteric crystal colors, suggesting that the longer molecules do not twist as much as the tri-decyl molecules, which would result in a larger repeat distance in the helical structure and, hence, a longer selective-reflection wavelength.

Following this same trend, the larger molecules of stigmasteryl S-heptadecyl thiocarbonate cause green, yellow, orange, and red cholesteric crystal colors. Rapid cooling from the liquid resulted in mostly yellowish green and red. Slow cooling produced green suggesting that the layers of molecules had more time to twist relatively to each other which would result in a shorter repeat distance (for molecules in different planes running parallel). When the liquid was cooled quickly to crystallization temperature and held steady, only red color appeared.

Stigmasteryl S-nonadecyl thiocarbonate produced only red cholesteric crystal colors which is consistent with the trend toward longer wavelengths with longer molecules.

⁸⁸ R. D. Ennulat, L. E. Garn, and J. D. White, *Mol Cryst Liq Cryst*, 26, 245 (1974).

⁸⁹ *Ibid.*

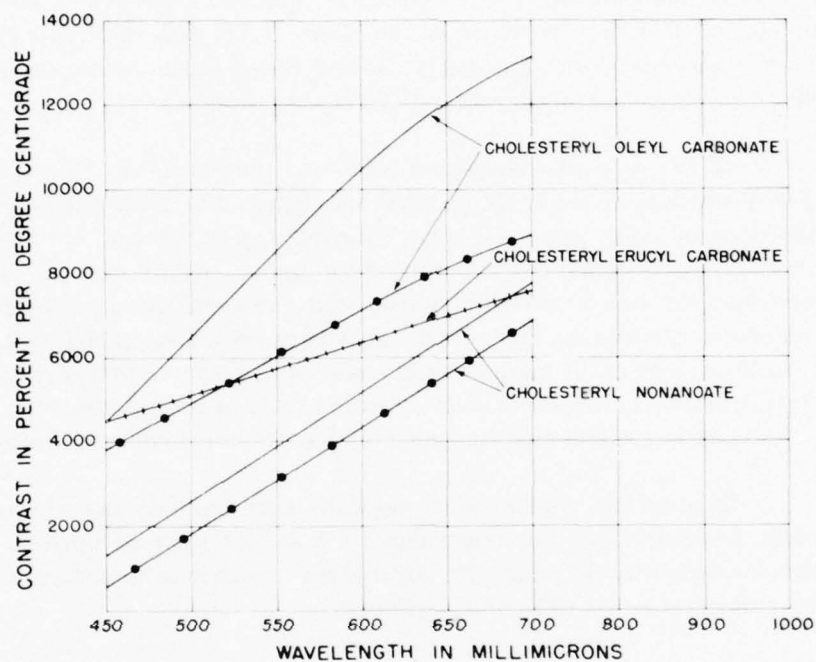


Figure 47. Maximum temperature coefficients of selective reflection as function of wavelength. Solid line = low-temperature side; broken line = high-temperature side of intensity curve at constant wavelength. [Reproduced from *Mol Cryst Liq Cryst* 13 337 (1971).]

The same thing was observed in the cholesteryl S-alkyl thiocarbonate series. Cholesteryl S-pentadecyl thiocarbonate exhibited mostly green crystal colors and the heptadecyl had mostly red crystal colors with some green, yellow, and orange. The colors, for the most part, shifted to longer and longer wavelengths as the crystals were heated slowly. (They did not seem to reverse on cooling, however.) This is opposite to the behavior of colors in the cholesteric mesophase where the shift is to shorter wavelengths on heating.

10. Mixtures and Impurities. Impurities can strongly influence the temperature dependence of selective reflection. They can suppress this effect in the visible and change the temperature and the temperature interval of the color band. Furthermore, certain impurities can introduce a hysteresis effect as indicated by the different temperatures of the maximum spectral reflectance observed for heating and cooling.^{90 91}

In mixed liquid crystals, the temperature region of the color band can be varied by changing type and concentration of the constituents. Since phase separation may be noticeable only after a prolonged period of time, it is difficult to establish the equilibrium concentration without knowing the phase diagram in sufficient detail. Although extensive literature deals with the concentration dependence of the color band, we did not find much information about the associated phase diagrams. Because of this and possible impurity effects, we doubt that the long-term stability of the temperature interval of the color band can presently be predicted for the known temperature-sensitive cholesteric mixtures.

The phase diagram of 16 binary mixtures of cholesteryl alkanoates was determined by differential scanning calorimetry in conjunction with microscopic investigations.^{92 93 94 95} Since this work was devoted to thermodynamic studies, it does not address the concentration dependence of the selective reflection. But we expect color bands, at least for compositions which contain a dominant amount of a constituent with a color band, if the mixture exhibits smectic-cholesteric transition temperatures. This is the case for binary mixtures of cholesteryl derivatives containing a high concentration of nonanoate and tetradecanoate,⁹⁶ pentanoate, isopentanoate, 2-methylbutyrate, or 2-ethylbutyrate.⁹⁷

⁹⁰ R. D. Ennulat, *Mol Cryst Liq Cryst*, 13, 337 (1971).

⁹¹ C. D. Dixon and L. C. Scala, *Mol Cryst Liq Cryst*, 10, 317 (1970).

⁹² A. V. Galanti and R. S. Porter, *J. Phys Chem* 76, 3089 (1972).

⁹³ C. W. Griffen and R. S. Porter, *Mol Cryst Liq Cryst*, 21, 77 (1973).

⁹⁴ R. J. Krzewski and R. S. Porter, *Mol Cryst Liq Cryst*, 21, 99 (1973).

⁹⁵ H. W. Gibson and J. M. Pochan, *J. Phys Chem*, 77, 837 (1973).

⁹⁶ C. W. Griffen and R. S. Porter, *Mol Cryst Liq Cryst*, 21, 77 (1973).

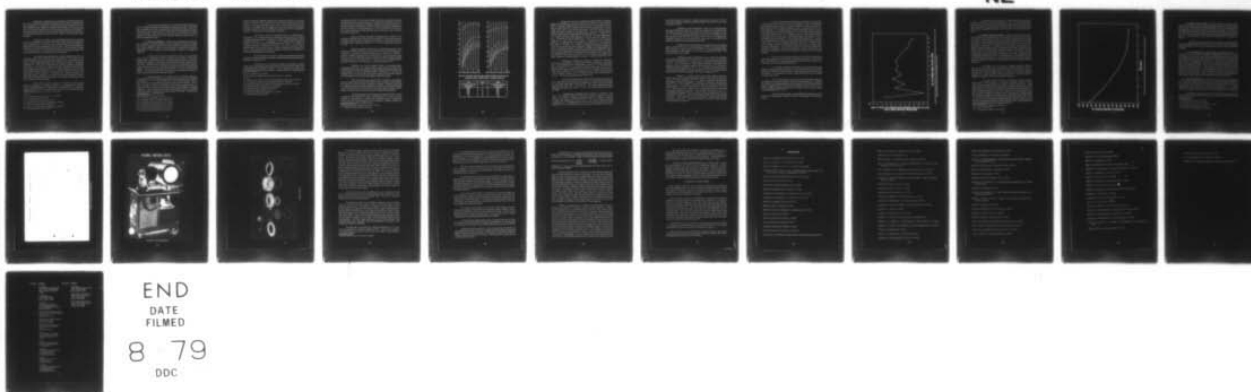
⁹⁷ H. W. Gibson and J. M. Pochan, *J. Phys Chem*, 77, 837 (1973).

AD-A070 539 ARMY ELECTRONICS RESEARCH AND DEVELOPMENT COMMAND FO--ETC F/G 7/4
PHYSICS OF MESOMORPHIC COMPOUNDS.(U)
SEP 78 A J BROWN, R D ENNULAT

UNCLASSIFIED DELNV-TR-0003

NL

2 OF 2
AD
A070539



END
DATE
FILMED
8 79
DDC



NATIONAL BUREAU OF STANDARDS
MICROCOPY RESOLUTION TEST CHART

Dilatometric measurements near the smectic-cholesteric phase transition of the cholesteryl oleyl carbonate-cholesteryl chloride system revealed first-order phase transitions for a cholesteryl oleyl carbonate mole fraction greater than 0.63 and second-order phase transitions for smaller mole fractions.⁹⁸ This result agrees with the theoretical prediction based on the theories of McMillan and Kobayashi.⁹⁹ Since these mixtures exhibit a very temperature-sensitive color band, it appears that the pretransitional selective reflection can occur near first- and second-order phase transitions.

The pitch of a mixture can be predicted from the pitch and concentration of the components if the effective rotary power follows the linear super-position law (see Section II.A.5). As we have seen, the latter should hold for compounds of similar molecules when pretransitional effects are absent. Since the high temperature sensitivity of the selective reflection is directly related to the pretransitional unwinding of the helical structure, it is impossible to determine the temperature region of the color band in mixtures from our present theoretical knowledge.

The experimental results indicate a nonlinear relationship between the temperature region of the color band and concentration.¹⁰⁰ For example, in the system cholesteryl nonanoate-cholesteryl oleyl carbonate, the color band shifts monotonically toward higher temperatures with increasing concentration of cholesteryl nonanoate.^{101 102} This effect is accompanied by a gradual expansion of the temperature interval of the color band. However, the system cholesteryl decanoate-cholesteryl hexanoate behaves quite differently.^{103 104} The temperature level of the color band is substantially depressed in the mid-concentration region to below the values characteristic of either component. Concurrently, the temperature width of the color band assumes a maximum. Note that the former system consisting of substantially different component molecules exhibits less nonlinearity than the latter system which is composed of similar homologs.

Other binary systems reported in the literature consist of the following combinations of cholesteryl derivatives: decanoate-chloride, decanoate-acetate, decanoate-cinnamate, decanoate-oleate, octanoate-oleate, and acetate-cinnamate.^{105 106} They behave essentially like the binary mixture cholesteryl decanoate-

⁹⁸ W. V. Müller and M. Stegemeyer, *Chem Phys Lett*, 27, 130 (1974).

⁹⁹ *Ibid.*

¹⁰⁰ J. Adams, W. Haas, and J. Wysocki, *Phys Rev Lett*, 22, 92 (1969).

¹⁰¹ J. L. Fergason, *Appl Opt*, 7, 1729 (1968).

¹⁰² J. H. J. Vogelzangs, *Ned Tijdschr Natuurk*, 38, 18 (1972).

¹⁰³ B. Böttcher, D. Gross, and E. Mundry, *Materialprüfung* 11, 156 (1969).

¹⁰⁴ B. Böttcher, *Chem-Ztg; Chem-Techn*, 1, 195 (1972).

¹⁰⁵ B. Böttcher, D. Gross, and E. Mundry, *Materialprüfung*, 11, 156 (1969).

¹⁰⁶ B. Böttcher, *Mater Constr (Paris)*, 4, 241 (1971).

The same thing was observed in the cholesteryl S-alkyl thiocarbonate series. Cholesteryl S-pentadecyl thiocarbonate exhibited mostly green crystal colors and the heptadecyl had mostly red crystal colors with some green, yellow, and orange. The colors, for the most part, shifted to longer and longer wavelengths as the crystals were heated slowly. (They did not seem to reverse on cooling, however.) This is opposite to the behavior of colors in the cholesteric mesophase where the shift is to shorter wavelengths on heating.

10. Mixtures and Impurities. Impurities can strongly influence the temperature dependence of selective reflection. They can suppress this effect in the visible and change the temperature and the temperature interval of the color band. Furthermore, certain impurities can introduce a hysteresis effect as indicated by the different temperatures of the maximum spectral reflectance observed for heating and cooling.^{90 91}

In mixed liquid crystals, the temperature region of the color band can be varied by changing type and concentration of the constituents. Since phase separation may be noticeable only after a prolonged period of time, it is difficult to establish the equilibrium concentration without knowing the phase diagram in sufficient detail. Although extensive literature deals with the concentration dependence of the color band, we did not find much information about the associated phase diagrams. Because of this and possible impurity effects, we doubt that the long-term stability of the temperature interval of the color band can presently be predicted for the known temperature-sensitive cholesteric mixtures.

The phase diagram of 16 binary mixtures of cholesteryl alkanoates was determined by differential scanning calorimetry in conjunction with microscopic investigations.^{92 93 94 95} Since this work was devoted to thermodynamic studies, it does not address the concentration dependence of the selective reflection. But we expect color bands, at least for compositions which contain a dominant amount of a constituent with a color band, if the mixture exhibits smectic-cholesteric transition temperatures. This is the case for binary mixtures of cholesteryl derivatives containing a high concentration of nonanoate and tetradecanoate,⁹⁶ pentanoate, isopentanoate, 2-methylbutyrate, or 2-ethylbutyrate.⁹⁷

⁹⁰ R. D. Ennulat, *Mol Cryst Liq Cryst*, 13, 337 (1971).

⁹¹ C. D. Dixon and L. C. Scala, *Mol Cryst Liq Cryst*, 10, 317 (1970).

⁹² A. V. Galanti and R. S. Porter, *J. Phys Chem* 76, 3089 (1972).

⁹³ C. W. Griffen and R. S. Porter, *Mol Cryst Liq Cryst*, 21, 77 (1973).

⁹⁴ R. J. Krzewski and R. S. Porter, *Mol Cryst Liq Cryst*, 21, 99 (1973).

⁹⁵ H. W. Gibson and J. M. Pochan, *J. Phys Chem*, 77, 837 (1973).

⁹⁶ C. W. Griffen and R. S. Porter, *Mol Cryst Liq Cryst*, 21, 77 (1973).

⁹⁷ H. W. Gibson and J. M. Pochan, *J. Phys Chem*, 77, 837 (1973).

cholesteryl hexanoate, regardless of whether the temperature width of the color band is wide or narrow for both components or wide for one and narrow for the other. Moreover, the smallest temperature interval of the color bands exhibited by these mixtures is not smaller than the smallest one of the two respective components. The system cholesteryl nonanoate-cholesteryl butyrate seems to be an exception to the latter,¹⁰⁷ possibly because of the influence of impurities.

A few binary systems were investigated only over a limited range of concentration. They include mixtures of cholesteryl nonanoate with the cholesteryl derivatives propionate, butyrate, isobutyrate, crotonate, 3-phenylpropionate, methyl carbonate,¹⁰⁸ acetate,¹⁰⁹ ¹¹⁰ and chloride;¹¹¹ ¹¹² ¹¹³ binary mixtures of cholesteryl decanoate with several cholesteryl β -alkoxypropionates,¹¹⁴ and a 1:1 mixture of cholesteryl decanoate and cholesteryl hexanoate.¹¹⁵ For the last system, selective-reflection data, such as spectral profiles at various temperatures, the angular dependence of peak wavelength and selective reflectance, and the peak wavelength as a function of temperature, have been reported.

The dependence of the pitch on temperature and composition has been discussed for mixtures of cholesteryl chloride and the cholesteryl alkanoates-nonanoate, decanoate, and dodecanoate.¹¹⁶

Ternary mixtures of cholesteric materials were developed to achieve a wider choice of temperature region and temperature width of the color band. Woodmansee selected the constituents as follows:¹¹⁷ a base compound that exhibits a narrow color band of relatively low temperature (cholesteryl oleate), a second component

¹⁰⁷ S. P. Brown, *Mater Eval*, 26, 163 (1968).

¹⁰⁸ J. L. Fergason, N. N. Goldberg, and R. J. Nadalin, *Mol Cryst Liq Cryst*, 1, 309 (1966).

¹⁰⁹ Ibid.

¹¹⁰ T. Ishikawa, T. Mizuno, F. Kato, Y. Yashiro, and H. Nagao, *Bull Soc Nagoya Inst Technol*, 22, 243 (1970).

¹¹¹ J. L. Fergason, N. N. Goldberg, and R. J. Nadalin, *Mol Cryst Liq Cryst*, 1, 309 (1966).

¹¹² T. Ishikawa, T. Mizuno, F. Kato, Y. Yashiro, and H. Nagao, *Bull Nagoya Inst Technol*, 22, 243 (1970).

¹¹³ J. Adams, W. Haas, and J. Wysocki, *Phys Rev Lett*, 22, 92 (1969).

¹¹⁴ D. Grass and B. Bottner, *Z. Naturforsch*, 25, B, 1099 (1970).

¹¹⁵ B. Böttcher, *Chem-Ztg*, *Chem Techn* 1, 195 (1972).

¹¹⁶ J. Adams, W. Haas, and J. Wysocki, *Phys Rev Lett*, 22, 92 (1969).

¹¹⁷ W. E. Woodmansee, *US*, 3,441,513 (1969).

that reduces the width of the color band (cholesteryl octanoate, nonanoate, decanoate, p-nitrobenzoate), and a third component that increases the temperature level of the color band without significantly widening it (cholesteryl acetate, propionate). By properly selecting the constituents and their respective concentrations, Woodmansee was able to shift the color band from about 21° to 45° and from 50° to 58°, respectively, while maintaining the width within the range of about 0.3° to 0.4°. Figure 48 shows some of his results.

Magne and Pinard thoroughly investigated ternary mixtures of the cholesteryl alkanoates oleate, nonanoate, and propionate.¹¹⁸ They measured the peak wavelength versus temperature relationships for compositions which selectively reflect the visible within a temperature interval of 1° to 3° over a temperature range from 5° to 75°.

Melamed and Rubin studied relatively temperature-insensitive ternary mixtures of cholesteryl chloride (22-45 weight percent) with a 40:60 weight percent composition of cholesteryl nonanoate-cholesteryl oleyl carbonate.¹¹⁹ Although the peak wavelength was shifted by only about 50 Å/°C over the temperature range from 20° to 35°, the 50μm-thick sample containing 32% cholesteryl chloride changed its optical rotation up to the rate of 60°/°C. This means that the readily measurable variation of rotation of 0.2° corresponds to a temperature change of 3 m°C.

Obviously, even with the limited number of temperature-sensitive compounds known to date, it is possible to prepare a large number of mixtures. Since most of the newer temperature-sensitive materials, such as the S-cholesteryl 14-Phenyltetradecanethioate, are not commercially available, cholesteryl oleyl carbonate and cholesteryl oleate are still the basic materials for close-to-room temperature operation and cholesteryl nonanoate or decanoate for higher-temperature regions.

Many experiments were performed here to determine what happens when one liquid crystal is mixed with another or with a nonliquid crystal impurity. One reason for mixing two liquid crystals was to produce a cholesteric color band in a temperature range between the temperatures at which such color bands normally exist in two liquid crystals. Impurities were also added to liquid crystals in order to produce a cholesteric color spectrum where one was not previously observable.

Cholesteryl S-hexadecyl thiocarbonate was originally observed as having a cholesteric color spectrum 0.2° wide at approximately 55°. However, we later observed no such spectrum in a freshly made and purified sample. Consequently, we set out to find out just what percent of an impurity, cholesteryl chloride, was needed in order to produce cholesteric colors.

¹¹⁸ M. Magne and P. Pinard, *J. Phys (Paris)*, 30, Colloq. C 4, 117 (1969).

¹¹⁹ L. Melamed and D. Rubin, *Appl Opt.*, 10, 1103 (1971).

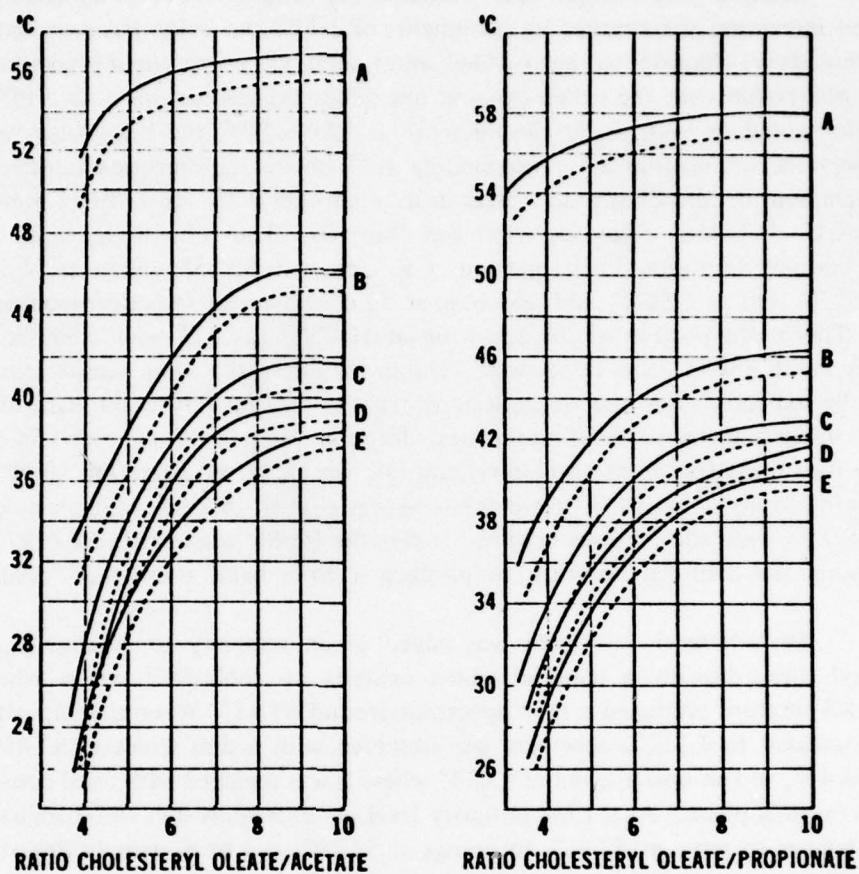


Figure 48. Temperature range (red to blue) of selective reflection of ternary mixtures.
Basic binary system: cholesteryl oleate — cholesteryl propionate.

Left	Curve	Right
% nonanoate, octanoate, or decanoate	No.	% nonanoate, octanoate, or decanoate
68.25	A	68.2
35.8	B	35.8
20.8	C	23.7
11.4	D	11.4
0.0	E	0.0

Starting with one part per thousand (by weight) (PPT) of cholesteryl chloride and increasing the amount by increments of 1 PPT, no color was seen until 4 PPT of cholesteryl chloride had been added; and then it was only a slight bluish cast which was observable with the naked eye and not under the microscope. At 5 PPT, a slight color could be seen under the microscope. At 8 PPT, the blue color was readily observable on heating at approximately 0.1° above the smectic-cholesteric transition temperature and disappeared after heating another 0.2° . At 9 PPT (1.5 mol %), a complete cholesteric color spectrum was observed. The color disappeared at 53.1° . On cooling, very dim violet appeared at 53° , green at 52.85° , yellow at 52.8° , orange at 52.7° , red at 52.65° , and no color at 52.6° where the smectic mesophase appeared. The bright portion of the spectrum at 10 PPT was 0.2° wide, about the same width as at 8 PPT, and it occurred at approximately the same temperature. As was to be expected, the smectic-cholesteric transition temperature gradually declined with increasing amounts of impurities, dropping from approximately 54.5° to 52.6° as the concentration of cholesteryl chloride was increased from 0 to 10 PPT. It is interesting to note that when this compound was studied in 1966, it had a color band about 0.2° wide since it was impure. It was the freshly made material (1970) which required the artificial impurity to produce a color band about 0.25° wide.

Dicholesteryl carbonate was added as an impurity to 5α -cholestan- 3β -yl S-decyl thiocarbonate, a material which exhibits no cholesteric colors when pure. A 0.8% mixture produced a flash spectrum around 53.45° . When the impurity level was increased to 1.2%, a spectrum was observed with a dim violet at 53.45° , yellow at 53.40° , and an unstable red at 53.53° where it was replaced with focal conics of the smectic mesophase. At a 1.6% impurity level, an extremely dim violet appears at 53.4° , changes to aqua at 53.35° , to orange at 53.29° , and to extremely dim red at 53.26° . The smectic mesophase appears at about 53.20° .

The 5α -cholestan- 3β -yl S-decyl thiocarbonate changed in appearance from a slight bluish haze seen only with the naked eye at 0 PPT cholesteryl chloride to a very narrow, faint partial spectrum at 4 PPT, and at 8 PPT to an easily observable spectrum $0.052 \pm 0.004^\circ$ wide — just above 52° . The smectic-cholesteric transition temperature decreased from 54.15° to 52.05° as the impurity was increased from 0 to 8 PPT.

Thiocholesteryl 10-phenyldecanoate exhibited no cholesteric colors until a level of 80 PPT cholesteryl chloride was reached, and then it was hard to observe. At 100 PPT, a normal color spectrum with a 0.11° width was observed, the bright part ranging from 27.84° to 27.95° . The smectic-cholesteric transition temperature was 27.7° , dropping from 39.8° for the pure material. The closely related thiocholesteryl 12-phenyldodecanoate showed no colors until 70 PPT, where a 0.14°

wide color spectrum was observed. Impurity increments were in steps of 10 PPT. The smectic-cholesteric transition temperature dropped from 43.45° to 33.2° as the impurities were added.

S-cholesteryl undecyl thiocarbonate, which has a smectic-cholesteric transition temperature of about 69.15° , shows no color until a level of 12 PPT cholesteryl chloride is reached, and a violet color is seen under the microscope at around 65° . At 18 PPT, blue and green also appear at around 63.5° . At 36 PPT, the complete spectrum, about 0.18° wide, is seen from 61.96° to about 62.14° although the separation between red and the smectic focal conics is poor. At 48 PPT, the red appears as it should and the spectral width is about 0.25° .

Cholesteryl S-octyl thiocarbonate has a partial spectrum (violet through green) of about 0.19° wide at a concentration of 20 PPT of cholesteryl chloride which increases to a width of about 0.37° at 48 PPT. The smectic-cholesteric transition temperature is approximately 67.5° for the pure material, about 66.55° at 20 PPT, and about 60.55° at 48 PPT.

S-cholesteryl tridecyl thiocarbonate is one of those rare compounds which exhibits a partial spectrum in its pure state. In this case, the material changes from black to bright indigo at 67.2° , to blue at 67.16° , and into the smectic mesophase at 67.15° . At a concentration of 5 PPT cholesteryl chloride, a violet-indigo color appears at 65.84° on cooling and greenish yellow comes in at 65.76° . The smectic-cholesteric transition temperature is 65.71° . At a concentration of 10 PPT, the entire color spectrum is produced, with blue appearing at 65.14° and red appearing and disappearing below 65.6° and changing to the smectic mesophase at 65.0° .

Professor E. J. Ambrose of the Chester Beatty Research Institute in London asked us for a liquid crystal which exhibited a color spectrum somewhere between 37° (body temperature) and 37.5° , in order to work with mammalian cells and malignant cells in the laboratory. In response, we produced a color spectrum from 37.15° to 37.5° by adding 7% cholesteryl chloride to S-cholesteryl 14-phenyltridecanethioate. The pure compound has a color spectrum between 47.3° and 47.35° . We also found that a mixture of 6.5% cholesteryl chloride in S-cholesteryl 12-phenyldodecanethioate produced a color spectrum between 36.9° and 37.1° . No cholesteric color appears in the pure material except for a slight bluish cast when viewed with the naked eye. The smectic mesophase appears at 36.9° on cooling in the mixture – a drop from 43.45° for the pure material. A broader cholesteric color band, from 35.7° to 38.3° , is produced by mixing 30% cholesteryl erucyl carbonate with 70% cholesteryl nonanoate.

In the case of 5 α -cholestan-3 β -yl S-decyl thiocarbonate, which exhibits no colors under the microscope when pure, the addition of about 1% S-cholesteryl octadecyl thiocarbonate produces a partial flash spectrum of violet, blue, and some green, with the smectic mesophase appearing at 53.05° as compared with 54.15° for the pure material. A 2% mixture produces a narrow, stable partial spectrum at around 52.6°, with the smectic mesophase starting at 52.5°. On faster cooling, cholesteric orange and red can be seen. A 2.5% mixture produced a stable yellow in addition to the higher end of the spectrum. This partial spectrum was estimated to have a temperature interval of about 0.11°. The smectic mesophase started at 52°. A mixture of approximately 3% produced an entire stable color spectrum with a bandwidth of about 0.12°. The smectic mesophase appeared at about 51.8°. Further increases of the "impurity" resulted in broader and broader color spectra occurring at lower and lower temperatures. As the mixture becomes more and more predominantly composed of S-cholesteryl octadecyl thiocarbonate, the color band narrows and increases in temperature, having a spectrum width of about 0.18° and occurring around 63°.

Each of the first fourteen members of the cholesteryl ω -phenylalkanoate series was mixed one at a time with cholesteryl nonanoate in a ratio of one to nine. The temperatures at which maximum color intensity occurred at 6000 Å were recorded for each mixture and plotted (Figure 49).

A 7:4 mixture of cholesteryl chloride and cholesteryl hexadecanoate produced a nematic-appearing (threaded structure) material which exhibited an interesting effect in regions of solid color where a constant jumping around of tiny specks was observed. It was similar to watching a grainy motion picture from a position very close to the screen.

A 5% to 10% mixture of the free radical α , γ -bis(diphenylene- β -phenylallyl) (BDPA) in p-azoxyanisole likewise produced a motion picture effect. In general, the mixing of free radicals with liquid crystals produced lowering of transition temperatures, as normally observed for other types of impurities, except in the case of a 1% mixture of BDPA or galvinoxyl ethyl 4,4'-azoxy benzoate, which increased transition temperatures slightly (0.1° to 0.6°).

The other liquid crystals into which BDPA and galvinoxyl were dissolved were p-azoxyanisole, cholesteryl nonanoate, and stigmasteryl S-hexylthiocarbonate.

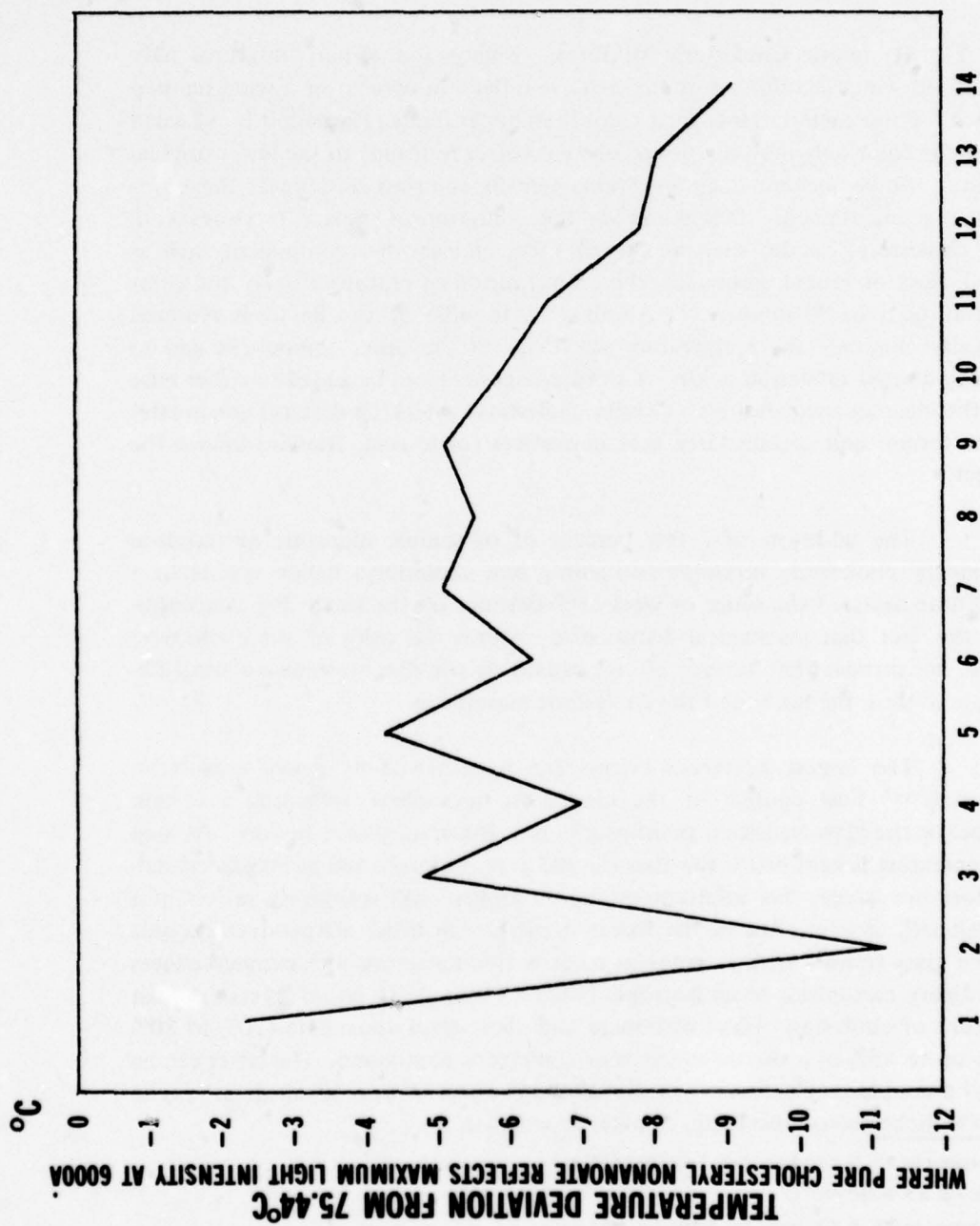


Figure 49. Effect of mixing 10% cholesteryl ω -phenylalkanoate with 90% cholesteryl nonanoate on the temperature at which maximum cholesteric color intensity occurs with 6000 Å incident light.

To demonstrate the deterioration of a liquid crystal with time, we held cholesteryl nonanoate at a constant temperature of 75.55° for 9 days and observed the decrease in the wavelength at which maximum color intensity occurred (Figure 50). On the first day, the wavelength was 6340 Å (red) and on the ninth day it was 4460 Å (blue), representing a lowering of the temperature of the color spectrum by about 1°.

11. Hysteretic Cholesteric Mixtures. Binary and ternary mixtures have been developed which exhibit a certain, selective-reflection color over a wide temperature region. These materials lose their color if an upper temperature limit is exceeded and reflect the color only minutes, hours, or weeks after returning to the lower original temperature. Some hysteretic compositions remain colorless as long as the lower temperature is maintained. Depending on the composition, binary mixtures containing a cholesteryl halide, such as the chloride, and another component such as cholesteryl oleyl or erucyl carbonate, cholesteryl oleate or erucate, display the color with a delay of 3 to 30 minutes.¹²⁰ About 15% to 40% of the halide is required to practically eliminate the temperature sensitivity of the other component and to establish the desired reflection color. A third component can be added to either raise or lower the clearing temperatures. Certain cholesteryl esters (cholesteryl nonanoate) induce the former and certain fatty acid derivatives (oleic acid, triolein) induce the latter effect.

The addition of a few percent of oil-soluble nigrosine or indulene dyes to binary cholesteric mixtures containing one cholesteryl halide results in a hysteretic time delay of the order of weeks.¹²¹ Because of the small dye concentration and the fact that mechanical disturbance restores the color of the cholesteric mesophase, we surmise that surface effects caused by the dye molecules control the alignment and thus the texture of the cholesteric mesophase.

The largest hysteresis effects can be achieved by glassy cholesteric liquid crystals.¹²² Fast cooling of the cholesteric mesophase reflecting a certain color to below the glass-transition point results in a frozen-in planar texture. As long as the temperature is kept below the glass-transition temperature and as long as crystallization does not occur, this solid cholesteric mesophase will selectively reflect at a peak wavelength characteristic of the frozen-in pitch. Once the temperature exceeds that of the glass transition, the frozen-in color is eliminated and the sample behaves like an ordinary mesophase or an isotropic liquid. These glassy liquid crystals consist of a mixture of cholesteryl oleyl carbonate and cholesteryl nonanoate (20% to 80% each) and up to 45% of a viscosity-increasing cholesteric compound. The latter can be cholesteryl p-nonylphenylcarbonate or dicholesteryl esters of α , ω -alkanedicarboxylic acids such as dicholesteryl succinate, adipate, or sebacate.

¹²⁰ J. L. Fergason and N. N. Goldberg, *Brit.* 1,153,959 (1969).

¹²¹ F. Davis, *US*, 3,576,761 (1971).

¹²² J. L. Fergason and N. N. Goldberg, *US*, 3,594,126 (1971).

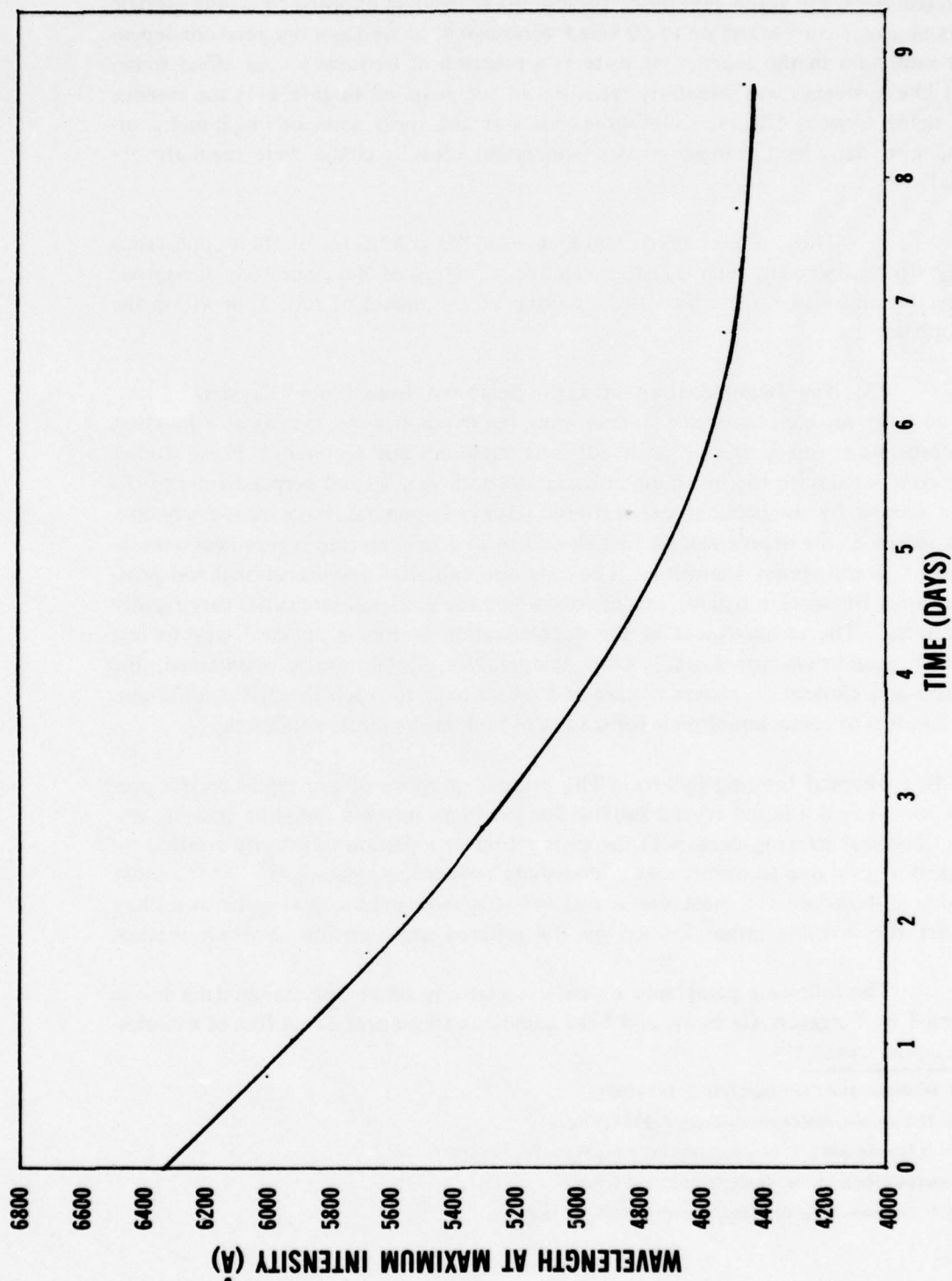


Figure 50. Deterioration of cholesteryl nonanoate with time at a constant temperature of 75.55°C.

12. Effects of Electric Fields.¹²³ Increased intensity of light selectively scattered from the plane texture of cholesteryl nonanoate exposed to strong electric fields at direct current and up to 30 kHz was observed, as well as a temperature-dependent minimum in the average intensity as a function of frequency. An effect somewhat like hysteresis was shown by retention of the acquired brightness in the absence of a field. Curious effects such as three classes of dark spots, some of which metamorphose into bars, light maltese crosses, and bright cross-hatchings were regularly observed.

These effects taken together with the conditions of their appearance imply strong alignment such that the selective reflection of the cholesteric mesophase is greatly enhanced by the increased ordering of the planes of reflection within the mesophase.

13. The Depolarization of Light Scattered from Liquid Crystals.¹²⁴ A helium-neon gas laser was used to determine the depolarization factors as a function of temperature and scattering angle for bulk mesomorphic materials. These studies were conducted with the incoming polarization both parallel and perpendicular to the plane formed by the incident and scattered waves. In general, there exist fairly constant values of the depolarization factors except in a temperature region near a mesophase or clearing-point transition. The data also exhibited pre-transitional and post-transitional fluctuation regions, i.e., regions where the scattered intensities vary rapidly with time. The measurement of the depolarization factors is an ideal way to test thermal equilibrium processes. After temperature equilibrium is maintained, the smectic and cholesteric phases require at least an hour to reach thermal equilibrium. This result is of prime importance for studies of bulk mesomorphic materials.

B. Thermal Imaging System. The primary purpose of our liquid crystal program was to find a liquid crystal suitable for use in an infrared radiation imaging system. Thermal imaging deals with the registration of radiation inherently emitted by physical objects due to differences in emissivity and/or temperature.¹²⁵ ¹²⁶ Thermal imaging systems are the most useful and versatile radiographic devices because they convert the invisible image formed by the infrared radiation into a visible replica.

The following paragraphs describe a relatively simple thermal-imaging device invented by Ferguson, Garbuny, and Vogl using as a transducer a thin film of a cholesteric liquid crystal.¹²⁷

¹²³ J. H. Muller, *Mol Cryst Liq Cryst*, 2, 167 (1966).

¹²⁴ L. M. Cameron, *Mol Cryst Liq Cryst*, 7, 235 (1969).

¹²⁵ R. D. Ennulat and J. L. Ferguson, *Mol Cryst Liq Cryst*, 13, 149 (1971).

¹²⁶ Infrared Imaging Issue, *Applied Optics*, Vol 7, Sep 68.

¹²⁷ J. L. Ferguson, T. H. Vogl, and M. Garbuny, US, 3,114,836.

This device utilizes the temperature dependence of the light selectively reflected from the plane texture of a cholesteric liquid crystal. Figure 51 shows the spectral profiles of the light selectively reflected by regions of temperature T_A and T_B of the cholesteric film. If this film is illuminated with monochromatic light of wavelength λ_0 , the region of temperature T_A has a much lower reflected intensity for light of wavelength λ_0 than the surrounding region of temperature T_B . Thus the observer perceives regions of different temperatures as regions of different brightness.

Figure 52 shows the schematics of a thermal imaging device based on this conversion principle. The infrared image of the scene is focused on the absorbing side of a membrane and converted by absorption into the corresponding heat pattern. Thermal conduction establishes an equivalent temperature pattern in the cholesteric liquid crystal deposited on the other side of the membrane. Because of the temperature-dependent selective reflectivity of the liquid crystal, this temperature image — and thus the original infrared image — is made visible by illumination with monochromatic light. To keep the liquid crystal at the proper operating temperature, the sensing layer is inclosed in a coarsely temperature-controlled chamber. A radiation heater provides fine control of the operating temperature. By varying the output of the radiation heater, desired temperature levels of the temperature image in the liquid crystal can be brought into the selective-reflection region and can thus be made visible. This capability and the extreme nonlinearity of the temperature dependence of the selective reflection (i.e., its cutoff characteristics) are essential to suppress the unwanted effect of high-background radiance of the scene without reducing the effect of the radiance coming from objects of interest.

The experimental studies were conducted with a device designed by Hansen and Ferguson of the Westinghouse Corporation (as shown in Figure 53). It consists of reflective optics, a thermoelectric thermostat, and a thermostated chamber containing illuminator, radiation heater, and the evacuated cell unit enclosing the transducer film. The thermostat generates water heated or cooled by a thermoelectric converter and pumps it through the grooves of the chamber. A contact thermometer mounted in a water reservoir permits adjustment and control of the water temperature. A circularly shaped He gas discharge lamp and a radiation heater, consisting of a ring of eight light bulbs, blackened to eliminate visible light, are mounted in the plate closing the chamber toward the observer. The cell unit (shown in Figure 54) is a blackened brass cylinder closed on one side by a germanium window for the infrared input and on the other side by an ordinary glass window to admit viewing light and heater radiation. The transducer membrane is suspended in the inside with the infrared absorber directed toward the germanium window. The cell unit is evacuated by a mechanical pump to prevent the degradation of the image resolution due to heat conduction through the surrounding air. A liquid nitrogen cold trap prevents the contamination of the liquid crystal film due to backstreaming pump oil.

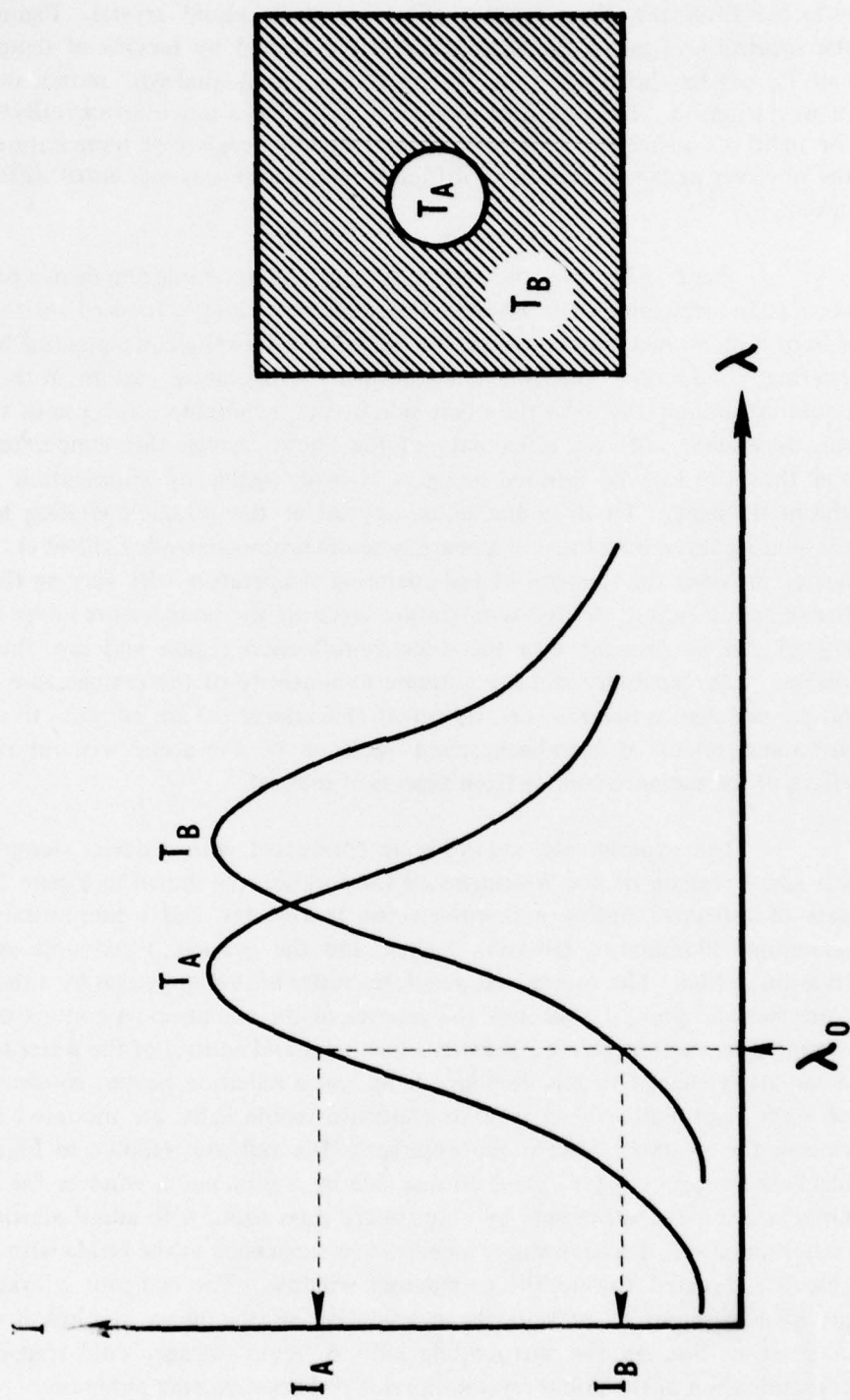


Figure 51. Conversion principle.

LABORATORY THERMAL IMAGING DEVICE

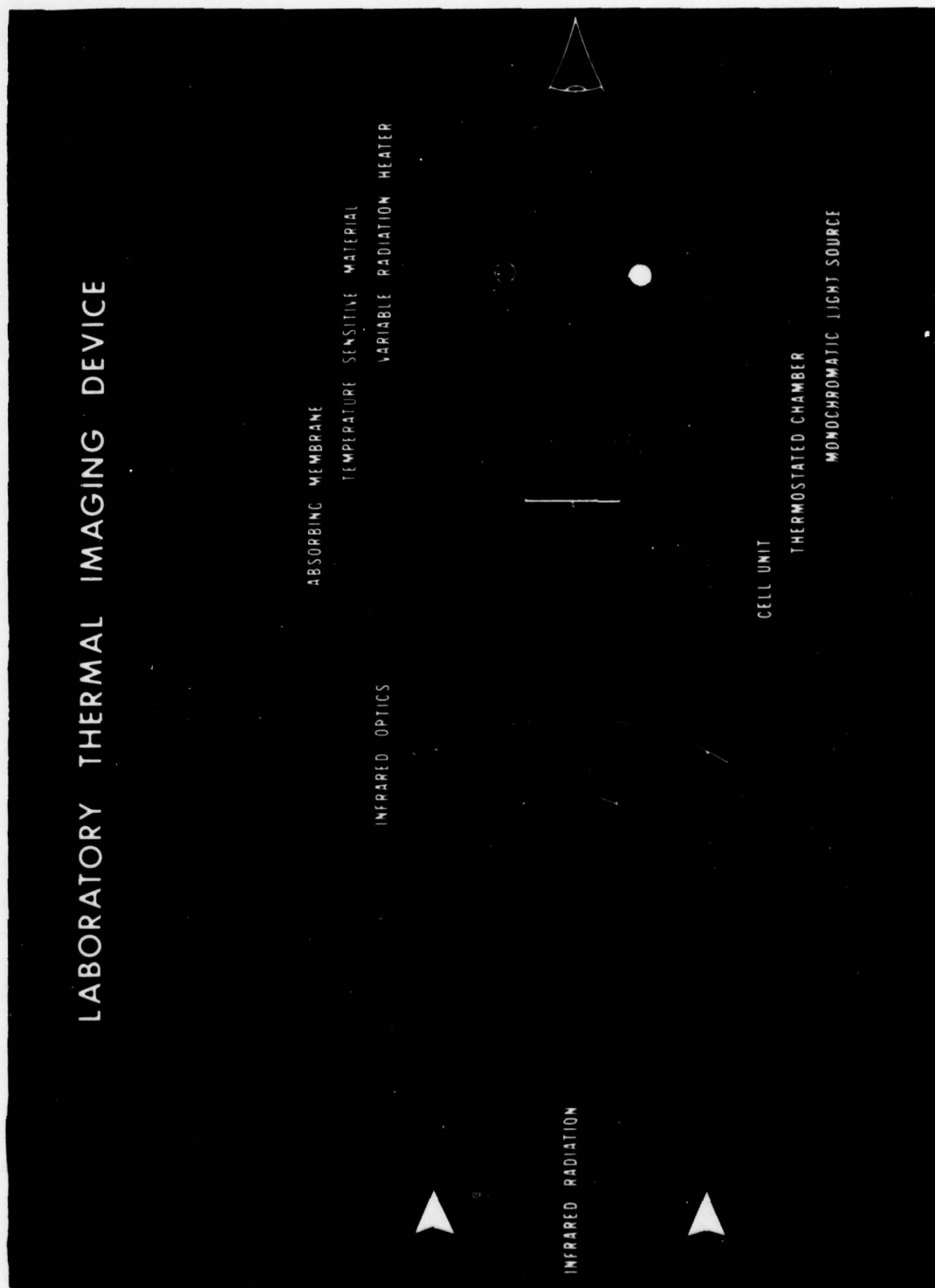


Figure 52. Laboratory thermal imaging device.

THERMAL IMAGING DEVICE

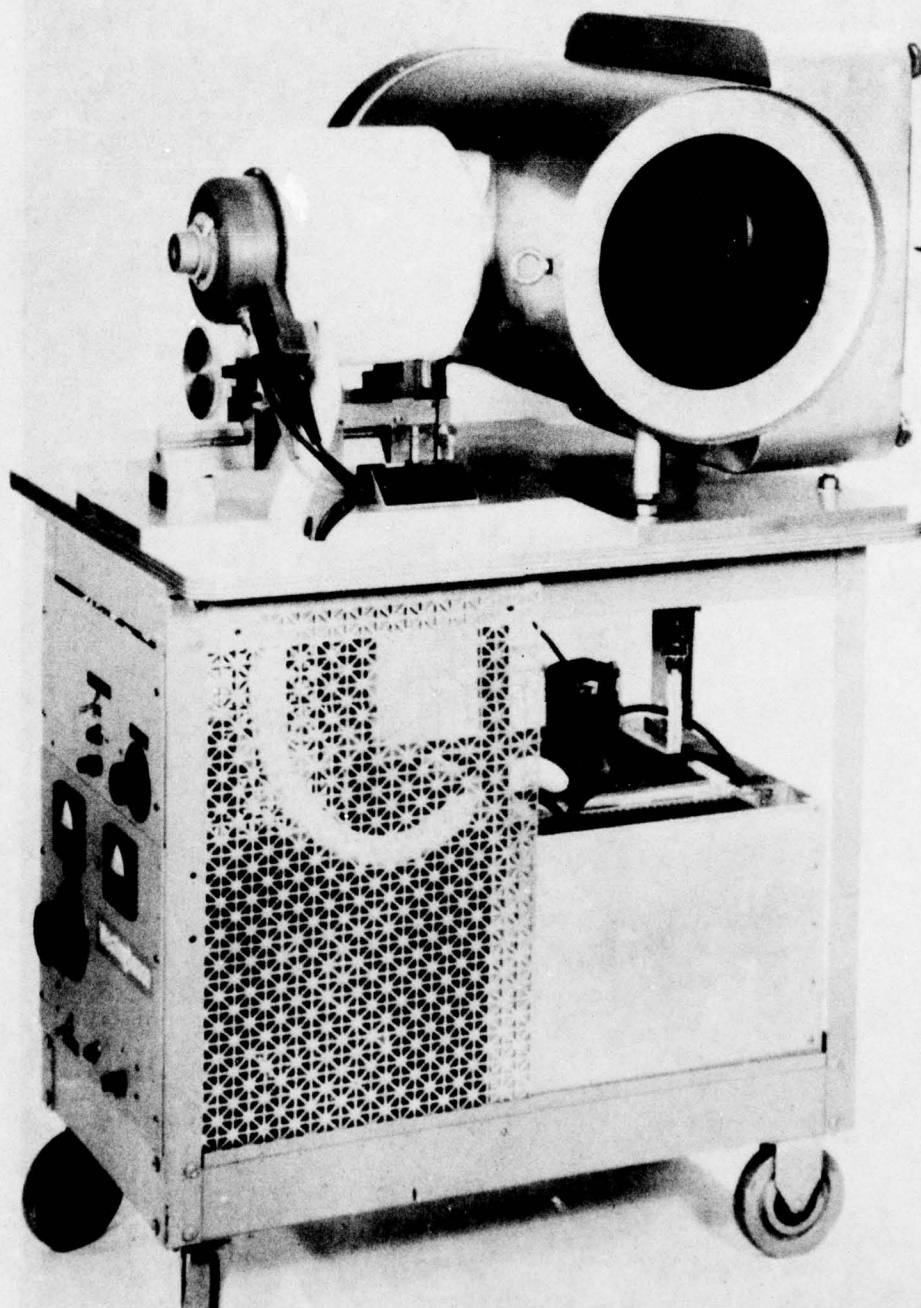


Figure 53. Thermal imaging device.

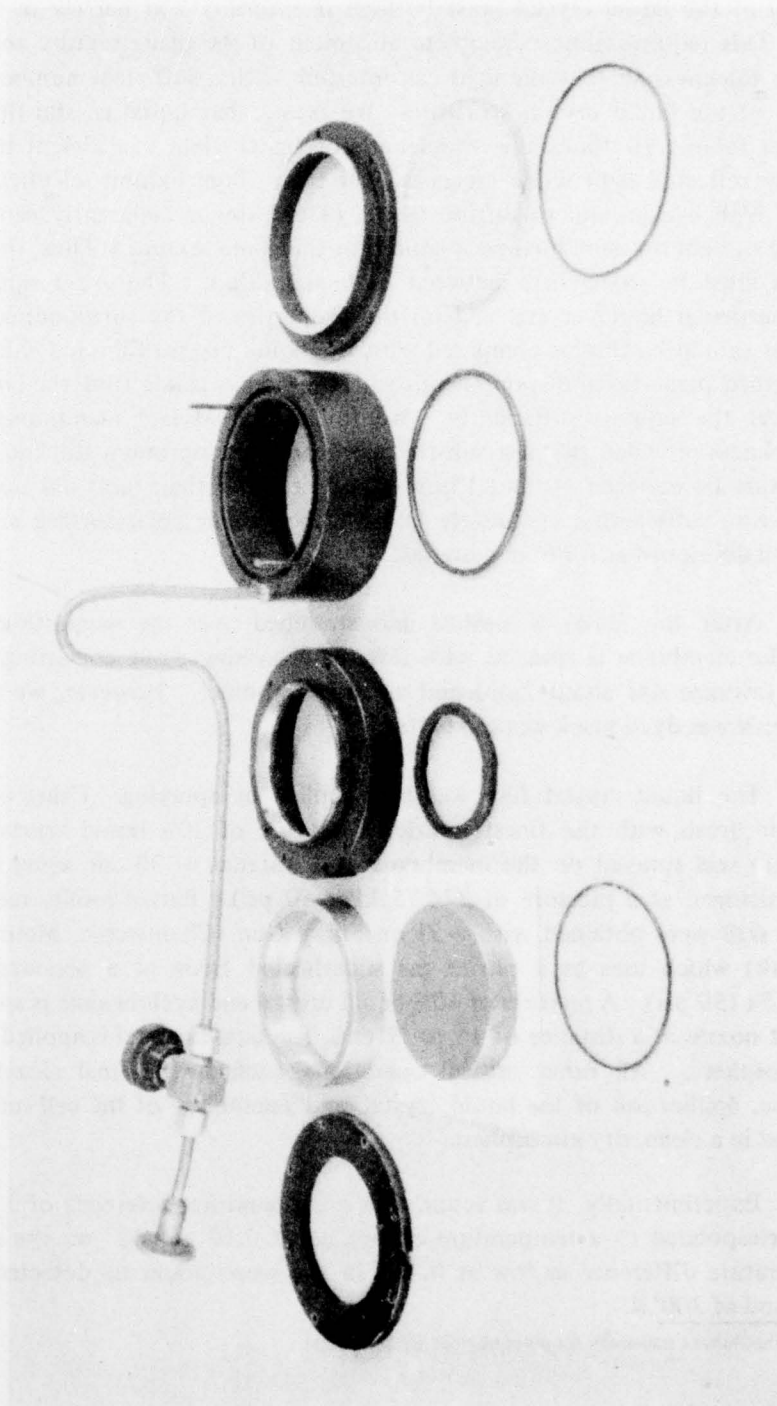


Figure 54. Cell unit.

To obtain the highest resolution and the smallest observable temperature difference, ΔT_{\min} , the transducer film must be as thin as possible and the selective reflection of the liquid crystal must be high in intensity and narrow in spectral response. This requires almost complete alignment of the plane texture and a certain optimum thickness so that the light can interfere with a sufficient number of repeat distances of the liquid crystal structure. We found that liquid crystal films thinner than $5\mu\text{m}$ (about 10 times the wavelength of light) yield insufficient intensity of selectively reflected light while layers thicker than $20\mu\text{m}$ exhibit selective reflection against a high background of diffuse light. (The latter is apparently caused by the scattering of light on small unaligned regions of the plane texture.) Thus the optimum thickness must be somewhere between $5\mu\text{m}$ and $20\mu\text{m}$. The exact value depends on the particular liquid crystal and on the properties of the surrounding substrate. The latter should be thin as compared with the liquid crystal film and should induce a well-aligned plane texture spontaneously. To obtain a stable film, the liquid crystal should wet the support sufficiently. We found that Mylar* membranes of about $6\mu\text{m}$ thickness provided the best substrates and that the optimum thickness of liquid crystal must be between 10 and $15\mu\text{m}$. Mylar thinner than $6\mu\text{m}$ did not align the plane texture sufficiently, apparently because the proper polar surface regions were not as well developed as for $6\mu\text{m}$ material.

After the Mylar is cleaned and stretched over the supporting ring, one side of the membrane is sprayed with infrared-absorbing paint consisting of carbon granules (average size about $2\mu\text{m}$) and an organic binder. However, we found that Mylar which was dyed black worked better.

The liquid crystal film was best applied by spraying. Using an ordinary artist's air brush with the finest nozzle, a mixture of 20% liquid crystal and 80% chloroform was sprayed on the membrane at a distance of 30 cm, using as a carrier gas dry nitrogen at a pressure of 344.75 kPa (50 psi). Better results requiring less operator skill were obtained with a Zicon Spray Gun (Chemtronic, Mount Vernon, New York) which uses as a carrier gas superheated freon at a pressure of about 344.75 kPa (50 psi). A mixture of 10% liquid crystal and cyclohexane is sprayed with the finest nozzle at a distance of 15 to 20 cm. The liquid crystal is applied in a clean, dry atmosphere. All other critical operations, such as the final cleaning of the membrane, application of the liquid crystal, and assemblage of the cell unit, are also performed in a clean, dry atmosphere.

Experimentally it was found that a temperature difference of 11.5° in the scene corresponded to a temperature difference of $0.17 \pm 0.02^\circ$ on the membrane. A temperature difference as low as 0.2°K in the scene could be detected against a background of 300°K .

* Mylar is the DuPont trademark for poly(ethylene terephthalate).

It was estimated that as much as 85% of the received radiation was lost by the obscuring optics, the germanium window, and the five reflective elements. The performance of this thermal imaging device is also greatly limited by the high background luminance of the viewing light. By using collimated, linear polarized viewing light and doubling the transmission of the optics, the minimum observable temperature difference in the scene would probably drop from 0.2° to less than 0.02° .

The observed spatial resolution was severely limited to the order of one line pair per millimeter. This was due to various factors. For example, the thickness of liquid crystalline layers cannot be reduced substantially below $10\mu\text{m}$ without adversely affecting the selective reflectivity.

Excessive lateral heat conduction across the membrane was a major problem. Elimination of the layer of carbon paint and the substitution of dyed Mylar for ordinary clear Mylar significantly improved the image. One of the problems with the carbon IR absorbing layer was that the IR radiation was being absorbed so far from the liquid crystal layer (on opposite sides of the Mylar membrane) that the resulting heat spread too far laterally (parallel to the membrane) as compared with the preferred perpendicular direction.

One of many possible ways to reduce lateral heat conduction might be to create thousands of square or hexagonal microsensory elements by punching tiny slits into the stretched Mylar membrane preferably with the liquid crystal in the crystallized phase at room temperature. A below-room-temperature liquid crystal, such as cholesteryl oleyl carbonate (which was unsatisfactory in virtually every way), would have complicated the slit-cutting process.

The sensing "islands" could easily be made as small as $50\mu\text{m}$ as shown by preliminary experiments. In addition to providing better image resolution, contrast, and faster heating time response, the slits would help to reduce "creeping" of the liquid crystal due to gravity and might enable a reduction in the size of a thermal imaging system, since less IR radiation would have to be gathered.

An entire thermal imaging system could be uniformly reduced in size without losing any radiation intensity on the liquid crystal membrane. By reducing lateral heat conduction, the tendency for the resulting smaller image to smear can be reduced.

Retaining the same aperture size for the incoming target IR radiation and concentrating it somewhat so as to form a smaller image on the membrane would also improve resolution, contrast, detectivity, and heating time response in addition to allowing a reduction in the size of the system. This would involve a slight reduction in the f/number of the optics.

If resolution were to improve to the point where the naked eye could not utilize it all, then eyepieces or a magnifying glass could be used to increase the apparent image size. At a wavelength of $10\mu\text{m}$, our thermal imaging system had an angular

$$\text{theoretical resolution limit of } \phi = \frac{1.22\lambda}{\text{aperture diameter}} = \frac{1.22 \times 10\mu\text{m}}{250 \times 10^3 \mu\text{m}} = 0.05 \text{ mr, which is}$$

equivalent to $12.5\mu\text{m}$ on the liquid crystal membrane, or 80 times better than our actual resolution of $1000\mu\text{m}$.

Another problem was how to effectively cool the membrane as IR energy from the target increased the membrane temperature. Since the heated membrane could not radiate heat energy away fast enough, conduction cooling was used whereby helium gas, under controlled pressure, absorbed heat by direct contact with the membrane and then was removed from the chamber by an applied vacuum. However, this was like walking a tightrope. Cooling too rapidly did not allow enough time for the incoming IR radiation to build up an image of weak targets, while cooling too slowly did not cause an image to disappear quickly enough to properly respond to changes in the scene. The problem was how to allow an image time to form with virtually no cooling and then quickly apply cooling to remove the excess heat in order to permit a new image to form. Operator controls might have been added to enable the observer to regulate the degree and the duration of the cooling as well as the type, i.e., pulsed or steady. Pulsed cooling might have been regulated by the observer as to the relative duration of the fast cooling fraction to the slow cooling fraction of the cooling cycle, in addition to the frequency of the cooling cycles.

Whether the imaging system is scanning or still and whether the target is moving or still must also be considered as well as the target temperature. A hot object will, of course, have a fast heating response time and a slow cooling response time as compared with the image of a target close to ambient temperature which has a slow heating response time and a fast cooling response time. The rate of cooling depends on several variables, such as the pressure and temperature of the helium gas and the distance from the membrane to the nearby window which affects the mean free path of the gas molecules and thus the degree of cooling. Much greater cooling occurs when the membrane is very close to the window. This could be another way that the observer might control the rate of cooling, such as with a knob to vary the membrane-window distance, in addition to controlling the pressure of the incoming helium gas and the opening of the vacuum exhaust. The feasibility of this approach, including the type of cyclical cooling used (i.e., rapidly changing the gas pressure and/or the membrane-window distance), would have to be determined experimentally. The number of cooling pulses, or cycles per second, would vary according to the ΔT between target and background which affects the response time of the liquid crystal.

We found that the time constant of cholesteryl oleyl carbonate was extremely long (several seconds) at its very low operating temperature of about 19°. In general, the lower the temperature of a liquid crystal, the more viscous it is. It is also inconvenient to cool to below ambient temperature. The high-temperature liquid crystals are very fluid and respond very quickly to temperature changes.

S-cholesteryl 14-phenyltetradecanethioate had a spectral width of about 0.07° and operated at 47°, with a very low crystallization temperature. A higher operating temperature was ruled out because too much power would be required to maintain operating temperature, especially in cold weather. Another potential disadvantage is that the hot membrane, although it might be made very small, could possibly be detected by the enemy. Also, deterioration of the liquid crystal proceeds more rapidly at higher temperatures, leading to uneven operating temperatures across the membrane and thereby requiring more frequent membrane replacement.

V. SUMMARY AND CONCLUSIONS

From a historical viewpoint, when our liquid crystal program was initiated, the only thermal-imaging system we had was the Barnes Thermograph which produced one picture in 20 minutes. A year later it produced a picture in 2 minutes. Liquid crystals had the same responsivity and could generate an image in 3 to 4 seconds, giving us the impetus to proceed with our program.

Over a period of many years, our chemists did an excellent job of synthesizing hundreds of new liquid crystals and in purifying them to a high degree. The characterization of the physical properties of the liquid crystals also proceeded smoothly. The difficult part of the overall program was the practical application of liquid crystals to the thermal imaging system. The major problem was in getting cholesteryl oleyl carbonate to work well in the system. But it never did. Many difficulties were encountered with it, such as the slow response time and a broad color band occurring at unpredictable temperatures. The material also required cooling to below room temperature. With one minor exception, the super-sensitive materials which operated above room temperature, with fast time responses and reasonably stable color ranges, were never studied in the thermal imaging system.

Toward the end of our 10-year effort, it appeared that the electronics revolution in conjunction with modern detectors was more promising than our uncertain liquid crystal approach. This was a major factor in terminating our program.

There are, however, many radiation image sensing systems where liquid crystals may represent the lowest cost, such as detection of HCN laser radiation, mode studies, and plasma studies, all using very long wavelengths.

BIBLIOGRAPHY

- Adams, J. E. and Haas, W., *Mol Cryst Liq Cryst*, 15 (1971).
- Adams, J. E. and Leder, L. B., *Chem Phys Lett*, 6 (1970).
- Adams, J. E., Haas, W.; and Wysocki, J.; *J. Chem Phys*, 50 (1969).
- Adams, J. E.; Haas, W.; and Wysocki, J.; "Liquid Crystals and Ordered Fluids," R. S. Porter and J. F. Johnson, eds, Plenum Press, NY (1970).
- Adams, J. E.; Haas, W.; and Wysocki, J.; *Phys Rev Lett*, 22 (1969).
- Alben, R., *Mol Cryst Liq Cryst*, 20 (1973).
- Applied Optics*, Infrared Imaging Issue, Vol 7 (Sep 68).
- Baessler, H. and Labes, M. M., *J. Chem Phys*, 52 (1970).
- Berremann, D. W. and Scheffer, T. J., *Mol Cryst Liq Cryst*, 11 (1970).
- Berremann, D. W. and Scheffer, T. J., *Phys Rev Lett*, 25 (1970).
- Böttcher, B., *Chem-Ztg, Chem-Techn*, 1 (1972).
- Böttcher, B., *Mater Constr (Paris)*, 4 (1971).
- Böttcher, B., Gross, D., and Mundry, E., *Materialpruefung*, 11 (1969).
- Brown, S. P., *Mater Eval*, 26 (1968).
- Cameron, L. M., *Mol Cryst Liq Cryst*, 7 (1969).
- Cano, R., *Bull Soc Franc Mineral*, 90 (1967).
- Chatelain, P., *Bull Soc Franc Mineral*, 66 (1943).
- Coates, D. and Gray, G. W., *Phys Lett*, 45A (1973).
- de Gennes, P. G., "The Physics of Liquid Crystals," Clarendon Press, Oxford (1974).

- Dixon, C. D. and Scala, L. C., *Mol Cryst Liq Cryst*, 10 (1970).
- Dreher, R., *Dissertation*, Freiburg (1971).
- Dreher, R.; Meier, G.; and Saupe, A.; *Mol Cryst Liq Cryst*, 13 (1971).
- Elser, W. and Ennulat, R. D., "Advances in Liquid Crystals," G. E. Brown, ed, Academic Press, NY, Vol 2 (1976).
- Elser, W.; Pohlmann, J. L. W.; and Boyd, P. R.; *Mol Cryst Liq Cryst*, 20 (1973).
- Elser, W.; Pohlmann, J. L. W.; and Boyd, P. R.; *Mol Cryst Liq Cryst*, 27 (1974).
- Ennulat, R. D., "Analytical Calorimetry," R. S. Porter and J. F. Johnson, eds, Plenum Press, NY (1968).
- Ennulat, R. D., *Mol Cryst Liq Cryst*, 3 (1968).
- Ennulat, R. D., *Mol Cryst Liq Cryst*, 6 (1970).
- Ennulat, R. D., *Mol Cryst Liq Cryst*, 13 (1971).
- Ennulat, R. D. and Brown, A. J., *Mol Cryst Liq Cryst*, 12 (1971).
- Ennulat, R. D. and Ferguson, J. L., *Mol Cryst Liq Cryst*, 13 (1971).
- Ennulat, R. D.; Garn, L. E.; and White, J. D.; *Mol Cryst Liq Cryst*, 26 (1974).
- Ferguson, J. L., *Appl Opt*, 7 (1968).
- Ferguson, J. L., *Mol Cryst Liq Cryst*, 1 (1966).
- Ferguson, J. L., *US Nat Tech Inform Serv Rep No. AD741898* (1971).
- Ferguson, J. L.; Goldberg, N. N.; and Nadalin, R. J.; *Mol Cryst Liq Cryst*, 1 (1966).
- Ferguson, J. L.; Taylor, T. R.; and Harsch, T. B.; *Electro-Technology (NY)*, 85 (1970).
- Friedel, G., *Ann Phys (Paris)*, 18 (1922).
- Galanti, A. V. and Porter, R. S., *J. Phys Chem*, 76 (1972).
- Gerritsma, C. J. and Van Zanten, P., *Phys Lett*, 42A (1972).

- Gibson, J. W. and Pochan, J. M., *J. Phys Chem*, 77 (1973).
- Grass, D. and Bottner, B., *Z. Naturforsch*, 25B (1970).
- Gray, G. W., "Molecular Structure and the Properties of Liquid Crystals," Academic Press, London & NY (1962).
- Griffen, C. W. and Porter, R. S., *Mol Cryst Liq Cryst*, 21 (1973).
- Hakemi, H. and Labes, M. M., *J. Chem Phys*, 58 (1973).
- Hampel, B., *Z. Werkstofftech*, 3 (1972).
- Hareng, P. M., *Rev Techn Thomson - CSE*, 5 (1973).
- Hartshorne, N. H. and Stuart, A., "Crystals and the Polarizing Microscope," E. Arnold, London (1960).
- Hermann, C., *Z. Kristallogr*, 79 (1931).
- Hosemann, R. and Bagchi, S. N., "Direct Analysis of Diffraction by Matter," Interscience Publ, NY (1962).
- Ishikawa, T.; Mizuno, T.; Kato, F.; Yashiro, Y.; and Nagao, H.; *Bull Nagoya Inst Technl*, 22 (1970).
- Kahn, F. J. *Appl Phys Lett*, 18 (1971).
- Kassubek, P. and Meier, G., *Mol Cryst Liq Cryst*, 8 (1969).
- Keating, P. N., *Mol Cryst Liq Cryst*, 8 (1969).
- Kelker, H. and Hatz, R., *Chem-Ing Techn*, 45 (1973).
- Keyes, P. H.; Weston, H. T.; and Daniels, W. B.; *Phys Rev Lett*, 31 (1973).
- Ko, K.; Teuscher, I.; and Labes, M. M.; *Mol Cryst Liq Cryst*, 22 (1973).
- Krzewki, R. J. and Porter, R. S., *Mol Cryst Liq Cryst*, 21 (1973).
- Laves, F. and Ernst, T., *Naturwissenschaften*, 31 (1943).

- Leder, L. B., *Chem Phys Lett*, 6 (1970).
- Lehmann, O., *Z. Phys Chem (Leipzig)*, 4 (1889).
- Mabis, A., *Acta Crystallogr*, 15 (1962).
- Magne, M. and Pinard, P., *J. Phys (Paris)*, 30, Colloq C4 (1969).
- Mainusch, K. J. and Stegemeyer, H., *Z. Phys Chem (Frankfort)*, 77 (1972).
- Melamed, L. and Rubin, D., *Appl Opt*, 10 (1971).
- Muller, J. H., *Mol Cryst Liq Cryst*, 2 (1966).
- Müller, W. V. and Stegemeyer, M., *Chem Phys Lett*, 27 (1974).
- Pohlmann, J. L. W., *Mol Cryst Liq Cryst*, 2 (1966).
- Pollmann, P. and Stegemeyer, H., *Ber Bunsenges, Phys Chem* 78 (1974).
- Sackmann, E., *J. Am Chem Soc*, 93 (1971).
- Sackmann, E. and Voss, J., *Chem Phys Lett*, 14 (1972).
- Saeva, F. D., *J. Am Chem Soc*, 94 (1972).
- Saeva, F. D. and Wysocki, J. J., *J. Am Chem Soc*, 93 (1971).
- Stegemeyer, H. and Finkelmann, H., *Ber Bunsenges, Phys Chem*, 78 (1974).
- Stegemeyer, H. and Finkelmann, H., *Chem Phys Lett*, 23 (1973).
- Stegemeyer, H. and Mainusch, K. J., *Naturwissenschaften*, 58 (1971).
- Toliver, W. H.; Ferguson, J. L.; Sharpless, E.; and Hoffman, P. E., *Aerosp Med*, 41 (1970).
- Vogelzangs, J. H. J., *Ned Tijdschr Natuurk*, 38 (1972).

Vorlander, D., *Z. Phys Chem (Leipzig)*, 61 (1973).

Voss, J. and Sackmann, E., *Z. Naturforsch.* 28A (1973).

Wahlstrom, E. E., "Optical Crystallography," J. Wiley and Sons, NY (1951).

DISTRIBUTION FOR NV&EOL REPORT DELNV-TR-0003

No. Copies	Addressee	No. Copies	Addressee
12	Defense Documentation Center ATTN: DDC-TCA Cameron Station (Bldg 5) Alexandria, VA 22314	1	AFSPCOMMEN/SUR San Antonio, TX 78243
1	Director National Security Agency ATTN: TDL Fort George G. Meade, MD 20755	1	Armament Development & Test Ctr ATTN: DLOSL, Tech Library Eglin Air Force Base, FL 32542
1	Office of Naval Research Code 427 Arlington, VA 22217	1	HQDA (DACE-CMS) Washington, DC 20310
1	Director Naval Research Laboratory ATTN: Code 2627 Washington, DC 20375	1	OSASS-RD Washington, DC 20310
1	Commander Naval Electronics Laboratory Ctr ATTN: Library San Diego, CA 92152	1	Commander US Army Training & Doctrine Cmd ATTN: ATCD-SI Fort Monroe, VA 23651
1	Commander US Naval Surface Weapons Center ATTN: Technical Library White Oak, Silver Spring, MD 20910	1	Commander US Army Training and Doctrine Cmd ATTN: ATCDOCI Fort Monroe, VA 23651
1*	Commandant, Marine Corps HQ, US Marine Corps ATTN: Code LMC Washington, DC 20380	1	CDR, US Army Materiel Development and Readiness Command ATTN: DRCMA-EE 5001 Eisenhower Avenue Alexandria, VA 22333
1	HQ, US Marine Corps ATTN: Code INTS Washington, DC 20380	1	CDR, US Army Materiel Development and Readiness Command ATTN: DR-CRD-FW Alexandria, VA 22333
1	Command, Control & Communi- cations Div Development Center Marine Corps Development & Educ Comd Quantico, VA 22314	1	Commander US Army Training & Doctrine Cmd ATTN: ATCD-F Fort Monroe, VA 23651
1	HQ ESD (XRR1) L. G. Hanscom Field Bedford, MA 01730	1	Commander US Army Missile Research and Development Command ATTN: DRSMI-RR, Dr. J. P. Hallows Redstone Arsenal, AL 35809
2	Air Force Avionics Laboratory ATTN: AFAL/TSR, STINFO Wright-Patterson AFB, OH 45433	1	Commander US Army Armament Research and Development Command ATTN: DRSAR-RDP (Library) Rock Island, IL 61201
		3	Commander US Army Combined Arms Combat Developments Activity ATTN: ATCAIC-IE Fort Leavenworth, KS 66027

No. Copies	Addressee
1	Commander US Army Logistics Center ATTN: ATCL-MA Fort Lee, VA 23801
1	Commandant US Army Ordnance School ATTN: ATSOR-CTD Aberdeen Proving Ground, MD 21005
1	Commander US Army Intelligence School ATTN: ATSIT-CTD Fort Sill, OK 73503
1	Commander Picatinny Arsenal ATTN: SARPA-TS-S #59 Dover, NJ 07801
1	Commander Frankford Arsenal ATTN: (Dr. Wm. McNeill) PDS Philadelphia, PA 19137
1	Commander USASA Test & Evaluation Center Fort Huachuca, AZ 85613
1	US Army Research Office - Durham ATTN: CRDARD-IP Box CM, Duke Station Durham, NC 27706
1	US Army Research Office - Durham ATTN: Dr. Robert J. Lontz Box CM, Duke Station Durham, NC 27706
1	Commander HQ MASSTER Technical Information Center ATTN: Mrs. Ruth Reynolds Fort Hood, TX 76544
1	USA Security Agency ATTN: IARD Arlington Hall Station Arlington, VA 22212
1	Commandant US Army Engineer School ATTN: ATSE-CTD-DT-TL Fort Belvoir, VA 22060

No. Copies	Addressee
1	Commander US Army Tank-Automotive Research and Development Command ATTN: DRSTA-RW-L Warren, MI 48090
1	Commandant US Army Air Defense School ATTN: C&S Dept, Msl Sci Div Fort Bliss, TX
1	Commander US Army Combined Arms Combat Developments Activity ATTN: ATCACC Fort Leavenworth, KS 66027
2	Commander US Army Yuma Proving Ground ATTN: STEYP-MTD (Tech Lib) Yuma, AZ 85364
1	Commander US Army Arctic Test Center ATTN: STEAC-PL APO Seattle 98733
1	CO, US Army Tropic Test Center ATTN: STETC-MO-A (Tech Lib) Drawer 942 Fort Clayton, Canal Zone 09827
1	Commander US Army Logistics Center ATTN: ATCL-MC Fort Lee, VA 22801
1	Directorate of Combat Developments US Army Armor School ATTN: ATSB-CD-AA Fort Knox, KY 40121
1	Commandant US Army Inst for Military Assistance ATTN: ATSU-CTD-OMS Fort Bragg, NC 28307
1	Commander US Army Missile Research and Development Command ATTN: DRSMI-RE (Mr. Pittman) Redstone Arsenal, AL 35809

No. Copies	Addressee	No. Copies	Addressee
1	Commander US Army Systems Analysis Agency ATTN: (Mr. A. Reid) DRXSY-T Aberdeen Proving Ground, MD 21005	1	Study Center National Maritime Research Center ATTN: Rayma Feldman King's Point, NY 11024
1	Commandant US Army Signal School ATTN: ATSN-CTD-MS Fort Gordon, GA 30905	1	HQ, USAEUR & Seventh Army Deputy Chief of Staff, Engineer ATTN: AEAEN-MT-P APO New York 09403
1	Commander US Army Tank-Automotive Research & Development Cmd ATTN: DRSTA-RHP, Dr. J. Parks Warren, MI 48090	1	HQ, USAEUR & Seventh Army Deputy Chief of Staff, Operations ATTN: AEAGC-FMD APO New York 09403
2	NASA Scientific & Tech Info Facility ATTN: Acquisitions Branch (S-AK/DL) P.O. Box 33 College Park, MD 20740		
2	Advisory Group on Electron Devices 201 Varick St, 9th Floor New York, NY 10014		
1	Ballistic Missile Radiation Anal Ctr Env Research Inst of Michigan Box 618 Ann Arbor, MI 48107		
2	Chief Ofc of Missile Electronic Warfare Electronic Warfare Lab, ECOM White Sands Missile Range, NM 88002		
1	Chief Intel Materiel Dev & Support Ofc Electronic Warfare Lab, ECOM Fort Meade, MD 20755		
2	Commander US Army Electronics Research and Development Command ATTN: DRSEL-MS-TI Fort Monmouth, NJ 07703		
1	TACTEC Battelle Memorial Institute 505 King Avenue Columbus, OH 43201		
1	Commander US Army Electronics Research and Development Command ATTN: DRSEL-PL-ST Fort Monmouth, NJ 07703		